Enhancement of Critical Loading for Electric Power Distribution Systems

A THESIS

Submitted in fulfillment of the requirement for the award of the degree of

DOCTOR OF PHILOSOPHY

in

ELECTRICAL ENGINEERING

by

Kultar Deep Singh
(900804001)

Under the Supervision of

Dr. Smarajit Ghosh
Professor, EIED

Department of Electrical & Instrumentation Engineering
Thapar University
Patiala – 147 004

Certificate

I hereby certify that the work which is being presented in the thesis entitled "**Enhancement of Critical loading for Electric power Distribution Systems**" in partial fulfillment of the requirement for the award of degree of "Doctor of Philosophy" submitted in Department of Electrical and Instrumentation Engineering of Thapar University, Patiala, is an authentic record of my own work carried out under the supervision of Dr. Smarajit Ghosh and refers other research work which are duly listed in the reference section.

The matter presented in this thesis has not been submitted for the award of any other degree of this or any other university.

(Kultar Deep Singh)

Regn. No. 900804001

This is to certify that the above statement made by the candidate is correct and true to the best of my knowledge.

S. Ghosh

(Dr. Smarajit Ghosh)

Professor

Department of Electrical and Instrumentation Engineering

Thapar University, Patiala.

Punjab, INDIA-147004

Acknowledgements

I would like to express my sincere appreciation to my supervisor, **Prof. Smarajit Ghosh**, for his support and encouragement throughout my research work. His experience, strength, tenderness and willfulness, has taught me the lessons of life, which are of immense help to me to take the decisions in my every endeavour.

I am thankful to my doctoral committee members, **Dr. S. S. Bhatia**, Prof. and head of School of Mathematics and Computer Applications (SMCA), Thapar University, Patiala, and **Dr. Mandeep Singh**, Associate Professor, Department of Electrical and Instrumentation Engineering for their constructive comments and regularly ensuring the progress of my research work. I am thankful to Dean of Research and Sponsored Projects **Dr. P. K. Bajpai** for his affection and blessing during this thesis work. I am thankful to all the faculty members and staff members of Department of Electrical and Instrumentation Engineering for their cordial behavior.

I am also thankful to **Mr. S. P. Yadav** for his kind support from starting of thesis work to the completion of the work

I offer deepest gratitude to my family members for their love and moral support.

(Kultar Deep Singh)

Dedicated to my grand mother

ABSTRACT

In this thesis it has been tried to explore the possibilities of enhancement of critical loading of radial electrical power distribution networks. It has been found that the critical loading can be enhanced by optimal conductor size selection, optimal capacitor placement, and network reconfiguration. To apply these corrective steps on the distribution networks an efficient load-flow solution method is required so that the actual condition related to node voltage and its angle, branch current, real power loss, reactive power loss, branch losses etc. of the network can be studied and analyzed. A new efficient method is proposed for load-flow solution of radial distribution networks. Simple transcendental equations are used to relate the sending-end voltage, receiving-end voltage and voltage drops in each branch of the distribution system. The effect of charging capacitance of the line has been incorporated in load-flow solution. A computer algorithm is developed in such a way that there is no need to adopt any sequential node numbering scheme for the solution of the networks. The angle of the receiving-end voltage is also computed along with the magnitude of the voltage. It is an iterative method. The flat voltage (1p.u.) start from substation to every end-node is considered. The voltage magnitude and angle are updated after each successive iteration and the voltage drops are then computed by using the new obtained values of voltage magnitude and angle. The comparison of speed and memory requirement by the proposed method with the other methods has been verified to show its efficiency.

To investigate the present state of loading and loadability limit, a line loadability index is derived. The change in resistance with the change in operating temperature of the

branch conductors is incorporated in the computation of voltage stability index and line loadability index. The voltage stability index computes the voltage stability limit of the radial distribution network in the fault conditions or at the time of load contingency, it identifies the most sensitive node of the distribution network and gives information about time within which the voltage collapse will occur for above said conditions. The line loadability index is based on the maximum permissible steady state operating temperature of the line conductors. The loadability limit of the distribution network is supposed to be within the maximum permissible operating temperature of the conductor. Line loadability index gives the loadability limit of the network in normal steady state conditions and identifies the most sensitive branch of the network. The values of voltage stability limit and line loadability limit are not unique for a distribution networks, the values might be different for the same network in different ambient conditions. So a very practical aspect is incorporated in the proposed work. The importance of the proposed voltage stability index is discussed in context of over current protection. The proposed voltage stability index and line loadability index can be used for voltage stability study and the loadability margin, optimal conductor size selection, capacitor placement studies, reconfiguration of distribution networks, over current protection system design etc. at planning stage as well as in operation of the electrical power distribution system.

The current carrying capacity, critical loading and voltage stability of distribution networks depend upon the conductor sizes applied to each branch of distribution network. Hence the optimal conductor size selection is utmost necessary. A method for optimal conductor size selection is proposed in this work. The conductor sizes are first selected according to the current carrying capacity of the available conductor sizes, then upgraded

through economical optimization. After selecting the economical conductor sizes, the constraints regarding the maximum limit of branch operating temperature and the minimum voltage level at the end nodes are applied and the up gradation of the candidate branches is carried out. While selection of the optimal conductor size for each branch of the distribution network, the effect of change of resistance with the change of temperature is incorporated. This incorporation leads to exact computation of real power losses of the network, actual thermal behavior of branch conductor in practical situations and optimal conductor size selection according to weather conditions of the region. The results are compared with the existing methods to establish the goodness of the proposed approach.

The critical loading and voltage stability are related to the system's voltage profile. The voltage profile of distribution network can be improved by reducing the reactive component of power by optimal capacitor placement. Capacitor placement problem is dealt with different way in this work. Capacitors are placed at the nodes where the reactive power demand is occurred. The capacitor sizes are selected on the basis of economical analysis. The shunt capacitor is more economical when it is placed as near as possible to the load causing low power factor. In the proposed, method it has been computed at first the summation of real power losses from substation to each node. The node having highest value of losses is taken as the candidate node and the smallest capacitor size is placed at that node and the objective function is again computed. The level of reactive power compensation is increased till it generates the economical benefits. All the nodes are tried in this manner. The results are compared with the existing method and the proposed method is found better in each aspect.

The enhancement of critical loading and voltage stability can be achieved from the existing network through network reconfiguration. The reconfiguration of distribution network is dealt with different point of view in this work. The possibilities of network reconfiguration are identified from the chronological load curves of the laterals of distribution network. The load can be shifted from one lateral of distribution network to the other lateral due to the seasonal change in load demand. The enhancement in critical loading and enhancement in voltage stability after network reconfiguration are shown with the help of a test system.

TABLE OF CONTENTS

LIST OF FIGURES

LIST OF TABLES

LIST OF SYMBOLS

N: Total number of nodes.

SN, RN: Sending-end node and receiving-end node.

k: Node Number :1, 2, 3,……. N.

jj: Branch number :1, 2, 3,……. N-1.

V_k: Sending-end voltage.

$V_{k+1:}$ Receiving-end node's voltage.

δ_k: Sending-end node's voltage angle.

δ_{k+1}: Angle of Receiving-end node's voltage.

I_{jj} : Branch current.

Z_{jj} : $R_{jj} + jX_{jj}$, Branch impedance.

y_m^c : Admittance of the charging capacitance.

P_m and Q_m : Real load and reactive power load respectively connected to the node (m).

L_1, L_2, L_3……. are the arrays to store node numbers of feeder and laterals the distribution network.

JN and LN are two dimensional arrays.

q_{jjc} : Convicted heat loss rate per unit length W/m

Δq_{jj} : Additional heat in the heat balance equation

Q_{jjse} : Total solar and sky radiated heat flux rate elevation corrected W/m^2

q_{jjs} : Heat gain rate from sun W/m

q_{jjr} : Radiated heat loss rate per unit length W/m

K_{ang} : Wind direction factor

k_{jj} : Thermal conductivity of air at temperature T film W/(m-°C)

v : Speed of air stream at conductor m/s

d_{jj} : Conductor diameter in mm

φ : Angle between wind and axis of conductor

ε : Emissivity

A'_{jj} : Projected area of conductor per unit length m^2/m

θ : Effective angle of incidence of the sun's rays degrees

α : Solar absorptivity (0.23 to 0.91)

Z_1 : Azimuth of line degrees

Z_c : Azimuth of sun degrees

H_c : Altitude of sun degrees

$T_{jj\,film}$: Film temperature.

T_a : Ambient air temperature °C

T_{jj} : Conductor temperature °C

ΔT_{jj} : Conductor temperature increment corresponding to time step °C

$T_{jj(high)}$: Maximum conductor temperature for which Ac resistance is specified °C

$T_{jj(low)}$: Minimum conductor temperature for which Ac resistance is specified °C

$T_{jj(old)}$: Conductor temperature prior to step increase °C

μ_{jj} : Dynamic viscosity of air Pa-s

H_e : Elevation of conductor above sea level m

ρ_{jj} : Density of air kg/m^3

S_{spc} : Specific heat of conductor material J/(kg-°C)

M_{jj} : Mass per unit length of conductor material kg/m

Δt : Time step used in transient calculations

$R_{jj(low)}$: Ac resistance of conductor at minimum specified temperature.

$R_{jj(high)}$: Ac resistance of conductor at maximum specified temperature.

$R_{jj(Tjj)}$: AC resistance of conductor at temperature, T_{jj} Ω/m

K_p : Annual demand cost of power loss (Rs. kW^{-1})

K_e : Annual demand cost of energy loss (Rs. kWh^{-1})

$Loss_{(jj,k,pp)}$: Real power loss of network branch -jj with load contribution factor.

ΔK_p : Annual growth in cost of power.

ΔK_e : Annual growth in cost of energy.

pp: Plan period in years for which the feeder is designed.

Lf : Load factor.

Lsf : Loss factor.

ΔLf : Annual growth in loss factor.

$CC_{(jj,k)}$: Capital investment for the conductor k of branch -jj.

$Cost_{(k)}$: Cost of the conductor (Rs./kg/km).

$Scrap_{(k)}$: Value of scrap material of the branch conductor after the plan period.

F_c : Contribution factor

ΔF_c : Annual change in contribution factor.

$l_{(jj)}$: Length of the conductor -jj (km).

dr: Annual discount rate.

N: Total number of nodes.

K: Node Number :1, 2, 3,……. N.

jj: Branch number :1, 2, 3,……. N-1.

V_K: Sending-end voltage.

$V_{K+1:}$ Receiving-end node's voltage.

I_{jj} : Branch current.

Z_{jj} : $R_{jj} + jX_{jj}$, Branch impedance.

P_m and Q_m : Real load and reactive load respectively connected to the node (m).

$S_m = P_m + jQ_m$: Total power at node m.

$\cos\phi_{1m}$: Present power factor.

$\cos\phi_{2m}$: Required power factor.

Q_{cmreq} : Required capacitive reactive power

Q_{cmp} : Reactive power of capacitor actually placed.

C_c : Cost of capacitor \$/kVAr.

Q_{cl} : Reactive power of capacitor at a location (node).

C_e : Cost of energy \$/kWh.

P_{LP} : Real power loss of a branch.

ss: Substation node

Q_{cmreqf} : Reactive power of fixed capacitor.

$Q_{c\min}$: Minimum value of capacitor size available in inventory.

CHAPTER 1

INTRODUCTION

1.1 Introduction:

Electricity provides a very convenient form of energy for lighting, heating, cooling, motive power for driving various types of loads and power for a number of utilization applications. Electricity is transmitted and distributed to the consumers through transmission and distribution systems. The losses in power transmission system are small as compared to distribution system due to higher voltage level. So chances of further improvement in efficiency are bleak. Therefore, nowadays extra attention is paid to the distribution systems.

The configuration of distribution networks is quite different from transmission networks. Distribution systems are typically radial in nature. This network configuration produces low voltages at the load buses, especially those, located far away from the substation. Additionally, in a distribution system low voltages at load ends will cause large power losses and the power factor, therefore, becomes poorer than expected.

A distribution system connects consumers to high voltage transmission system. Because of lower voltage and hence higher current, the $I^2 R$ loss in distribution system is significantly high compared to transmission system.

The modern power distribution network is constantly being faced with an ever-growing load demand. Distribution networks experience distinct change of load from a lower to higher level every day. It has been seen that above certain critical loading conditions, the distribution system experiences violation of critical loading conditions, which leads to permanent deformation of conductors. In case of several sever fault, the system voltage may collapse before the protection system clears the fault.

Line loadability and voltage collapse problems have become a point of concern for many researchers. Line loadability is a term related to steady state loading of the distribution network. Analysis of line loadability of each branch of the network shows the extent of loading of each branch under given load and most sensitive branch of the network and margin between present loading and critical loading. Voltage stability analysis is important at the time of faults or fault like situations. The protection system usually isolates the faulty portion of the network. But in some conditions the voltage collapse may occur when fault level is so high. Voltage collapse is a local phenomenon that may have consequent serious fallouts. Future increase in the demand for electric power has been projected to far exceed the planned generation of existing power system in the coming decades. This has led to increasingly complex interconnected systems that are forced to operate ever closer to the limits of loadability and stability. This operation has necessitated close examination of line loadability and voltage stability assessment capabilities of distribution systems. Many new types of instabilities are beginning to afflict the operating status of critically balanced system. The instability may be manifested in different ways, depending upon the character and configuration of the system and upon its operating mode. Of these, line loadability and voltage instability has been responsible for collapse of several major networks. Line loadability and voltage stability studies of a power distribution system are consequently essential.

Improving the performance of distribution systems to meet the required target is a matter of selecting the most cost–effective technologies and operating practices. The distribution systems tend to be very extensive with a long life span for conductors and plant. It is not sufficient to analyze how a particular portion of the network may be modified to improve its performance on date. It is a matter of determining the expected optimum solution when allowance is made for the uncertainties in the prediction of the future scenario of

customer demand. It is valuable to investigate long–term solutions especially when the implementation of the solutions may require large–scale investments. Arising from these issues, the realization by the utilities and the increasing reliance on having accurate up–to–date information for decisions on increasing revenues, improving customer service must be set up. No doubt, the vast field and organizational experience of the power utilities will continue to provide the required inputs into the total process.

To operate the distribution network near to critical loading conditions to exploit maximum benefits from installed capacity, an accurate and efficient load-flow method is necessary, to compute voltage at each node, current through each branch, branch losses, branch voltage drop and total real power losses and total reactive power losses with less computer memory utilization and less CPU time. Form the above said parameters of distribution network the line loadability of each branch and voltage stability of each node of the network can be computed. The corrective measures for enhancement of critical loading like optimal conductor size selection for each branch, optimal capacitor placement and distribution network reconfiguration can be applied.

1.2 Critical Loading:

Every part of distribution network is designed to take certain load. The load equal to the maximum limit of network is called the critical load. The word ‘critical load’ is used for maximum limit of load that can be carried by the system because beyond this load one or more than one part of the network starts to get damaged. So the loading of the network should be within this limit. In case of distribution networks, the loadability limit is decided by the temperature of the branch conductors. The temperature of the branch conductors is a function of load current and the ambient conditions. So the critical loading limit is decided by the load current, resistance of branch conductors and ambient conditions. To increase the critical

loading limit of a distribution network, the load current for the given load and resistance of the network has to be reduced. The reduction of load current can be achieved by optimal capacitor placement and reconfiguration of network. The reduction of resistance is achieved by optimal conductor size selection for each branch of the network.

1.3 Objectives of research:

The research endeavors to derive a new load-flow solution method, a new line loadability index and voltage stability index, optimal conductor size selection method, optimal capacitor placement method and network reconfiguration method for radial distribution networks. The objectives of the research are divided into following:

- A new accurate and efficient load-flow solution method for radial networks is to be proposed. By using this load-flow solution the node voltage, branch current, branch voltage drop, branch real power losses and reactive power losses are computed.
- A new expression of line loadability index (*LLI*) is to be derived that gives the information of level of loading of each branch and the most sensitive branch of the network. The critical loading of the distribution network(s) is computed for different load models.
- A new expression for voltage stability index is to be derived that gives the information of voltage stability index of each node and the most sensitive node of the network. The voltage stability of the network(s) under fault conditions is checked for different load models.
- A new method is to be proposed to select the optimal conductor for radial distribution networks incorporating *LLI*. The critical loading and voltage stability under fault conditions of the distribution network(s) is checked for different load models.

- A new method is to be proposed for optimal capacitor placement of radial distribution networks. The critical loading and voltage stability of the distribution network(s) is checked for different load models.
- A new method is to be proposed for network reconfiguration of radial distribution networks. The critical loading and voltage stability of the distribution network(s) is checked for different load models.

1.4 Scope of research:

After the rigorous literature survey the following areas of research are marked as the scope of further research.

- The load-flow solutions reported so far were not developed to carry out the reconfiguration of radial distribution networks without renumbering the branches and nodes. For renumbering the branches and nodes after reconfiguration needed large manual and computation effort. To save the computation effort in renumbering the branches and nodes, a new load-flow solution method that can solve the network without renumbering after reconfiguration is required.
- The term line loadability index (LLI) is used with same meaning as the voltage stability index by Juan ***et al.*** [41]. The new definition and formulation of line loadability index is required so that the line loadability index can be used for analysis of steady state loading condition of distribution networks.
- The voltage stability indices reported in literature had not incorporated the effect of change in resistance with the change in temperature due to flow of current through branch conductors. A new procedure and formulation for computation is required so that the effect of change in resistance with the change in temperature due to flow of current

through branch conductors can be incorporated to get the more realistic results can be obtained.

- The previous researchers had only considered the current carrying capacity of conductors as the constraint, but they did not incorporate the change in resistance or the change in current carrying capacity due to change in operating temperature of the conductors and the effect of ambient conditions on current carrying capacity of conductors. The optimal conductor size selection method can be proposed by incorporating the *LLI* as a constraint.
- Almost all previous researchers solved the capacitor placement problem according to the line reactive power demand and proposed the optimal location and size after economic analysis. Procedure for optimal capacitor placement is required to be proposed according to reactive power demand of each node. The improvement in *LLI* and *VSI* is to be investigated after capacitor placement.

The previous researchers had suggested the procedures for network reconfiguration with very much flexibility. They almost tried every possible combination for network reconfiguration but it is not possible in real distribution networks. Because it not possible to stretch tie line from any node to any other node in a distribution network. So this led to theoretical exercise but had no practical significance. A procedure for network reconfiguration is required that considers the practical constraints like seasonal change in load, maintenance of radial nature of network, same direction of flow of current as in base network and possible practically tie-lines of network reconfiguration.

1.5 Organization of research:

Chapter 1 has presented the introduction of basic nature and problems of distribution network, critical loading, objectives of research, scope of research and organization of research.

Chapter 2 presents the literature survey on load-flow, line loadability index and voltage stability index, optimal conductor selection, optimal capacitor placement and network reconfiguration for radial distribution networks.

Chapter 3 presents a new load-flow solution method for radial distribution networks. The results obtained by proposed load-flow method are compared with other existing methods to show the reliability of proposed method. The comparison of computer memory and CPU time for existing and proposed method is also shown in this chapter to show the goodness of proposed method.

Chapter 4 presents the formulation and computation of new line loadability index and voltage stability index by incorporating the change in resistance of branch conductors with the operating temperature. The results of voltage stability index are compared with the existing voltage stability indices to show the goodness of proposed method. The proposed method has been investigated for different types of load models.

Chapter 5 presents a new method for optimal conductor size selection for radial distribution networks incorporating the line loadability index as one of the constraints. The results are compared with the existing method of optimal conductor size selection to show the goodness of proposed method. The enhancement of critical loading and voltage stability by optimal conductor placement are also shown.

Chapter 6 presents a new method for optimal capacitor placement for radial distribution network. It is based on the node wise reactive power demand compensation. The results are compared with the exiting methods to show the goodness of the proposed method. Enhancement of critical loading and improvement in voltage stability of network is investigated after optimal capacitor placement.

Chapter 7 presents a new method for network reconfiguration based on chronological load curve. Enhancement of critical loading and improvement in voltage stability of network is investigated after network reconfiguration.

Chapter 8

Conclusion and future scope of research.

References show the list of previous papers, books, reports etc. published by researchers those are discussed in literature survey and other chapters of this thesis on various topics related to this research.

Appendix-A

Proof of convergence of load-flow solution.

Appendix-B

Line data and load data for 33-node network.

Appendix-C

Line data and load data for 69-node network.

Appendix-D

Line data, load data and conductor data for 41-node network.

Appendix-E

Line data, load data and conductor data for 30-node network.

Appendix-F

Line diagram, line data, load data and conductor data for 32-node network.

Appendix-G

Line data, load data and conductor data for 123-node network.

List of Publication

Biography

Biography of author.

Biography of supervisor.

CHAPTER 2

LITERATURE SURVEY

2.1 Literature survey of electric power distribution networks:

Exhaustive literature survey on the following areas

i. Load-flow solution of electric power distribution networks.
ii. Line loadability index and voltage stability index for radial electric power distribution networks.
iii. Optimal conductor size selection for radial electric power distribution networks.
iv. Optimal capacitor placement procedure for radial electric power distribution networks.
v. Network reconfiguration for radial power distribution networks.

are shown in the following sub articles

2.2 Survey on load-flow of electric power distribution networks:

The load-flow analysis has an utmost important role for the design of distribution network. An efficient and good converging load-flow of distribution system is not only useful to obtain voltage and power loss of the network but also necessary for accurate selection of branch conductor and other aspect of planning. Load-flow methods like Newton-Raphson, and fast decoupled load-flow method proposed by Tinny and Hart [1] and Scott and Alsac [2] could be efficiently used for transmission systems having high X/R ratio. Since the distribution systems have high R/X ratio, the above methods could not converge. Some researchers Iwamoto and Tamura [3] and Rajcic and Tamura [4] suggested the modified conventional methods to solve the distribution networks. Ladder network theory was used by Kersting [5]. A compensation based method was proposed by Shirmohammadi ***et al.*** [6] to

solve the weakly meshed networks. The branch numbering scheme was developed to enhance the numerical performance. Baran and Wu [7] proposed a Newton –Raphson based method, which needs the computation of Jacobian matrix to solve the radial distribution networks. Hence this method needed more computational efforts. Renato [8] used the bi-quadratic equations to relate the sending-end and receiving-end voltages. But the angle of the voltage was not considered in his method. Goswami and Basu [9] proposed a direct method for solving the radial networks but they had put the limit that no node could be a junction of more than three branches. Jasmon and Lee [10] reduced the network in a single line equivalent model and used the power-flow equations in which the sending-end voltage was involved. Das ***et al.*** [11] proposed a unique numbering scheme for nodes and branches. They had used the simple algebraic equations to solve the radial distribution system. Haque [12] had proposed a solution method for radial and mesh power distribution networks. Backward and forward sweep technique was used for final solution. Initially the substation voltage was taken as the voltage of each node, which was updated after each successive iteration. Ghosh and Das [13] proposed a method for load-flow solution using forward backward technique. But only the magnitude of voltage at each node was computed. They had used the concept of nodes beyond branch and provided the proof of convergence. Aravindhababu ***et al.*** [14] proposed a technique to compute the branch currents and loads from the node branch matrix, voltage drops and node voltages were then computed. Mekhamer ***et al.*** [15] used the equations of Baran and Wu [7] for load-flow solution of radial distribution system but the solution methodology was different. The load of the lateral branches was supposed as the single equivalent load. After computation of the voltages of the main feeder nodes, the laterals were expanded and the voltage of the first node of the lateral was taken equal to the node voltage to which the lateral was connected. Same solution technique was used for the laterals. Eminoglu and Hocaoglu [16] presented a method for load-flow solution based on

Kirchhoff's law equations and applied the proposed method on different load models. Satyanarayana ***et al.*** [17] developed the load-flow equations from the ABCD parameter model of short transmission line and applied the method on the different load models. Sherpa and Ghosh [18] proposed a new algorithm for load-flow solution that needed no sequential numbering of nodes and branches, even the sending end-node and receiving-end nodes were not required if the nodes and branches are sequentially numbered. Nagaraju ***et al.*** [19] proposed a method for load-flow of radial distribution networks using sparse technique. But this method was only suitable for the sequentially numbered networks. If the network was not sequential numbered, manual work had to be done to make it sequentially numbered.

They used the 33-node distribution network and 69-node network given in Baran and Wu [20] to show the reliability of their approach. Hamouda and Zehar [21] proposed an algorithm for load-flow solution of radial distribution networks in which branch-to-node matrix was constructed and then inverse of this matrix was formed to obtain the node-to-branch network. From node-to-branch matrix a branch matrix, was formed. Hence this method needed ample amount of computational effort and computer memory to store the matrices.

2.3 Survey on line loadability index and voltage stability index of electric power distribution networks:

In the present era the cost of erection and up-gradation of the distribution system to cope-up the load demand, are increasing day by day. The cost of energy is also shooting up. The utilities are forced by the circumstances to operate the distribution systems near to its maximum capacity. In such operating conditions, a small disturbance can cause the voltage collapse in the system. So it is very urgent to mark the maximum loadability of the system and the margin between present operating point and the maximum loadability of the distribution system. In this concern some researchers proposed the voltage stability indices,

line loadability indices and loadability margin indices. Kwatny ***et al.*** [22] proposed the load-flow solution using bifurcation on the point of voltage stability limit. Chiang ***et al.*** [23] proposed that the voltage collapse was a dynamic phenomenon. Flatabo ***et al.*** [24] proposed an iterative method to check the sensitivity of the system. Load was increased till the operating limit of the system reached. Clark [25] and Gupta ***et al.*** [26] used the P-V or Q-V curves to show the stability limit of the system. Jasmon and Lee [27] derived the voltage stability index and shown that the voltage stability limit can be computed with the help of the voltage stability index. Jacobian matrix was used to derive the voltage stability index and the margin between the operating point and the voltage collapse limit had been shown with the help of voltage stability index by Hill ***et al.*** [28]. Sterling ***et al.*** [29] used the Thevenin's equivalent of the circuit to compute the stability limit of the circuit. Gubina and Strimcnik [30] reduced the radial distribution network into the two-bus equivalent model and derived the voltage stability index from the Jacobian matrix of the reduced model. Hong and Gau [31] proposed that the study of the S-V curve could depict the stability margins of the system. They applied Newton's optimal power flow method to study the S-V curve. Mohamed and Jasmon [32] used the bus clustering technique for the voltage stability analysis, because the buses of the same type behave in same manner so that a single bus could represent the group. Cutsem ***et al.*** [33] showed that the voltage stability analysis was very crucial under heavily loaded systems. They had studied the operating conditions for normal and contingency conditions. Moghavvemi and Faruque [34, 35] derived the line stability index from the receiving-end reactive power equation of the reduced two-bus equivalent of the distribution network. Chakravorty and Das [36] proposed a voltage stability index, which was derived from the bi-quadratic equation of the receiving-end voltage. It was shown that the discriminant of the equation will be zero at the critical point of voltage stability. Haque [37] used the Thevenin's equivalent of the network to derive the voltage stability limit. Chaturvedi

et al. [38] used the Kirchhoff's law to obtain the voltage equation for the derivation of the stability index. Kataoka ***et al.*** [39] proposed a voltage margin proximity index considering the voltage limits of the power system. They had shown the limit of the active power to be transmitted within the operating range of the voltage. Eminoglu ***et al.*** [40] proposed a bus stability index using bi-quadratic equation of the receiving-end voltage of the distribution system where the smallest value of the index showed the most sensitive bus in the system. Juan ***et al.*** [41] used the discriminant of voltage equation as the indicator of voltage stability of the bus was under consideration. Hamada ***et al.*** [42] proposed a voltage stability index that had linear change in index values with the change in load. Chen ***et al.*** [43] derived a voltage stability prediction index from the concept of P-V curve. They also proposed the stability margin of the distribution system. The improvement of voltage stability limit was discussed by Sakthivel and Mary [44]. Hosseini [45] proposed the contingency ranking and voltage stability analysis of power system efficiently with the help of neural networks.

2.4 Survey on optimal conductor size selection for electric power distribution networks:

Funk Houser [49] had proposed a method for economical conductor size selection for radial distribution network. They had assumed that the load was uniformly distributed throughout the network. A mathematical model had been developed by Ponnavaiko and Rao [50] for objective function, which was to be minimized. They considered the increase in cost of energy with time as well as the change in load factor etc. and used the dynamic programming method for decision making. A dynamic model for distribution networks had been proposed by Kirn and Adler [51]. In the optimal conductor size selection procedure, the annual revenue requirements and capital requirement for energy losses were considered. That method could not be employed on large sized system. Nagendra Rao [52] proposed a new algorithm

considering the same objective function as developed by Ponnavaiko and Rao [50]. The algorithm developed by Tram and Wall [53] based on realistic assumptions that was quite complicated. Hence software coding was a tedious task. But that method showed its limitations when used for large and complex distributions. Anders ***et al.*** [54] proposed a method for economical selection of cables analyzing various parameters necessarily to be considered, their effect on the economics was studied by sensitivity analysis. Leppert and Allen [55] proposed conductor selection procedure by considering load growth and wholesale power cost escalation along with the current capacity and voltage drop constraints.

Wang ***et al.*** [56] proposed a conductor size selection procedure with the combination of economical current density based method and heuristic approach method that showed the satisfactory results. Sivanagaraju ***et al.*** [57] proposed a method for selection of optimal conductor size for each branch of radial distribution network. In their method current carrying capacity as well as the minimum allowable voltage at the end nodes are taken as constraints and it was very much similar to Tram and Wall [53]. Kaur and Sharma [58] proposed a procedure for conductor size selection for radial distribution system using zero-one integer formulation of the system and formulated the skip rules to reduce the computational effort.

In the approach proposed by Kaur and Sharma [58] the method adopted for computation of voltage at each node was not clear because voltage at the nodes common for different routes would be different. The value, which would be the correct one, was not discussed. In a situation when the conductor placed in some branches were of the maximum size available in inventory and the receiving-end nodes of these branches violate the maximum voltage drop, the method suggested would upgrade the next branch where the upgradation was possible but this very branch might or might not be the right candidate branch for conductor upgradation. The term load factor has been misunderstood by the authors because it is the ratio of average load to the maximum load for a pre specified period of time. So the maximum load would

have to be served by the feeder for at least a minimum period of time. So the conductor sizes selected must be able to bear the peak load of the network. In their example of 123-node network, the proposed conductor sizes near the substation node would not be able to take that much load current.

Sivanagaraju ***et al.*** [57] proposed that the voltage of each node was to be checked against the minimum acceptable node voltage. Suppose an end node, or a node near the end node, violates the condition according to that approach, the conductor size of this very branch had to be upgraded. But practically it was seen that the branches at the end node were least responsible in voltage drop. So such upgradation of conductor was neither economically nor technically justified. The term load factor was also misunderstood by the authors of this paper.

The current carrying capacity of the conductor is not a constant parameter for a particular conductor, because the environment conditions and the heat generated in the conductor due to the current through it made the considerable change in the current carrying capacity. This fact has not been incorporated in any of the reported works.

In 11kV or of higher voltage feeders the connected loads were generally not the single load rather they were the group of load in the consumer premises or loads connected to 11kV/440V transformer. Usually these were not switched on simultaneously. Hence a load contribution factor was observed. Contribution factor was defined in Gonen [59]. In conductor size selection the effect of load contribution factor should be incorporated.

2.5 Survey on optimal capacitor placement for electric power distribution networks:

Reactive power compensation is an important aspect of the power distribution system, because power and energy loss reduction, power supply reliability, power quality, voltage

regulation, system capacity release can be achieved via it. The reactive power compensation is achieved with the application of shunt capacitors. Series compensation is seldom used at distribution level. As investment and benefits are associated with the reactive power compensation, so from early days of electrification many researchers and practicing engineers worked on the issue of reactive power compensation.

Initially the problem of capacitor placement was dealt for special cases with number of assumptions as proposed by Cook [60]. Duran [61] used the dynamic programming technique to deal with optimal capacitor placement problem and the capacitor sizes were taken as discrete values. Cook [62] and Chang [63] solved the capacitor placement problem by analytical approach via computer programming. Grainger and Lee [64] proposed an approach in which capacitor sizes were taken as continuous variables. They applied the non-linear programming, but the assumption to take the capacitor sizes as linear variable was unrealistic. Lee and Grainger [65] had considered the switched and fixed capacitors for reactive power compensation. Grainger and Lee [66] proposed a voltage dependent model for loss reduction and capacity release in distribution networks. Grainger ***et al.*** [67] suggested a real time switching scheme for reactive power control with switched capacitors. Ponnavaikko and Rao [68] considered the fixed and switched capacitors for compensation, capacity release and voltage improvement, while optimization of the load growth was also considered. Baran and Wu [7, 20] proposed a method for optimal reactive power compensation. They decomposed the problem as master and slave problem. Salama ***et al.*** [69] identified the sensitive node as the candidate nodes for capacitor placement with heuristics strategy. In their approach, they also considered the voltage regulator to be placed in the network. Chis ***et al.*** [70] used the heuristic approach for capacitor placement problem. Haque [71] proposed a method for loss reduction by capacitor placement that approach failed to recognize importance of cost and benefit constraints. Chiang ***et al.*** [72] suggested the global optimal solution using simulated

annealing for capacitor placement problem. Huang ***et al.*** [73] used tabu search algorithm and sensitivity analysis to identify the most suitable locations for capacitor placement. Miu ***et al.*** [74] used two-stage genetic algorithms (GA) and heuristic based algorithms for solving capacitor placement problems. Levitin ***et al.*** [75] proposed a genetic algorithms-based capacitor placement technique and also proposed a fast energy loss computation technique. Masoum ***et al.*** [76] used a Fuzzy approach for capacitor placement and sizing. They also considered the harmonics present due to non-linear loads. Das [77] proposed a Fuzzy-GA based method for capacitor sizing and location. Sarkar and Chakravorty [78] proposed an approach for capacitor placement in radial distribution networks to improve the voltage profile and loss minimization. They used the Genetic Algorithms to find the optimal location of capacitors. Goswami and Singh [79] used FACTS devices for reactive power control to minimize the voltage dip at the time of faults.

2.6 Survey on network reconfiguration for electric power distribution networks:

In earlier stage of network reconfiguration the problem was dealt to optimization of feeder cost at planning stage was proposed by Sun ***et al.*** [80]. Merlin and Back [81] proposed the network reconfiguration for loss reduction for distribution networks. The radial network was first converted to mesh by closing all the tie-lines and by applying branch-and-bound-type optimization technique for loss minimization so that the radial configuration was again restored. Shirmohammadi and Hong [82] proposed a technique for network reconfiguration by closing all the tie-lines first and followed the heuristic approach for optimization. However, they overcame some of the approximation made by Merlin and Back [81]. Borozan ***et al.*** [83] proposed a technique, which was not principally different from Shirmohammadi and Hong [82]. They incorporated in their methodology the real-time load estimation, effective determination of power loss configuration, and cost/benefit evaluation. Civanlar

et al. [84] used the heuristic approach for network reconfiguration but they proposed a branch-exchange technique to keep the network radial in nature throughout the procedure. They proposed that when a tie switch was closed a sectionalizing switch should be opened to keep the network radial. Baran and Wu [85] used the load-balance index and proposed the approximate load-flow method, which was used in network reconfiguration. Their method was an improvement of Civanlar ***et al.*** [84]. Lu ***et al.*** [86] proposed network reconfiguration for loss minimization in distribution networks. Taylor and Lubekaman [87] proposed a heuristic method for distribution network reconfiguration for loss reduction and capacity release of transformer and feeders. Chiang and Jean-Jumean [88, 89] and Jeon ***et al.*** [90] used simulated annealing algorithm for the reconfiguration. Wagner ***et al.*** [91] established that the heuristic approach could be used for real-time implementation for distribution network reconfiguration. Chen and Cho [92] suggested a branch-and-bound method for network reconfiguration by using binary integer programming for optimal switching scheme to loss minimization. Zhou ***et al.*** [93] used fuzzy technique and heuristic approach for optimization. They proposed network reconfiguration for service restoration and load balancing. They also proposed a method to minimize the operating cost of distribution network by reconfiguration. Taleski and Rajicic [94] suggested energy loss minimization by reconfiguration. Borozan and Rajakovic [95] proposed the application assessment for network reconfiguration. Lin and Chin [96] used voltage index, ohmic index, and decision index to determine the switching operation for network reconfiguration. Liu ***et al.*** [97] used the artificial–intelligence application for network reconfiguration. Nara ***et al.*** [98, 99] proposed network reconfiguration techniques for minimum loss using genetic algorithm (GA). Das [100] used the fuzzy multi objective approach using heuristic techniques for feeder reconfiguration.

Huang [101] presented an evolutionary genetic algorithm (EGA)-based fuzzy multi-objective approach to solve the network reconfiguration problem by maximizing the fuzzy satisfaction

in a radial distribution system. Savier and Das [102] proposed a quadratic-loss allocation scheme for allocating losses to consumers connected to a radial distribution system before and after reconfiguration. The algorithm used was based on heuristic rule and fuzzy multi-objective approach. Bouhouras and Labridis [103] investigated the effect of load alterations in distribution systems on optimal configurations for loss minimization. The network reconfigurations were implemented utilizing heuristics techniques while load variations were simulated by stochastic procedures. Miu ***et al.*** [104] used the network reconfiguration for service restoration of radial distribution network in the environment of majority of manually operated switches. Kashem ***et al.*** [105] proposed an approach to use network reconfiguration for enhancement of voltage stability. Venkatesh ***et al.*** [106] proposed a fuzzy adaptation of the evolutionary programming algorithm for optimal reconfiguration due to the discrete nature of the problem for radial distribution networks to maximize loadability. González ***et al.*** [107] presented a heuristic reconfiguration algorithm to minimize the Non-Delivered Power of distribution networks. The thermal limits and radial nature of the network were taken as constraints.

Amanulla ***et al.*** [108] used the binary particle swarm optimization-based search algorithm for maximizing the reliability and minimizing the power losses. Load point reliability was evaluated by probabilistic reliability models. Zin ***et al.*** [109] proposed a heuristic approach for reconfiguration of radial distribution networks for minimizing the branch current. Gomes ***et al.*** [110] proposed a technique for network reconfiguration to achieve optimum power flow. All the switches were considered closed and a heuristic procedure was adopted to open the appropriate switches to maintain the radial nature of the network. Sarma ***et al.*** [111] used the reconfiguration for immediate service restoration. The candidate loads were identified by specially designed algorithm. Hong and Ho [112] proposed a method for network reconfiguration using genetic algorithms for minimizing the power loss in normal operating

conditions and minimizing the voltage drop in fault conditions. The problem was formulated as multi-objective fuzzy problem.

Fan ***et al.*** [113] formulated the problem as a nonlinear integer optimization problem and made it linear. They applied intuitive heuristic approach for solution. Sua ***et al.*** [114] suggested an ant colony search algorithm to solve the optimal network reconfiguration problem for power loss reduction using positive feedback as well as greedy search to reach the final solution. Chakravorty and Ghosh [115] investigated the effect of different configuration of distribution feeder on the reliability and contingency behavior. Remesh ***et al.*** [116] investigated the effect of different techniques on the loss minimization. They used network reconfiguration as a tool for loss minimization.

Rao and Narasimham [117] used the heuristic approach to suggest the best combination of switching arrangement for loss minimization. They reduced the computational effort by choosing first the tie switches having large voltage difference. Khodr ***et al.*** [118] used a specific approach of the Generalized Benders decomposition algorithm for reconfiguration to achieve loss minimization and load balancing in distribution networks within the applied constraints of current limit and voltage limit. Oliveira ***et al.*** [119] proposed a solution technique by using a mixed integer non-linear programming approach, in which a continuous function was used to handle the discrete variables. The primal–dual interior point technique was applied to solve the optimization problem at each step. The Lagrange multipliers were used to evaluate a new proposed sensitivity index for distribution system reconfiguration. Kumar and Jayabarathi [120] proposed a method based on bacterial foraging optimization algorithm for distribution network reconfiguration for loss minimization. They formulated the problem as non-linear optimization problem. The radial nature of the network was finally restored.

In all the above discussed reported work on network reconfiguration, the problem was dealt with lot of flexibility. But in practical distribution networks the chances of network reconfiguration are very limited because the distribution networks are erected in the residential, commercial, industrial areas etc. The feeders may or may not be touching each other and even some times the tie-lines cannot be stretched from any one point to another point due to various constraints. So the application of optimization techniques is not justified in this case as it leads to only theoretical exercise. However, in spite of all these constraints, still network reconfiguration is considered to optimize the available capacity of the distribution network.

CHAPTER 3

LOAD-FLOW SOLUTION FOR RADIAL ELECTRIC POWER DISTRIBUTION NETWORKS

3.1. Introduction:

Load-flow is an important aspect of study, analysis, planning and design of electric power distribution network. To study the above said aspects of distribution network the node voltage and its angle, branch current, real power loss and reactive power loss etc. are needed. The accuracy and reliability of study, analysis and planning of distribution network depends upon the accuracy and efficiency of load-flow method. So load-flow solution method should be efficient, reliable and should require less memory space of computer. The main aim of the chapter is to propose a new method for load-flow solution of radial distribution networks. The following features are incorporated in the proposed load-flow method.

1. No sequential numbering of nodes is required. So one or more load points can be added or eliminated from the network without the requirement of renumbering of nodes. Considerable effort for data preparation is reduced.
2. No need to store the nodes beyond the branch, the branch to node incident matrix. So the computer memory requirement is considerably reduced.
3. This method gives node voltages as well as their angle and can handle the effect of charging capacitances of the network. So this method can be used for reactive power compensation studies.

The proposed method has been tested with different types of load modeling and convergence has been obtained satisfactorily.

3.2. Assumptions:

It is assumed that the three-phase radial distribution networks are balanced and can be represented by their equivalent single-line diagrams. Line shunt capacitances are considered even at the distribution voltage levels.

3.3. Formulation of load-flow method:

Figure 3.1 shows the electrical equivalent of the radial distribution system. It is assumed that the charging capacitance of each branch is lumped at the receiving-end node of that branch.

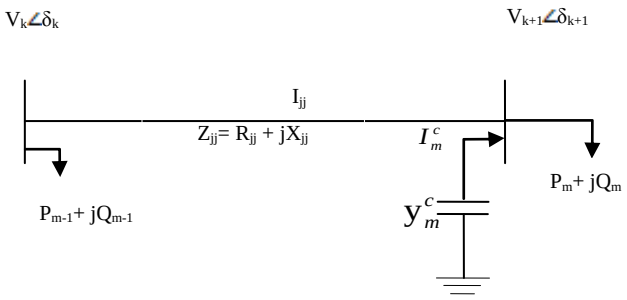

Fig.3.1 Two-bus equivalent of distribution network

3.3.1. Derivation of expression of magnitude of voltage and angle of the voltage at each node:

The sending-end voltage can be related to the receiving-end voltage as:

$$V_k\angle\delta_k = V_{k+1}\angle\delta_{k+1} + I_{jj}Z_{jj} \tag{3.1}$$

The current through a particular branch is the sum of all load currents due to the loads connected to the nodes minus the charging current due to line shunt capacitances beyond that branch and the receiving-end node of that very branch.

$$I_{jj} = \sum_{m=k+1}^{N}\left[\left(\frac{P_m - jQ_m}{V_m\angle -\delta_m}\right) + \; j\; V_m\angle\delta_m \;\; y_m^c\right] \tag{3.2}$$

$$I_{jj} = I_{jj}^{a} + jI_{jj}^{r} \tag{3.3}$$

$$I_{jj}^{a} = \sum_{m=k+1}^{N} \left\{ \frac{P_m \cos\delta_m + \ Q_m - V_m^2 y_m^c \ \sin\delta_m}{V_m} \right\} \tag{3.4}$$

$$I_{jj}^{r} = \sum_{m=k+1}^{N} \left\{ \frac{P_m \sin\delta_m - \ Q_m - V_m^2 y_m^c \ \cos\delta_m}{V_m} \right\} \tag{3.5}$$

Real and imaginary parts of the node current can be expressed as

$$I_m^a = \frac{P_m \cos\delta_m + \ Q_m - V_m^2 y_m^c \ \sin\delta_m}{V_m} \tag{3.6}$$

$$I_m^r = \frac{P_m \sin\delta_m - \ Q_m - V_m^2 y_m^c \ \cos\delta_m}{V_m} \tag{3.7}$$

Let $Q_m^{'} = Q_m - V_m^2 y_m^c$ (3.8)

Here P_m and Q_m, are the real and reactive loads connected to the m th node. V_m and δ_m are the voltage and its angle respectively at m th node. I_{jj}^{a} and I_{jj}^{r} are active and reactive components of the branch current (I_{jj}). If the lengths of branches of the distribution system are considerably small compared to transmission system, the value of y_m^c will be very low. In Eq. (3.2), the charging current will also be zero. Hence the proposed method can be applied to both the cases either the charging currents are considered or neglected.

The voltage drop in each branch can be expressed by

$$I_{jj} Z_{jj} = \ I_{jj}^{a} + jI_{jj}^{r} \quad R_{jj} + jX_{jj} \tag{3.9}$$

So Eq. (3.1) can be expressed as

$$V_{k+1}\angle\delta_{k+1} = V_k\angle\delta_k - \ I_{jj}^{a} + jI_{jj}^{r} \quad R_{jj} + jX_{jj} \tag{3.10}$$

For the simplicity, the following are considered

$$C_{jj} = I_{jj}^{a} R_{jj} - I_{jj}^{r} X_{jj} \tag{3.11}$$

$$D_{jj} = I_{jj}^{a} X_{jj} + I_{jj}^{r} R_{jj} \tag{3.12}$$

$$V_{k+1} \cos \delta_{k+1} + j \sin \delta_{k+1} = V_k \cos \delta_k + j \sin \delta_k - C_{jj} + j D_{jj} \tag{3.13}$$

Separating real and imaginary parts of Eq. (3.13), we have

$$V_{k+1} \cos \delta_{k+1} = V_k \cos \delta_k - C_{jj} \tag{3.14}$$

$$V_{k+1} \sin \delta_{k+1} = V_k \sin \delta_k - D_{jj} \tag{3.15}$$

Squaring on both sides of Eq. (3.14) and Eq. (3.15), we have after addition

$$V_{k+1}^2 + 2V_{k+1}(C_{jj} \cos \delta_{k+1} + D_{jj} \sin \delta_{k+1}) + (C_{jj}^{\ 2} + D_{jj}^{\ 2} - V_k^2) = 0 \tag{3.16}$$

It is a quadratic equation of V_{k+1} and V_{k+1} can be computed as

$$V_{k+1} = \frac{-2(C_{jj} \cos \delta_{k+1} + D_{jj} \sin \delta_{k+1})}{2} \pm \frac{\sqrt{2(C_{jj} \cos \delta_{k+1} + D_{jj} \sin \delta_{k+1})^{\ 2} - 4(C_{jj}^{\ 2} + D_{jj}^{\ 2} - V_k^2)}}{2} \tag{3.17}$$

i.e. $$V_{k+1} = -(C_{jj} \cos \delta_{k+1} + D_{jj} \sin \delta_{k+1}) \pm \sqrt{(C_{jj} \cos \delta_{k+1} + D_{jj} \sin \delta_{k+1})^2 - (C_{jj}^{\ 2} + D_{jj}^{\ 2} - V_k^2)} \tag{3.18}$$

Since the receiving-end voltage has positive value, the following root is considered.

$$V_{k+1} = -(C_{jj} \cos \delta_{k+1} + D_{jj} \sin \delta_{k+1}) + \sqrt{(C_{jj} \cos \delta_{k+1} + D_{jj} \sin \delta_{k+1})^2 - (C_{jj}^{\ 2} + D_{jj}^{\ 2} - V_k^2)} \tag{3.19}$$

Divide Eq. (3.15) by Eq. (3.14) we have,

$$\delta_{k+1} = \tan^{-1}\left(\frac{V_k \sin \delta_k - D_{jj}}{V_k \cos \delta_k - C_{jj}}\right) \tag{3.20}$$

3.3.2. Formulation of power losses:

From Eq. (3.2) and Eq. (3.8) we have,

$$I_{jj}^2 = I_{jj} I_{jj}^* = (I_{jj}^a + jI_{jj}^r)(I_{jj}^a - jI_{jj}^r) = \sum_{m=k+1}^{N}\left(\frac{P_m^2 + Q'^2_m}{V_m^2}\right) \tag{3.21}$$

From Eq. (3.6) and Eq. (3.7), we have

$$I_m^2 = I_m I_m^* = (I_m^a + jI_m^r)(I_m^a - jI_m^r) = \left(\frac{P_m^2 + Q'^2_m}{V_m^2} \right) \quad (3.22)$$

Real power loss of branch-jj

$$= \left(\sum_{m=k+1}^{N} \frac{P_m^2 + Q'^2_m}{V_m^2} \right) R_{jj} \quad (3.23)$$

Reactive power loss of branch-jj

$$= \left(\sum_{m=k+1}^{N} \frac{P_m^2 + Q'^2_m}{V_m^2} \right) X_{jj} \quad (3.24)$$

Total real power loss of the network

$$= \sum_{jj=1}^{N-1} \left(\sum_{m=k+1}^{N} \frac{P_m^2 + Q'^2_m}{V_m^2} \right) R_{jj} \quad (3.25)$$

Total reactive power loss of the network

$$= \sum_{jj=1}^{N-1} \left(\sum_{m=k+1}^{N} \frac{P_m^2 + Q'^2_m}{V_m^2} \right) X_{jj} \quad (3.26)$$

3.4. Load modelling:

In constant power type of load model, the power demand of the load remains same irrespective to the change in terminal voltage. This is not true for most of the loads. Power demand changes with the change of terminal voltage of the loads. Due to the change in power demand of the loads with the change in terminal voltage, there is a worth noting effect on the convergence of the load-flow solution. The characteristics of exponential load models can be expressed as:

$$P = P_0 \left(\frac{V}{V_0} \right)^{n_p} \quad (3.27)$$

$$Q = Q_0 \left(\frac{V}{V_0} \right)^{n_q} \tag{3.28}$$

Here P_0 and Q_0 in Eq. (3.27) and Eq. (3.28) for active and reactive power respectively at nominal voltage, V and V_0 stand for node voltage and nominal load voltage respectively and n_p and n_q are the respective load exponents for real and reactive power. The values of the load exponents for various types of load used by Eminoglu and Hocaoglu [16] have been presented in Table 3.1.

Table 3.1 The values of the load exponents for various types of loads [16].

Sr. No.	Type of load	n_p	n_q
1	Battery charge	2.59	4.06
2	Fluorescent lamps.	2.07	3.21
3	Constant impedance	2.00	2.00
4	Air conditioner	0.50	2.50
5	Constant current	1.00	1.00
6	Resistance space heater	2.00	0.00
7	Pumps, fans other motors	0.08	1.60
8	Incandescent lamps	1.54	0.00
9	Compact fluorescent lamps	1.00	0.35
10	Small industrial motors	0.10	0.60
11	Large industrial motors	0.05	0.50
12	Constant power	0.00	0.00
13	Composite load = 30% constant power + 30% constant current + 40% constant impedance load.		
14	Practical load = Battery Charge 2% + Fluorescent lamps 11% + AC 8% + resistance space heating 5% + Pump, fans and other motors 18% + CFL 5% + Incandescent lamp 6% + Small motors 25% + Large motors 20%.		

3.5 Solution methodology:

For the load-flow solution of radial distribution network either sequential numbering scheme is adopted or non-sequential numbering scheme is followed. At first a two-dimensional array is formed through computer program, which contains the node number of link node between two interlinked laterals and the node number of first node of the linked

lateral in its each row. Next the arrays storing lateral node numbers are formed. The number of laterals' arrays is equal to the number of laterals present in the network. Main feeder, laterals and sub-laterals all are consider as laterals. Once the lateral arrays are formed, the load-flow solution can be easily carried out.

3.5.1. Formation of lateral arrays:

For any type of numbering scheme, sequential or non-sequential the following steps are used.

1. Read the sending-end nodes and receiving-end nodes.

2. Define an array JN[ ][ ] to store the junction nodes. It's a two dimensional array.

3. For every sending end node check if it appear more than once. For each repeated entry store the repeated node and its receiving end node in successive rows of the JN[ ][ ] array. The number of rows of the JN [ ][ ] array shows the number of lateral of the network.

4. Start from the substation node. Define a lateral array and put the substation node number as the first entry in the array. Check if the latest node stored in the array is the sending-end node of the next branch if YES put receiving-end node of this branch as the next entry in the lateral array. Repeat it till the condition is NO.

5. Define a lateral array to store the node numbers of the lateral. Put node numbers stored in the row under consideration of JN[ ][ ].

6. Check if last node in lateral array is the sending end node of the next branch. If YES, put receiving-end node of this branch in the lateral array and repeat step 6. If NO, go to step 5 and repeat the above procedure till all the rows of JN[ ][ ] are considered.

The detailed procedure presented in the flow-chart of the above procedure shown in Fig. 3.2.

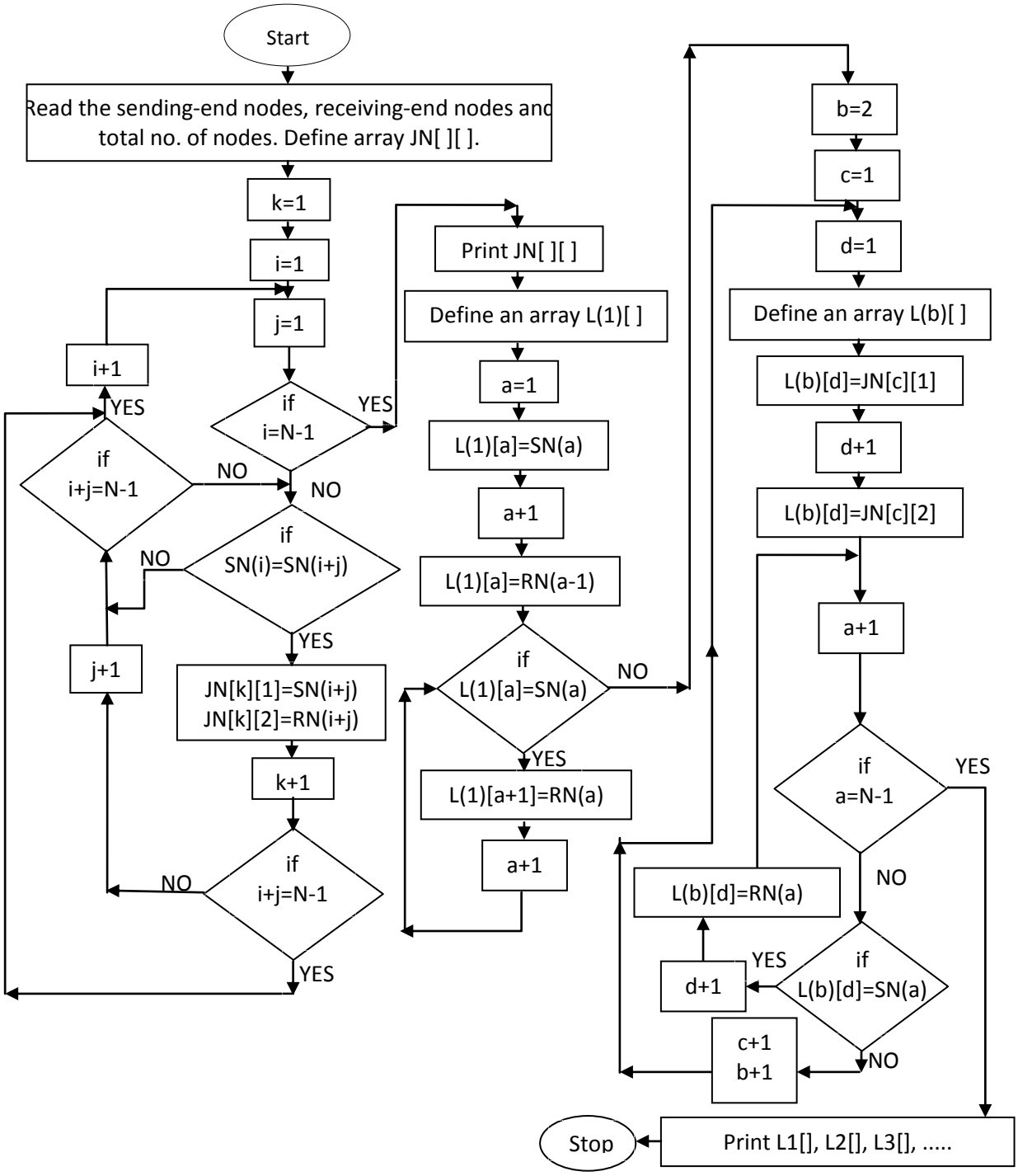

Fig. 3.2 Flow Chart for formation of lateral array

3.5.2. Load-flow solution:

Start from the first lateral and its first branch.

1. Consider a lateral. Compute the node current, for each of its nodes after the branch under consideration.

2. During computation of the node current it is checked whether the node under consideration is the source node of any other array. If YES, go to step 3.

3. Store first two nodes of the linked array in LN[ ][ ] array.

4. Consider the array that's first two nodes are stored in LN[ ][ ] and repeat steps 1-3 till all the entries of LN[ ][ ] are considered.

5. Compute voltage and its angle for the receiving-end node of the branch under consideration.

6. Steps 1-4 are repeated for each branch of the network.

7. Repeat the above procedures till the convergence of the load-flow solution is occurred.

8. Print the results.

The detailed procedure of the above steps is shown in Fig 3.3.

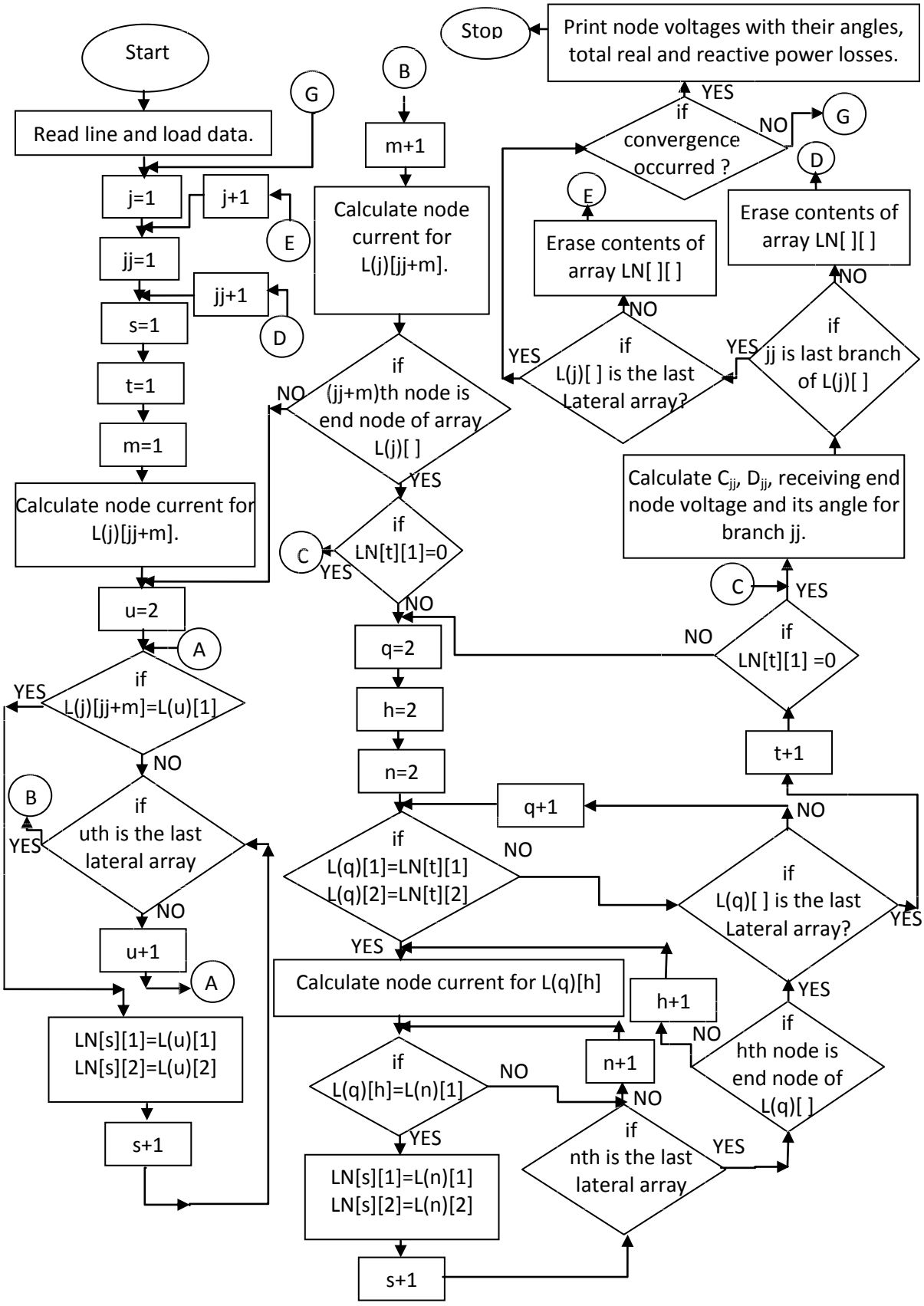

Fig. 3.3 Flow Chart for load-flow solution

3.6 Convergence criteria:

The difference of the voltage computed for any node in two successive iterations should be less than 0.00001 or 10^{-5}. Proof of convergence of load-flow solution is shown in **Appendix-A** for the proposed method.

3.7 Application of the proposed method:

To show the effectiveness of the proposed method three examples, 33-node, 69-node and 41-node radial distribution system have been considered. In first example (33-node) and second example (69-node) constant power load is considered and the effect of line shunt capacitance has been neglected. The results are compared with the existing methods. Third example (41-node) is taken to show the effect of load characteristics on convergence of load-flow solution for various types of loads and to show the effect of charging capacitances. The line data and load data of 33- node radial distribution network (Example 1) is available in Baran and Wu [7], which are shown in **Appendix-B**. Single line diagram of 33-node distribution network is shown in Fig. 3.4. The base kV and base MVA values are 12.66 kV and 100 MVA respectively. The load-flow results of 33-node radial distribution network obtained by proposed method are compared with the existing method proposed by Hamouda and Zehar [21], which is shown in Table 3.2.

The line data and load data of 69- node radial distribution network (Example 2) are available in Baran and Wu [20]. The line data and load data have been shown in **Appendix-C**. Single line diagram of 69-node distribution network is shown in Fig. 3.5. The base kV and base MVA values are 12.66 kV and 100 MVA respectively. The load-flow results are compared with the existing method proposed by Satyanarayana ***et al.*** [17] and have been presented in Table 3.3. Real and reactive power losses are also presented in Table 3.3. Third example is

41-node radial distribution network shown in Fig. 3.6. Line data and load data of 41-node distribution system are shown in **Appendix-D**. The technical data regarding conductors of 41-node distribution system is shown in Table D2 in **Appendix-D**. The base kV and base MVA values are 11 kV and 100 MVA respectively. Load-flow solutions have been carried out for various types of loads without considering the capacitance of the branches. The load-flow results of 41-node distribution network for different load modellings have been shown in Table 3.4, Table 3.5, Table 3.6, Table 3.7, Table 3.8 and Table 3.9. Only the magnitude of voltage and its angle, which are minimum values, are shown in Table 3.10. The corresponding node number is 13. The number of iterations required for the convergence of load-flow solution, real and reactive power losses for various types of loads are also presented in Table 3.10. Composite load consist of 30% of constant power load, 30% of constant current load and 40% of constant impedance load. Practical load consists of Battery Charge (2%) + Fluorescent lamps (11%) + AC (8%) + Resistance space heating (5%) + Pump, fans and other motors (18%) + CFL (5%) + Incandescent lamp (6%) + Small motors (25%) + Large motors (20%).

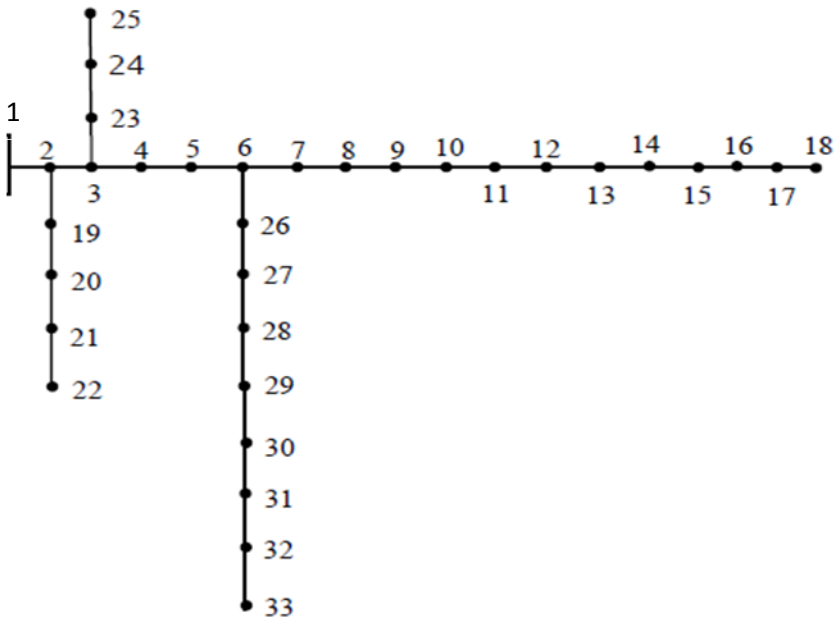

Fig. 3.4 Single line diagram of 33-node distribution network.

Table 3.2 The load-flow results of 33-node distribution network.

Node No.	Proposed method		Existing Method [21].	
	Voltage magnitude (p.u.)	Voltage angle in radian	Voltage magnitude (p.u.)	Voltage angle in radian
1	1.000000	0.000000	1.000000	0.000000
2	0.997015	0.000238	0.997170	0.000218
3	0.982882	0.001673	0.983040	0.001652
4	0.975373	0.002827	0.975566	0.002799
5	0.967946	0.003999	0.968170	0.003964
6	0.949468	0.002356	0.949754	0.002323
7	0.945943	-0.001688	0.946236	-0.001713
8	0.932287	-0.004367	0.932605	-0.004390
9	0.925955	-0.005667	0.926279	-0.005690
10	0.920097	-0.006789	0.920426	-0.006811
11	0.919229	-0.006660	0.919558	-0.006682
12	0.917714	-0.006455	0.918044	-0.006478
13	0.911538	-0.008081	0.911872	-0.008102
14	0.909248	-0.009482	0.909583	-0.009503
15	0.907821	-0.010153	0.908157	-0.010173
16	0.906439	-0.010568	0.906775	-0.010587
17	0.904391	-0.011944	0.904728	-0.011963
18	0.903778	-0.012115	0.904115	-0.012133
19	0.996486	0.000049	0.996584	0.000016
20	0.992909	-0.001120	0.993007	-0.001151
21	0.992204	-0.001458	0.992303	-0.001489
22	0.991567	-0.001813	0.991665	-0.001844
23	0.979297	0.001132	0.979486	0.001129
24	0.972625	-0.000417	0.972816	-0.000418
25	0.969300	-0.001179	0.969492	-0.001181
26	0.947539	0.003045	0.947870	0.003004
27	0.944974	0.004025	0.945310	0.003983
28	0.933532	0.005474	0.933883	0.005430
29	0.925312	0.006834	0.925669	0.006790
30	0.921754	0.008672	0.922113	0.008626
31	0.917592	0.007198	0.917952	0.007154
32	0.916676	0.006796	0.917037	0.006752
33	0.916392	0.006661	0.916754	0.006617

Power losses using the proposed method

Active power losses	Reactive power losses
205.25kW	**139.31kVAr**

Power losses using the existing method [21]

Active power losses	Reactive power losses
205.19kW	**139.23kVAr**

The ratio of CPU time of proposed the method with the existing method [21] is 1: 1.25.
The ratio of memory requirement of proposed the method with the existing method [21] is 1: 1.98.

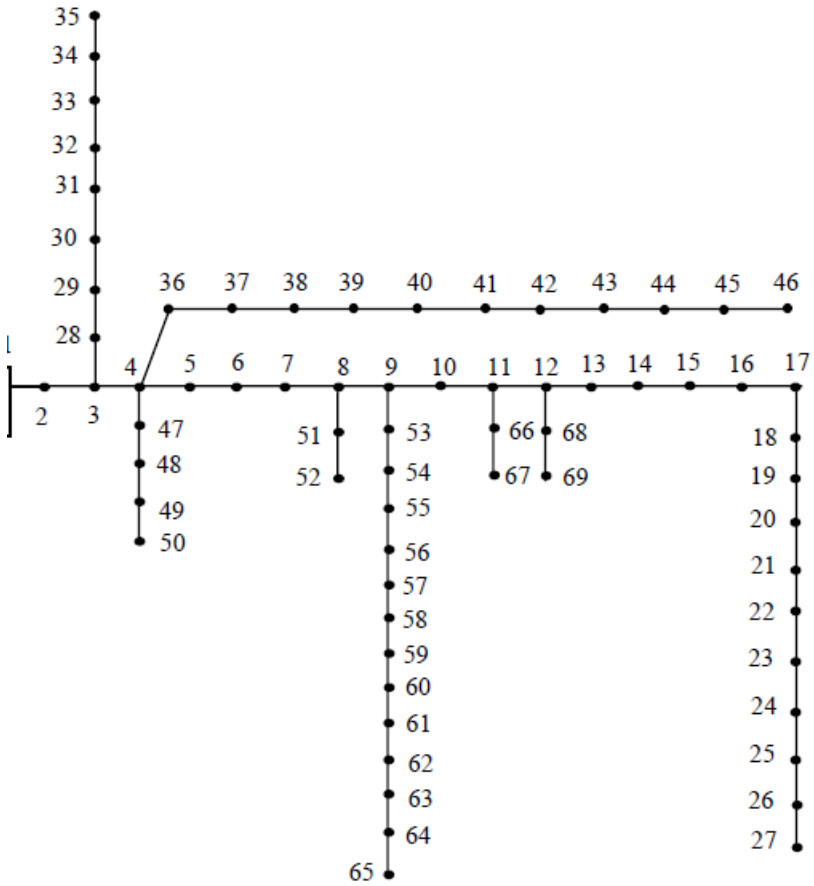

Fig. 3.5 Single line diagram of 69-node distribution network.

Table 3.3 The load-flow results of 69-node distribution system.

Node No.	Proposed Method		Existing Method [17]
	Voltage magnitude (p.u.)	Voltage angle in radian	Voltage magnitude (p.u.)
1	1.000000	0.000000	1.00000
2	0.999967	-0.000021	0.99997
3	0.999933	-0.000043	0.99993
4	0.999840	-0.000103	0.99984
5	0.999022	-0.000325	0.99902
6	0.990097	0.000840	0.99010
7	0.980813	0.002074	0.98082
8	0.978634	0.002364	0.97861
9	0.978291	0.002409	0.97748
10	0.973295	0.003873	0.97250
11	0.972249	0.004182	0.97140
12	0.969410	0.004999	0.96824
13	0.966491	0.005805	0.96533
14	0.963597	0.006611	0.96243
15	0.960732	0.007411	0.95957
16	0.960200	0.007560	0.95904
17	0.959321	0.007807	0.95816
18	0.959312	0.007809	0.95815
19	0.958848	0.007958	0.95769
20	0.958551	0.008054	0.95739
21	0.958070	0.008209	0.95691
22	0.958063	0.008211	0.95690
23	0.957991	0.008235	0.95683
24	0.957835	0.008285	0.95667
25	0.957666	0.008340	0.95650
26	0.957596	0.008362	0.95643
27	0.957577	0.008369	0.95641
28	0.999927	0.008365	0.99993
29	0.999859	0.008329	0.99986
30	0.999763	0.008375	0.99976
31	0.999746	0.008383	0.99975
32	0.999661	0.008423	0.99966
33	0.999457	0.008517	0.99946
34	0.999228	0.008655	0.99923
35	0.999161	0.008673	0.99916
36	0.999920	0.008664	0.99992
37	0.999748	0.008553	0.99975
38	0.999589	0.008510	0.99959

39	0.999543	0.008498	0.99954
40	0.999541	0.008498	0.99954
41	0.998843	0.008306	0.99884
42	0.998551	0.008225	0.99855
43	0.998512	0.008214	0.99851
44	0.998504	0.008211	0.99850
45	0.998406	0.008180	0.99841
46	0.998405	0.008180	0.99841
47	0.999790	0.008148	0.99979
48	0.998544	0.007365	0.99854
49	0.994693	0.004938	0.99470
50	0.994148	0.004592	0.99415
51	0.980777	0.004597	0.97857
52	0.980768	0.004600	0.97856
53	0.975851	0.004981	0.97469
54	0.972612	0.005427	0.97145
55	0.968144	0.006047	0.96697
56	0.963781	0.006656	0.96261
57	0.941293	0.013560	0.94013
58	0.930236	0.017086	0.92908
59	0.925963	0.018496	0.92480
60	0.920942	0.020315	0.91978
61	0.913553	0.021517	0.91238
62	0.913264	0.021564	0.91209
63	0.912877	0.021627	0.91170
64	0.910979	0.021938	0.90980
65	**0.910405**	**0.022032**	**0.90923**
66	0.973238	0.022053	0.97134
67	0.973238	0.022054	0.97134
68	0.971919	0.022158	0.96791
69	0.971918	0.022159	0.96791

Power losses using the proposed method Active power losses Reactive power losses **224.5695kW** **101.0474kVAr**	Power losses using the existing method [17] Active power losses Reactive power losses **224.63kW** **101.99kVAr**

The ratio of CPU time of proposed the method with the existing method [17] is 1: 1.89.

The ratio of memory requirement of proposed the method with the existing method [17] is 1: 1.98.

Table 3.4 Load-flow results of various types of load (Sr. No. 1, 2, 4 of Table 3.1) for 41-node distribution system

Load Type	Battery charge		Fluorescent lamp		Air conditioner	
Node	Voltage magnitude (p.u.)	Voltage angle	Voltage magnitude (p.u.)	Voltage angle	Voltage magnitude (p.u.)	Voltage angle
1	1.00000	0.00000	1.00000	0.00000	1.00000	0.00000
27	0.99071	-0.00482	0.99046	-0.00489	0.99000	-0.00533
35	0.97705	-0.00804	0.97642	-0.00812	0.97517	-0.00904
8	0.96609	-0.00991	0.96509	-0.00996	0.96305	-0.01132
33	0.95859	-0.01122	0.95733	-0.01127	0.95472	-0.01294
20	0.95277	-0.01228	0.95130	-0.01232	0.94818	-0.01428
39	0.94658	-0.01343	0.94486	-0.01345	0.94121	-0.01574
4	0.94162	-0.01437	0.93971	-0.01439	0.93560	-0.01695
34	0.93860	-0.01496	0.93656	-0.01496	0.93217	-0.01770
32	0.93373	-0.01591	0.93148	-0.01591	0.92664	-0.01893
16	0.92926	-0.01592	0.92682	-0.01588	0.92149	-0.01909
21	0.92734	-0.01546	0.92482	-0.01537	0.91926	-0.01861
17	0.92595	-0.01497	0.92338	-0.01485	0.91765	-0.01809
18	0.97936	-0.01698	0.97877	-0.01683	0.97759	-0.02052
22	0.97086	-0.01839	0.97004	-0.01823	0.96835	-0.02221
11	0.96215	-0.01989	0.96107	-0.01971	0.95880	-0.02402
13	0.95779	-0.02066	0.95657	-0.02047	0.95401	-0.02497
14	0.95278	-0.02156	0.95139	-0.02137	0.94847	-0.02608
40	0.94929	-0.02152	0.94780	-0.02129	0.94462	-0.02610
6	0.94677	-0.02149	0.94519	-0.02124	0.94182	-0.02612
12	0.94389	-0.02044	0.94222	-0.02014	0.93860	-0.02502
15	0.98551	-0.02129	0.98516	-0.02098	0.98451	-0.02598
30	0.98337	-0.02162	0.98299	-0.02131	0.98227	-0.02634
29	0.97811	-0.02145	0.97766	-0.02111	0.97678	-0.02620
41	0.97442	-0.02046	0.97391	-0.02010	0.97289	-0.02520
28	0.97218	-0.01987	0.97164	-0.01948	0.97052	-0.02459
2	0.96974	-0.01896	0.96916	-0.01855	0.96794	-0.02365
26	0.97292	-0.01884	0.97221	-0.01841	0.97080	-0.02357
24	0.96800	-0.01754	0.96722	-0.01706	0.96558	-0.02224
23	0.96475	-0.01633	0.96390	-0.01581	0.96211	-0.02099
37	0.96458	-0.01578	0.96356	-0.01524	0.96143	-0.02041
10	0.95529	-0.01458	0.95396	-0.01398	0.95112	-0.01916
5	0.95316	-0.01380	0.95177	-0.01317	0.94878	-0.01835
9	0.95190	-0.01335	0.95048	-0.01269	0.94739	-0.01787
3	0.94541	-0.01292	0.94367	-0.01225	0.93993	-0.01743
36	0.93219	-0.01237	0.92989	-0.01166	0.92490	-0.01684
31	0.92685	-0.01152	0.92432	-0.01075	0.91872	-0.01593
38	0.92621	-0.01112	0.92364	-0.01032	0.91795	-0.01551
7	0.94987	-0.01011	0.94837	-0.00922	0.94509	-0.01442
19	0.98160	-0.00947	0.98117	-0.00855	0.98031	-0.01375
25	0.97175	-0.00903	0.97104	-0.00810	0.96959	-0.01330

Table 3.5 Load-flow results of various types of load (Sr. No. 6, 7 of Table 3.1) for 41-node distribution system

Load type	Resistance space heater		Pump, funs other motors	
Node No.	Voltage magnitude (p.u.)	Voltage angle	Voltage magnitude (p.u.)	Voltage angle
1	1.00000	0.00000	1.00000	0.00000
27	0.98967	-0.00455	0.98968	-0.00540
35	0.97463	-0.00697	0.97438	-0.00908
8	0.96239	-0.00792	0.96180	-0.01130
33	0.95397	-0.00857	0.95314	-0.01289
20	0.94736	-0.00904	0.94632	-0.01419
39	0.94030	-0.00953	0.93904	-0.01562
4	0.93461	-0.00991	0.93316	-0.01680
34	0.93114	-0.01014	0.92957	-0.01753
32	0.92552	-0.01052	0.92376	-0.01874
16	0.92044	-0.00985	0.91837	-0.01881
21	0.91831	-0.00900	0.91603	-0.01827
17	0.91681	-0.00821	0.91435	-0.01769
18	0.97716	-0.00928	0.97686	-0.02007
22	0.96784	-0.01007	0.96732	-0.02172
11	0.95820	-0.01087	0.95746	-0.02348
13	0.95335	-0.01126	0.95249	-0.02440
14	0.94775	-0.01170	0.94674	-0.02549
40	0.94393	-0.01128	0.94276	-0.02546
6	0.94116	-0.01096	0.93987	-0.02544
12	0.93809	-0.00948	0.93654	-0.02426
15	0.98415	-0.01008	0.98408	-0.02520
30	0.98191	-0.01033	0.98181	-0.02556
29	0.97643	-0.00992	0.97624	-0.02539
41	0.97260	-0.00871	0.97228	-0.02435
28	0.97028	-0.00797	0.96989	-0.02371
2	0.96776	-0.00688	0.96726	-0.02274
26	0.97028	-0.00653	0.96993	-0.02263
24	0.96517	-0.00487	0.96462	-0.02123
23	0.96179	-0.00338	0.96108	-0.01993
37	0.96081	-0.00268	0.96015	-0.01932
10	0.95049	-0.00109	0.94945	-0.01800
5	0.94824	-0.00005	0.94705	-0.01713
9	0.94692	0.00057	0.94562	-0.01662
3	0.93906	0.00115	0.93771	-0.01615
36	0.92386	0.00195	0.92196	-0.01551
31	0.91782	0.00330	0.91547	-0.01451
38	0.91708	0.00395	0.91466	-0.01404
7	0.94458	0.00561	0.94321	-0.01284
19	0.98003	0.00650	0.97980	-0.01212
25	0.96909	0.00699	0.96870	-0.01166

Table 3.6 Load-flow results of various types of load (Sr. No. 8, 9, 10 of Table 3.1) for 41-node distribution system

Load type	Incandescent lamps		Compact fluorescent lamps		Small industrial motors	
Node No.	Voltage magnitude (p.u.)	Voltage angle	Voltage magnitude (p.u.)	Voltage angle	Voltage magnitude (p.u.)	Voltage angle
1	1.00000	0.00000	1.00000	0.00000	1.00000	0.00000
27	0.98957	-0.00470	0.98955	-0.00492	0.98941	-0.00528
35	0.97435	-0.00730	0.97423	-0.00785	0.97376	-0.00869
8	0.96192	-0.00842	0.96168	-0.00930	0.96086	-0.01060
33	0.95336	-0.00919	0.95304	-0.01031	0.95197	-0.01196
20	0.94663	-0.00976	0.94623	-0.01110	0.94495	-0.01306
39	0.93944	-0.01038	0.93896	-0.01196	0.93744	-0.01426
4	0.93364	-0.01087	0.93310	-0.01265	0.93138	-0.01525
34	0.93010	-0.01117	0.92952	-0.01308	0.92767	-0.01587
32	0.92437	-0.01165	0.92372	-0.01378	0.92166	-0.01688
16	0.91917	-0.01106	0.91842	-0.01337	0.91612	-0.01673
21	0.91698	-0.01023	0.91617	-0.01262	0.91374	-0.01606
17	0.91542	-0.00945	0.91457	-0.01189	0.91203	-0.01539
18	0.97689	-0.01069	0.97676	-0.01347	0.97630	-0.01745
22	0.96744	-0.01160	0.96724	-0.01460	0.96656	-0.01889
11	0.95767	-0.01252	0.95738	-0.01577	0.95647	-0.02042
13	0.95275	-0.01299	0.95242	-0.01637	0.95138	-0.02121
14	0.94706	-0.01352	0.94668	-0.01707	0.94548	-0.02214
40	0.94318	-0.01314	0.94275	-0.01679	0.94142	-0.02199
6	0.94036	-0.01285	0.93989	-0.01658	0.93847	-0.02189
12	0.93722	-0.01139	0.93667	-0.01519	0.93511	-0.02057
15	0.98401	-0.01204	0.98396	-0.01592	0.98374	-0.02143
30	0.98175	-0.01230	0.98169	-0.01621	0.98144	-0.02176
29	0.97623	-0.01192	0.97614	-0.01590	0.97582	-0.02152
41	0.97237	-0.01072	0.97224	-0.01474	0.97184	-0.02041
28	0.97002	-0.00999	0.96987	-0.01403	0.96943	-0.01973
2	0.96747	-0.00891	0.96729	-0.01297	0.96679	-0.01871
26	0.96996	-0.00858	0.96981	-0.01271	0.96926	-0.01852
24	0.96478	-0.00695	0.96458	-0.01114	0.96392	-0.01703
23	0.96136	-0.00547	0.96110	-0.00971	0.96035	-0.01564
37	0.96032	-0.00477	0.96006	-0.00903	0.95920	-0.01499
10	0.94982	-0.00321	0.94944	-0.00753	0.94825	-0.01355
5	0.94753	-0.00217	0.94710	-0.00653	0.94582	-0.01261
9	0.94618	-0.00155	0.94572	-0.00594	0.94438	-0.01205
3	0.93818	-0.00098	0.93768	-0.00540	0.93611	-0.01152
36	0.92267	-0.00018	0.92198	-0.00464	0.91985	-0.01081
31	0.91647	0.00113	0.91565	-0.00340	0.91319	-0.00966
38	0.91571	0.00177	0.91486	-0.00280	0.91235	-0.00911
7	0.94379	0.00341	0.94331	-0.00128	0.94189	-0.00770
19	0.97983	0.00429	0.97974	-0.00044	0.97941	-0.00691
25	0.96875	0.00478	0.96859	0.00003	0.96803	-0.00644

Table 3.7 Load-flow results of various types of load (Sr. No. 11, 14 of Table 3.1) for 41-node distribution system

Load type	Large industrial motors		Practical load	
Node No.	Voltage magnitude (p.u.)	Voltage angle	Voltage magnitude (p.u.)	Voltage angle
1	1.00000	0.00000	1.00000	0.00000
27	0.98937	-0.00529	0.98969	-0.00516
35	0.97366	-0.00869	0.97447	-0.00849
8	0.96069	-0.01060	0.96199	-0.01036
33	0.95176	-0.01195	0.95340	-0.01168
20	0.94470	-0.01305	0.94665	-0.01275
39	0.93715	-0.01424	0.93943	-0.01391
4	0.93105	-0.01522	0.93361	-0.01487
34	0.92732	-0.01584	0.93005	-0.01546
32	0.92128	-0.01684	0.92430	-0.01643
16	0.91570	-0.01668	0.91900	-0.01630
21	0.91330	-0.01600	0.91672	-0.01567
17	0.91159	-0.01532	0.91509	-0.01503
18	0.97620	-0.01738	0.97696	-0.01705
22	0.96643	-0.01881	0.96749	-0.01845
11	0.95629	-0.02033	0.95769	-0.01995
13	0.95118	-0.02112	0.95276	-0.02072
14	0.94525	-0.02205	0.94705	-0.02163
40	0.94117	-0.02189	0.94312	-0.02149
6	0.93821	-0.02178	0.94026	-0.02139
12	0.93483	-0.02045	0.93701	-0.02012
15	0.98368	-0.02131	0.98411	-0.02097
30	0.98138	-0.02164	0.98185	-0.02130
29	0.97575	-0.02139	0.97630	-0.02107
41	0.97177	-0.02028	0.97239	-0.01998
28	0.96935	-0.01960	0.97001	-0.01931
2	0.96671	-0.01857	0.96741	-0.01831
26	0.96915	-0.01838	0.97004	-0.01813
24	0.96379	-0.01687	0.96479	-0.01666
23	0.96022	-0.01548	0.96130	-0.01531
37	0.95903	-0.01483	0.96036	-0.01468
10	0.94802	-0.01338	0.94977	-0.01328
5	0.94559	-0.01243	0.94741	-0.01237
9	0.94415	-0.01186	0.94602	-0.01183
3	0.93581	-0.01134	0.93813	-0.01132
36	0.91945	-0.01062	0.92255	-0.01064
31	0.91275	-0.00945	0.91619	-0.00954
38	0.91190	-0.00889	0.91539	-0.00902
7	0.94164	-0.00747	0.94362	-0.00769
19	0.97934	-0.00667	0.97987	-0.00692
25	0.96792	-0.00620	0.96883	-0.00645

Table 3.8 Load-flow results of various types of load (Sr. No. 3, 5 of Table 3.1) for 41-node distribution system

Load type	Constant impedance		Constant current	
Node No.	Voltage magnitude (p.u.)	Voltage angle	Voltage magnitude (p.u.)	Voltage angle
1	1.00000	0.00000	1.00000	0.00000
27	0.99018	-0.00479	0.98973	-0.00500
35	0.97579	-0.00776	0.97464	-0.00811
8	0.96414	-0.00932	0.96230	-0.00976
33	0.95615	-0.01041	0.95381	-0.01093
20	0.94991	-0.01127	0.94714	-0.01185
39	0.94326	-0.01221	0.94002	-0.01286
4	0.93792	-0.01297	0.93429	-0.01368
34	0.93465	-0.01344	0.93078	-0.01418
32	0.92939	-0.01421	0.92511	-0.01502
16	0.92458	-0.01397	0.91991	-0.01476
21	0.92253	-0.01336	0.91769	-0.01409
17	0.92107	-0.01275	0.91610	-0.01343
18	0.97820	-0.01444	0.97713	-0.01522
22	0.96926	-0.01564	0.96775	-0.01648
11	0.96005	-0.01690	0.95804	-0.01781
13	0.95543	-0.01754	0.95316	-0.01849
14	0.95010	-0.01830	0.94751	-0.01929
40	0.94642	-0.01811	0.94363	-0.01909
6	0.94376	-0.01797	0.94081	-0.01894
12	0.94075	-0.01674	0.93762	-0.01764
15	0.98481	-0.01750	0.98419	-0.01843
30	0.98261	-0.01780	0.98194	-0.01874
29	0.97722	-0.01754	0.97642	-0.01847
41	0.97344	-0.01645	0.97253	-0.01735
28	0.97115	-0.01579	0.97018	-0.01667
2	0.96865	-0.01480	0.96760	-0.01565
26	0.97153	-0.01459	0.97025	-0.01544
24	0.96649	-0.01314	0.96504	-0.01393
23	0.96315	-0.01181	0.96159	-0.01255
37	0.96259	-0.01119	0.96069	-0.01191
10	0.95273	-0.00982	0.95024	-0.01048
5	0.95052	-0.00893	0.94791	-0.00954
9	0.94922	-0.00840	0.94654	-0.00898
3	0.94205	-0.00791	0.93875	-0.00846
36	0.92777	-0.00725	0.92339	-0.00776
31	0.92203	-0.00620	0.91716	-0.00662
38	0.92134	-0.00570	0.91639	-0.00607
7	0.94702	-0.00442	0.94418	-0.00468
19	0.98077	-0.00368	0.98000	-0.00389
25	0.97035	-0.00321	0.96904	-0.00342

Table 3.9 Load-flow results of various types of load (Sr. No. 12, 13 of Table 3.1) for 41-node distribution system

Load type	Constant power		Composite load	
Node No.	Voltage magnitude (p.u.)	Voltage angle	Voltage magnitude (p.u.)	Voltage angle
1	1.00000	0.00000	1.00000	0.00000
27	0.98920	-0.00525	0.98977	-0.00498
35	0.97327	-0.00853	0.97474	-0.00808
8	0.96009	-0.01029	0.96246	-0.00972
33	0.95100	-0.01154	0.95401	-0.01088
20	0.94381	-0.01254	0.94738	-0.01180
39	0.93611	-0.01363	0.94029	-0.01280
4	0.92989	-0.01453	0.93459	-0.01362
34	0.92607	-0.01508	0.93110	-0.01412
32	0.91990	-0.01599	0.92546	-0.01495
16	0.91422	-0.01572	0.92029	-0.01470
21	0.91179	-0.01498	0.91809	-0.01403
17	0.91005	-0.01424	0.91651	-0.01337
18	0.97585	-0.01615	0.97722	-0.01515
22	0.96594	-0.01749	0.96788	-0.01641
11	0.95565	-0.01891	0.95821	-0.01774
13	0.95046	-0.01963	0.95336	-0.01841
14	0.94444	-0.02049	0.94773	-0.01921
40	0.94031	-0.02027	0.94387	-0.01901
6	0.93730	-0.02012	0.94106	-0.01886
12	0.93390	-0.01872	0.93789	-0.01756
15	0.98347	-0.01954	0.98425	-0.01835
30	0.98115	-0.01986	0.98200	-0.01866
29	0.97549	-0.01958	0.97649	-0.01839
41	0.97149	-0.01843	0.97261	-0.01727
28	0.96906	-0.01773	0.97026	-0.01660
2	0.96640	-0.01668	0.96770	-0.01558
26	0.96872	-0.01645	0.97036	-0.01536
24	0.96334	-0.01489	0.96517	-0.01386
23	0.95975	-0.01346	0.96172	-0.01249
37	0.95841	-0.01279	0.96085	-0.01185
10	0.94724	-0.01128	0.95045	-0.01042
5	0.94478	-0.01028	0.94813	-0.00949
9	0.94333	-0.00969	0.94677	-0.00893
3	0.93476	-0.00914	0.93902	-0.00842
36	0.91806	-0.00838	0.92375	-0.00772
31	0.91123	-0.00713	0.91756	-0.00658
38	0.91037	-0.00653	0.91680	-0.00604
7	0.94078	-0.00499	0.94442	-0.00466
19	0.97909	-0.00416	0.98006	-0.00387
25	0.96749	-0.00367	0.96915	-0.00340

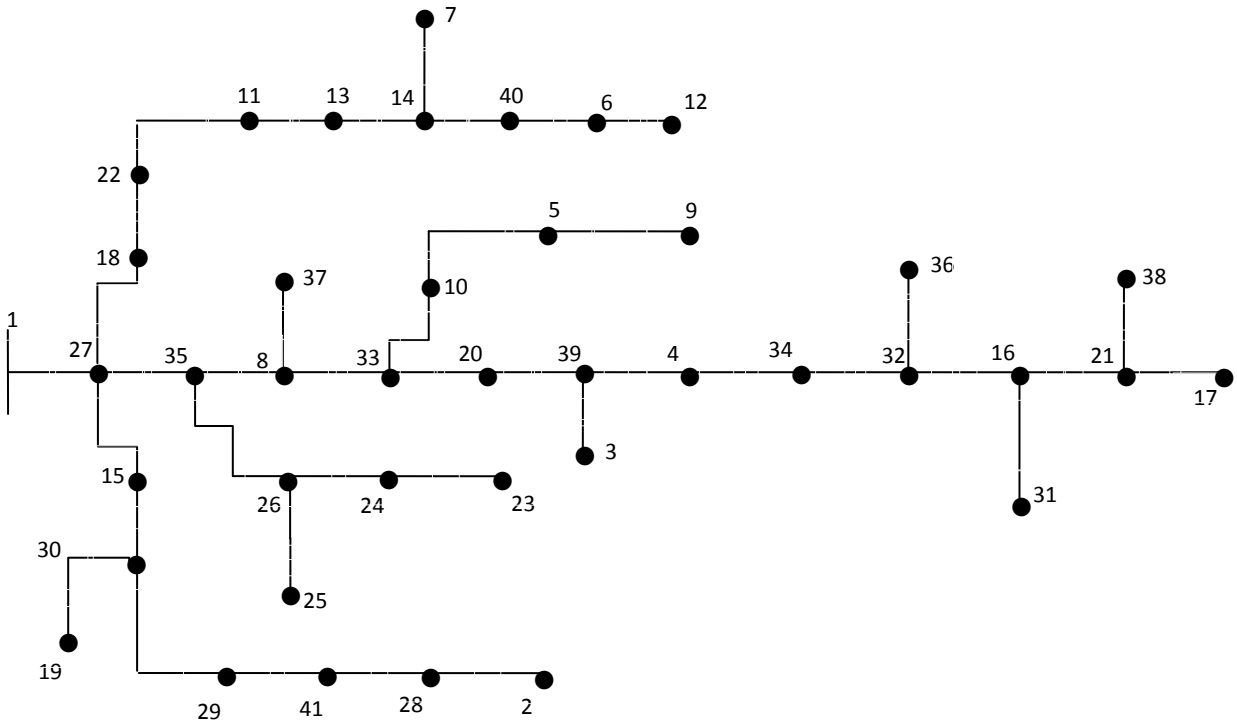

Fig. 3.6 Single line diagram of 41-node power distribution system

Table 3.10 Number of iterations for the convergence of the load-flow solution and the real and reactive power losses for various load models for 41-node network.

Sr. No.	Load model	No. of iterations	Real power losses in kW	Reactive power losses in kVAr	Min. voltage magnitude (p.u.) at node number 13	Angle of voltage at node number 13 in radians
1	Battery charge	4	172.8015	192.3338	0.92595	-0.01489
2	Fluorescent lamps	4	173.3655	192.9465	0.92338	-0.01485
3	Constant impedance	3	173.8920	193.5195	0.92107	-0.01275
4	Air conditioner	3	174.6066	194.2929	091765	-0.01909
5	Constant current	3	174.9854	194.7066	0.91610	-0.01343
6	Resistance space heater	3	174.8633	194.5766	0.91681	-0.00821
7	Pumps, fans other motors	3	175.3406	195.0899	0.91435	-0.01769
8	Incandescent lamps	3	175.1611	194.8993	0.91542	-0.00945
9	Compact fluorescent lamps	3	175.3353	195.0871	0.91457	-0.01189
10	Small industrial motors	3	175.8709	195.6667	0.91203	-0.01539
11	Large industrial motors	4	175.9700	195.7743	0.91159	-0.01532
12	Constant power	4	176.3188	196.1534	0.91005	-0.01414
13	Composite load*	3	174.8930	194.6062	0.91651	-0.01337
14	Practical load**	3	175.1937	194.9317	0.91509	-0.01503

* Composite load = 30% constant power + 30% constant current + 40% constant impedance load.
** Practical load = Battery Charge 2% + Fluorescent lamps 11% + AC 8%
+ Resistance space heating 5% + Pump, fans and other motors 18% + CFL 5%
+ Incandescent lamp 6% + Small motors 25% + Large motors 20%

The proposed load-flow method is capable of handling the effect of charging capacitances of the branches. The line shunt capacitance is computed from the line data is shown lumped at the receiving end node of the respective branch in Table D1 in **Appendix-D**. Table 3.11 compares the load-flow results with charging capacitance and without charging capacitance for constant power load only. Table 3.11 shows that not only the voltage magnitude of each node, has been improved but also the angle of voltage of each node has been improved due to the inclusion of shunt capacitance. The real and reactive power losses have been reduced when the shunt capacitances are in action.

Table 3.11 Load-flow results of 41-node system by considering the charging capacitance of the branches and without considering the charging capacitance.

Node No.	Results when capacitance is considered.		Results when capacitance is not considered.	
	Voltage magnitude (p.u.)	Voltage angle	Voltage magnitude (p.u.)	Voltage angle
1	1.00000	0.00000	1.00000	0.00000
27	0.98922	-0.00529	0.98920	-0.00530
35	0.97331	-0.00856	0.97327	-0.00859
8	0.96016	-0.01028	0.96009	-0.01034
33	0.95109	-0.01150	0.95100	-0.01157
20	0.94391	-0.01247	0.94381	-0.01255
39	0.93622	-0.01353	0.93611	-0.01362
4	0.93001	-0.01439	0.92989	-0.01449
34	0.92620	-0.01493	0.92607	-0.01504
32	0.92004	-0.01580	0.91990	-0.01592
16	0.91437	-0.01549	0.91422	-0.01562
21	0.91194	-0.01474	0.91179	-0.01487
17	0.91020	-0.01400	0.91005	-0.01414
18	0.97588	-0.00717	0.97585	-0.00719
22	0.96598	-0.00848	0.96594	-0.00851
11	0.95570	-0.00987	0.95565	-0.00991
13	0.95051	-0.01058	0.95046	-0.01062
14	0.94449	-0.01142	0.94444	-0.01146
40	0.94037	-0.01120	0.94031	-0.01125
6	0.93737	-0.01104	0.93730	-0.01109
12	0.93396	-0.00964	0.93390	-0.00969
15	0.98350	-0.00610	0.98347	-0.00611
30	0.98118	-0.00641	0.98115	-0.00643
29	0.97553	-0.00612	0.97549	-0.00615
41	0.97153	-0.00496	0.97149	-0.00500
28	0.96910	-0.00426	0.96906	-0.00430
2	0.96645	-0.00320	0.96640	-0.00324
26	0.96878	-0.00832	0.96872	-0.00836
24	0.96339	-0.00675	0.96334	-0.00680
23	0.95980	-0.00531	0.95975	-0.00537
37	0.95849	-0.00960	0.95841	-0.00966
10	0.94733	-0.00998	0.94724	-0.01006
5	0.94487	-0.00897	0.94478	-0.00906
9	0.94342	-0.00837	0.94333	-0.00847
3	0.93487	-0.01297	0.93476	-0.01307
36	0.91820	-0.01504	0.91806	-0.01516
31	0.91138	-0.01424	0.91123	-0.01437
38	0.91052	-0.01414	0.91037	-0.01427
7	0.94084	-0.00987	0.94078	-0.00993
19	0.97912	-0.00556	0.97909	-0.00559
25	0.96754	-0.00783	0.96749	-0.00788
When charging capacitance is considered. Total real power loss = **176.28550 kW** Total reactive power loss = **196.11720 kVAr**				
When charging capacitance is not considered. Total real power loss =**176.3188kW** Total reactive power loss =**196.1534kVAr**				

3.8 Conclusion:

An efficient load-flow method has been proposed in this chapter. The proposed method is capable of handling the effect of charging capacitance of the branches. It is a forward sweep method in which voltage drop in each branch is computed at a voltage. The voltage of each node is computed with the recent values of voltage drop, so the convergence is confirmed in this method. The solution algorithm does not need the numbering of the nodes in sequential order. Convergence of the method is shown with different types of the load. To show the efficiency of the method, the load-flow results are compared with the existing methods for 33-node distribution network and 69-node distribution network. The CPU time and the memory requirement is less for the proposed method.

As the proposed load-flow method is capable of handling the effect of capacitance, it is suitable to be used in networks with capacitor placed at various nodes. The proposed load-flow solution method is very much suitable for reconfiguration of radial distribution networks, because it does not need renumbering of nodes for load-flow after reconfiguration, which saves lot of time and computation effort.

CHAPTER 4

LINE LOADABILITY INDEX AND VOLTAGE STABILITY INDEX FOR RADIAL ELECTRIC POWER DISTRIBUTION NETWORKS

4.1. INTRODUCTION: Most of the reported works in the field of line loadability index and voltage stability index have been presented in **Section 2.3** of **Chapter 2**. The term line loadability index had been used in same context as voltage stability index by Juan ***et al.*** [41], this term has been redefined in the present work in entirely different context. The definition of line loadability is the maximum load that can be delivered by a distribution network without violating the maximum operating temperature limits of any branch of the network. The loadability index of each branch gives the margin for further loading. The line loadability analysis is related to steady-state loading conditions. None of the previous researchers has published this type of analysis.

Voltage stability indices reported till date, analyze the maximum loading or critical loading on the basis of voltage stability. But this type of analysis is quite misleading. The voltage instability never occur in steady operating conditions, instead it always occur at the time of sever faults. But in all the reported papers the researchers studied the steady state loading conditions of distribution network through voltage stability analysis.

The voltage stability indices and loadability margins reported so far have the following major limitations:

(i) The change in resistance of the line conductor with the change in operating temperature, which is further a function of branch current, ambient temperature and weather conditions. These had not been incorporated in computation of the voltage stability indices.

(ii) Thermal limits and current carrying capacity of the branch conductors used in distribution system had been neglected while computing the loadability limits of the distribution networks. The thermal limits of the branch conductors are also dependent on ambient temperature and weather conditions.

(iii) It was not reported that for how long the distribution system was capable to withstand the heavy currents before the voltage collapse occurs or the time required by the over current protection system of the distribution network to isolate the faulty portion of the system.

Without considering these constraints, it is difficult to obtain the correct voltage stability limit and line loadability limit of the power distribution system. The voltage stability indices already available in literature compute the voltage stability limit very near or at the point where the mathematical solution of the receiving-end voltage equation was no more possible but they had not considered the change in branch conductor resistance with temperature. The effect of weather and ambient conditions were also not considered in the previous reported research work. So the value of the critical loading or the voltage stability limit was a unique one for a particular distribution network. But practically, these were not true. The weather and ambient conditions have considerable effect on the voltage stability limit and line loadability limit. So these limits are dynamic in nature.

The significance of the voltage stability index is that sometimes the load may increase instantaneously due to some load contingency or fault. The voltage collapse may occur

before the protection system comes into play or in case when the protection system fails to actuate and the line conductor attain the temperature at which material melts and lose its mechanical strength. So voltage stability index gives the loading limit under the fault or load contingency conditions. At or near the divergence point of the load-flow solution, the system is very heavily loaded that leads to higher operating temperature of the line conductors so the resistance of the conductors changes. At the higher values of resistance, the voltage drops in the branch conductors increase, specially for the constant power loads and leads to further decrease in node voltages at the critical load, this phenomenon becomes cumulative and the voltage collapse occurs well before the limit marked by the voltage stability indices, those neglect the change in resistance with higher operating temperature.

The highest operating temperature of the line conductors for steady state conditions is constrained by the annealing of the conductors and the elongation of the conductors, which leads to larger sags, small ground clearances and permanent deformation of the conductors. For ACSR conductors, the maximum operating limit for safe steady state operation is about 75□ C to 80□ C. For very short durations, the temperature can rise to 250□ C or above. The proposed line loadability index is based on this constraint of the system. Significance of the line loadability index is that it gives the steady state loadability limit of the distribution network. The steady state loading of the distribution network is limited upto that extent when the steady state temperature of at least one branch reaches the maximum steady state temperature limit.

In this chapter a voltage stability index and a line loadability index have been proposed for electrical power distribution networks. The effect of rise in temperature on resistance is

incorporated while computation of the voltage stability index and the line loadability index. Some situations have been discussed when the voltage collapse can occur although the over current protection is present there.

4.2. Formulation of Voltage stability index and Line Loadability index:

The voltage stability index is derived from the basic equations of distribution system to relate the sending-end voltage to the receiving-end voltage in which resistance and reactance of the branch conductors, real and reactive power loads etc are involved. The line loadability index is based on the maximum allowable temperature rise of the branch conductors.

4.2.1. Voltage stability index (VSI):

The sending-end voltage can be related to the receiving-end voltage as:

$$V_k \angle \delta_k = V_{k+1} \angle \delta_{k+1} + I_{jj}(R_{jj} + jX_{jj}) \tag{4.1}$$

The current in a particular branch is the sum of all load currents due to the loads connected to the nodes beyond that branch plus the load current of that branch.

$$I_{jj} = \sum_{m=k+1}^{N} \left(\frac{P_m - jQ_m}{V_m \angle -\delta_m} \right) \tag{4.2}$$

Here P_m and Q_m are the real and reactive loads connected to the (k+1)th node. V_m and δ_m are the voltage and its angle at (k+1)th node. The voltage drop in each branch can be expressed by

$$V_{k+1} \angle \delta_{k+1} = V_k \angle \delta_k - \sum_{m=k+1}^{N} \left(\frac{P_m - jQ_m}{V_m \angle -\delta_m} \right) R_{jj} + jX_{jj} \tag{4.3}$$

For the simplicity,

$$C = \sum_{m=k+1}^{N} \left[\frac{(P_m R_{jj} + Q_m X_{jj}) \cos\delta_m - (P_m X_{jj} - Q_m R_{jj}) \sin\delta_m}{V_m} \right] \tag{4.4}$$

$$D = \sum_{m=k+1}^{N} \left[\frac{(P_m X_{jj} - Q_m R_{jj}) \cos\delta_m + (P_m R_{jj} + Q_m X_{jj}) \sin\delta_m}{V_m} \right] \tag{4.5}$$

$$V_{k+1} \cos \delta_{k+1} + j \sin \delta_{k+1} = V_k \cos \delta_k + j \sin \delta_k - C + j D \tag{4.6}$$

Separating real and imaginary parts in Eq. (4.6), we have

$$V_{k+1} \cos \delta_{k+1} = V_k \cos \delta_k - C \tag{4.7}$$

$$V_{k+1} \sin \delta_{k+1} = V_k \sin \delta_k - D \tag{4.8}$$

Squaring on both sides of Eq. (4.7) and Eq. (4.8), we have after addition

$$V_{k+1} = \sqrt{(C^2 + D^2 + V_k^2) - 2V_k (C \cos\delta_k + D \sin\delta_k)} \tag{4.9}$$

For the positive values of V_{k+1}

$$(C^2 + D^2 + V_k^2) - 2V_k (C \cos\delta_k + D \sin\delta_k) \geq 0 \tag{4.10}$$

Let

$$VSI = (C^2 + D^2 + V_k^2) - 2V_k (C \cos\delta_k + D \sin\delta_k) \tag{4.11}$$

where

$$\delta_{k+1} = \tan^{-1}\left(\frac{V_k \sin\delta_k - D_{jj}}{V_k \cos\delta_k - C_{jj}} \right) \tag{4.12}$$

Total real power loss of the network

$$= \sum_{jj-1}^{N-1} \left(\sum_{m=k+1}^{N} \frac{P_m^2 + Q_m^2}{V_m^2} \right) R_{jj} \tag{4.13}$$

Total reactive power loss of the network

$$= \sum_{jj-1}^{N-1} \left(\sum_{m=k+1}^{N} \frac{P_m^2 + Q_m^2}{V_m^2} \right) X_{jj} \qquad (4.14)$$

4.2.2. Line Loadability index (LLI):

The conductors used for the distribution of electrical power have particular current carrying capacity, which is governed by the thermal limits of the material. The steady state operating temperature is assumed to be less than or equal to 80 C.

Let the maximum operating temperature $T_{jj(max)}$ of the branch jj's conductor is 80 C.

The actual operating temperature is T_{jj} .

Line Loadability Index $LLI = \dfrac{T_{jj\ \max} - T_{jj}}{T_{jj\ \max}}$ (4.15)

For reliable operation of the system, value of the *LLI* should approach to 1. Lesser the value of *LLI*, lesser will be the margin for further loading of the system. The value of T_{jj} at particular load conditions changes with change in ambient temperature and weather conditions. The voltage stability limit and line loadability limit can be marked by computing both the *VSI* and *LLI*.

4.3. Incorporation of change in resistance with the change in temperature:

The temperature of the conductor is considered equal to the ambient temperature when the distribution network is not energized. But when system is serving the load, heat energy is generated in the conductors, which tend to increase the temperature of the conductors. Branch conductors are exposed in the sun so that heat energy form the sun also adds its effect to increase the temperature of the conductors. As the conductors gain heat due to

above said effects, their temperature is raised from the ambient temperature. Due to the temperature difference among conductor surface and surrounding air, the heat starts dissipating in the air. Heat dissipates due to convection and radiation. The balance between heat gained and dissipated gives the final operating temperature.

It is clearly stated above that the heat is gained and dissipated by the branch conductors simultaneously. The heat balance equation comes into play. The temperature at which this equation is balanced will be the final temperature of the conductor. It takes approximately an hour to attain a final steady state temperature. The heat balance equation is very well discussed in IEEE Std. 738™-2006 [46] with the support of explanation of various parameters and associated tables. The procedure for computation of the temperature rise of the branch conductors is discussed by Le ***et al.*** [47]. However, the procedure to compute the temperature rise is discussed below in brief.

Heat balance equation:

$$q_{jjc} + q_{jjr} = q_{jjs} + I_{jj}^2 R_{jj(Tjj)} \tag{4.16}$$

$$q_{jjc1} = \left[1.01 + 0.0372 \left(\frac{d_{jj} \rho_{jj} v}{\mu_{jj}} \right)^{0.52} \right] k_{jj} K_{ang} (T_{jj} - T_a) \tag{4.17}$$

$$q_{jjc2} = \left[0.0119 \left(\frac{d_{jj} \rho_{jj} v}{\mu_{jj}} \right)^{0.6} \right] k_{jj} K_{ang} (T_{jj} - T_a) \tag{4.18}$$

$$K_{\text{ang}} = 1.194 - \cos(\varphi) + 0.194 \cos(2\varphi) + 0.368 \sin(2\varphi) \tag{4.19}$$

Equation (4.17) and Eq. (4.18) show the heat loss from the conductor due to forced convection i.e., due to wind. Eq. (4.17) shows the correct value for slow wind speed and

Eq. (4.18) shows the correct value for high wind speed. For any wind speed the higher value among both is considered.

$$q_{jjcn} = 0.0205\rho^{0.5} d_{jj}^{0.75} (T_{jj} - T_a)^{1.25} \tag{4.20}$$

$$q_{jjr} = 0.0178 d_{jj} \varepsilon \left[\left(\frac{T_{jj} + 273}{100} \right)^4 - \left(\frac{T_a + 273}{100} \right)^4 \right] \tag{4.21}$$

$$q_{jjs} = Q_{jjse} \alpha \sin(\theta) A'_{jj} \tag{4.22}$$

$$\theta = \cos^{-1} \cos(H_c) \cos(Z_c - Z_1) \tag{4.23}$$

$$\mu_{jj} = \frac{1.458 \times 10^{-6} (T_{jj\,film} + 273)^{1.5}}{T_{jj\,film} + 383.4} \tag{4.24}$$

$$\rho_{jj} = \frac{1.293 - 1.525 \times 10^{-4} H_e + 6.379 \times 10^{-9} H_e^2}{1 + 0.00367 T_{jj\,film}} \tag{4.25}$$

$$k_{jj} = 2.424 \times 10^{-2} + 7.477 \times 10^{-5} T_{jj\,film} - 4.407 \times 10^{-9} T_{jj\,film}^{\ 2} \tag{4.26}$$

$$T_{jj\,film} = \frac{T_{jj} - T_a}{2} \tag{4.27}$$

Equation (4.20) shows the heat loss from the surface of conductor due to natural convection. Eq. (4.21) shows the heat loss from the surface of the conductor due to radiation. Eq. (4.22) shows the heat gained by the conductor surface due to the sun radiations. When the current through conductor is increased, its temperature starts rising. It takes some time to reach the steady state value. Before reaching the steady state condition,

the heat gained by the conductor is more than the heat dissipated from the conductor. Therefore, heat balance equation for this duration becomes

$$q_{jjc} + q_{jjr} = q_{jjs} + I_{jj}^2 R_{jj(Tjj)} + \Delta q_{jj} \tag{4.28}$$

$$\Delta q_{jj} = q_{jjs} + I_{jj}^2 R_{jj(Tjj)} - q_{jjc} - q_{jjr} \tag{4.29}$$

Heat energy gained by the conductor can be computed by dividing the total time taken to reach steady state temperature in short time intervals, i.e. Δt of 10 seconds for steady state operation and 0.01 or less for fault conditions.

$$\Delta t \times \Delta q_{jj} = M_{jj} \times S_{spc} \Delta \mathrm{T}_{jj} \tag{4.30}$$

$$\Delta \mathrm{T}_{jj} = \frac{\Delta t \times \Delta q_{jj}}{M_{jj} \times S_{spc}} \tag{4.31}$$

$$T_{jj} = T_{jj(old)} + \Delta \mathrm{T}_{jj} \tag{4.32}$$

The formula available in IEEE Std. 738™-2006 [46] for computation of conductor resistance at any temperature

$$R_{jj} = \left[\frac{R_{jj(high)} - R_{jj(low)}}{T_{jj(high)} - T_{jj(low)}} \right] (T_{jj} - T_{jj(low)}) + R_{jj(low)} \tag{4.33}$$

4.4. Computation of voltage stability index and line loadability index :

The procedural steps to compute the voltage stability index (*VSI*) and the line loadability index (*LLI*) are shown below.

(1) Read the load and line data, ambient conditions, global position of the network, time of the day, month of the year, etc.

(2) Compute heat gained by each branch conductor due to $I_{jj}^2 R_{jj(Tjj)}$, sun radiations and compute heat dissipated due to natural convection, forced convection and radiations for Δt .

(3) Compute the changed temperature and resistance for each branch of the conductor for Δt . $\Delta t = 10$ sec. for *LLI* and Δt can be very small as 0.01 sec in case of *VSI*.

(4) Run the load-flow using changed resistances of branches and compute *VSI* or *LLI* or both. For load-flow solution, the Eq. (4.9), Eq. (4.12), Eq. (4.13) and Eq. (4.14) have been used.

(5) For *LLI* the steps (2), (3), (4) are repeated for $\sum \Delta t = 3600$ for *VSI* it can be for $\sum \Delta t = 3600$ or the voltage collapse may occur within fraction of seconds so in this case the repetition of above procedure depends upon the time taken for voltage collapse but in this case Δt is taken very small.

(6) Print the results.

4.5. Examples:

A 30-node distribution network has been considered and shown in Fig. 4.1. The tie-lines and isolator switches shown in Fig. 4.1 are not considered at this stage. Only the base network shown with solid lines is considered. The line data and load data of the system are shown in Table E1 and Table E2 (respectively) in **Appendix-E**. Base MVA and base kV are 100 MVA and 11 kV respectively. Various aspects of behavior of the distribution networks during steady state and very heavily loaded (fault like) conditions are illustrated through this network. For load-flow studies the method proposed in **Chapter 3** is used.

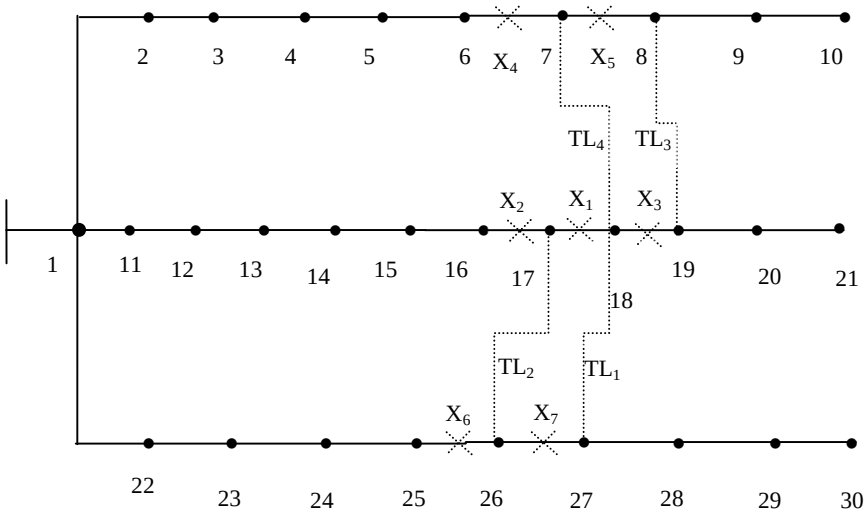

Fig. 4.1 Single line diagram of 30-node power distribution system

4.5.1 VSI at base load:

The index values of *VSI* for the condition when all the loads connected to the nodes considered equal to their maximum demands, are shown in Fig 4.2. Table 4.1 shows the line loadability index and voltage stability index for each node at base condition for 30-node radial distribution network. It is clear from the results that the node number 21 is the most sensitive node.

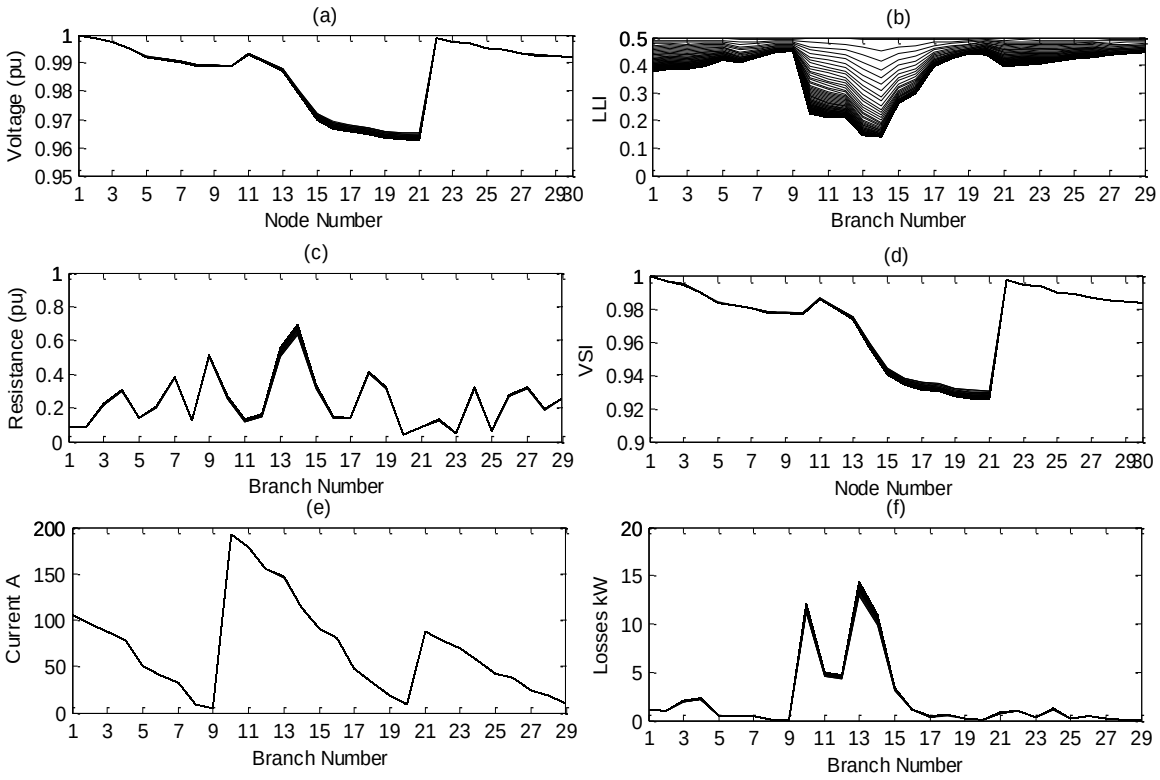

Fig. 4.2 The *VSI* of each node at normal load, resistance of each branch, current in each branch, *LLI* of each branch and real power losses in each branch at normal load for 30-node distribution network.

Table 4.1 The index values of *LLI* for each branch and index values of *VSI* for each node at base load conditions for 30-node distribution network.

Branch no.	Line loadability index	Node no.	Voltage Stability index
1	0.37533	1	1
2	0.38557	2	0.99755
3	0.38647	3	0.99532
4	0.397	4	0.9904
5	0.41859	5	0.98428
6	0.4118	6	0.98259
7	0.42707	7	0.98082
8	0.44842	8	0.97825
9	0.44984	9	0.978
10	0.22627	10	0.97752
11	0.21042	11	0.98626
12	0.21125	12	0.98045
13	0.14355	13	0.97453
14	0.14093	14	0.95686
15	0.25998	15	0.94084
16	0.29874	16	0.93469
17	0.39803	17	0.93229
18	0.4258	18	0.9309
19	0.44233	19	0.92814
20	0.43617	20	0.92692
21	0.39431	21	0.92681
22	0.4027	22	0.99797
23	0.40573	23	0.99525
24	0.41341	24	0.99434
25	0.42572	25	0.99007
26	0.42905	26	0.98943
27	0.4376	27	0.98698
28	0.44202	28	0.98539
29	0.44804	29	0.98463
		30	0.98409

4.5.2 Voltage stability limit:

The voltage stability limit of the distribution network can be computed by increasing the load on each node till the index value of *VSI* for one of the nodes becomes equal to or

approximately zero. The maximum value of λ is 3.5 for this particular network with CP load and *VSI* of most sensitive node (21) for this loading condition as shown in Fig.4. 3 (e). The value of the λ can be slightly more or less but the time taken for voltage collapse will vary inversely.

It is discussed in earlier sections of this thesis that the temperature of branch conductors increases from ambient temperature when the network is serving the load. This phenomenon is shown in Fig 4.3 (b). Width of curve shows the change, wider the curve more is the change in parameter, same is for all other parts of Fig. 4.3. With the change in temperature of branch conductor, the resistance of the branch conductors also change, which has been shown in Fig 4.3 (d).

Table 4.2 The voltage stability index of each node and temperature of each branch at critical loading for 30-node distribution network.

Node No.	Voltage Stability Index	Branch No.	Temperature (°C)
1	1	1	84.915
2	0.99192	2	77.795
3	0.98466	3	80.679
4	0.96852	4	73.037
5	0.94886	5	60.606
6	0.94357	6	74.442
7	0.93779	7	61.839
8	0.92967	8	45.303
9	0.92893	9	44.247
10	0.92747	10	326.3
11	0.80144	11	400.9
12	0.70706	12	472.8
13	0.59241	13	737.32
14	0.20589	14	900.59
15	0.0031439	15	555.14
16	0.012115	16	419.25
17	0.0057631	17	137.7
18	0.0043555	18	83.964
19	0.0029984	19	56.252
20	0.0028477	20	44.762
21	0.0028459	21	71.278
22	0.99352	22	65.746
23	0.98493	23	66.372
24	0.98205	24	64.008
25	0.96859	25	55.284
26	0.96661	26	52.973
27	0.95908	27	53.364
28	0.95419	28	50.025
29	0.95184	29	45.561
30	0.95022		

4.5.3. Comparison of results with existing methods:

The voltage stability index proposed by Moghavvemi and Faruque [35], Chakravorty and Das [36], Juan ***et al.*** [41] and Hamada [42] are computed for 30-node radial distribution network up-to voltage stability condition. The value of load multiplier λ beyond which the system voltage becomes instable, stability index of most sensitive node and voltage at most sensitive node are shown in Table 4.3. If the voltage stability limits computed by various voltage stability indices are compared, it is clear the existing stability indices give higher value than the proposed voltage stability. It is due to the fact that the effect of change in resistance due to change in temperature had not been incorporated in the existing voltage stability indices. Even the previous voltage stability indices are silent about the time for which the network can withstand the critical load.

Table 4.3 Comparison of index values, voltage stability limit and minimum node voltage of 30-node distribution network.

	λ^*	Stability index	Mini. Voltage magnitude (p.u..)
Proposed *VSI*	3.5	*VSI*= 0.002845	0.386520
Moghavvemi and Faruque[35]	4.6576	L_p = 1.000010	0.47467
Chakravorty and Das[36]	4.6153	SI(m_2)=0.00003	0.43786
Juan ***et al.***[41]	4.6245	L_s= 1.00198	0.41844
Hamada[42]	4.4567	L_v= 1.000001	0.50324
* multiplier of load power.			

4.6. The conditions practically possible when voltage collapse can occur in radial distribution networks:

The voltage stability limit of a practical distribution network can never occur as it is discussed in **Section 4.5.2** due to following reasons.

(i) The possibility of load increase in such a way that the maximum demands of all the loads are 3.5 times the original maximum demand is impractical.

(ii) It is clear from the Fig. 4.3(e) that the voltage collapse occurred approx. 110 seconds after the step increase in λ from 1 to 3.5. The over-current protection of the network will trip the circuit within few seconds.

(iii) The branch conductors cannot withstand such high temperatures for long time.

But the importance of **Section 4.5.2** is not diminished due to the above discussion, because the concept of the *VSI* and the behavior of the network are comprehensively explained through graphical representation of various parameters in this section. Moreover, **Section 4.5.3** included in the thesis to show effectiveness of the proposed method in comparison with previous methods and to show, how the previous methods are unable to compute exact voltage stability limit.

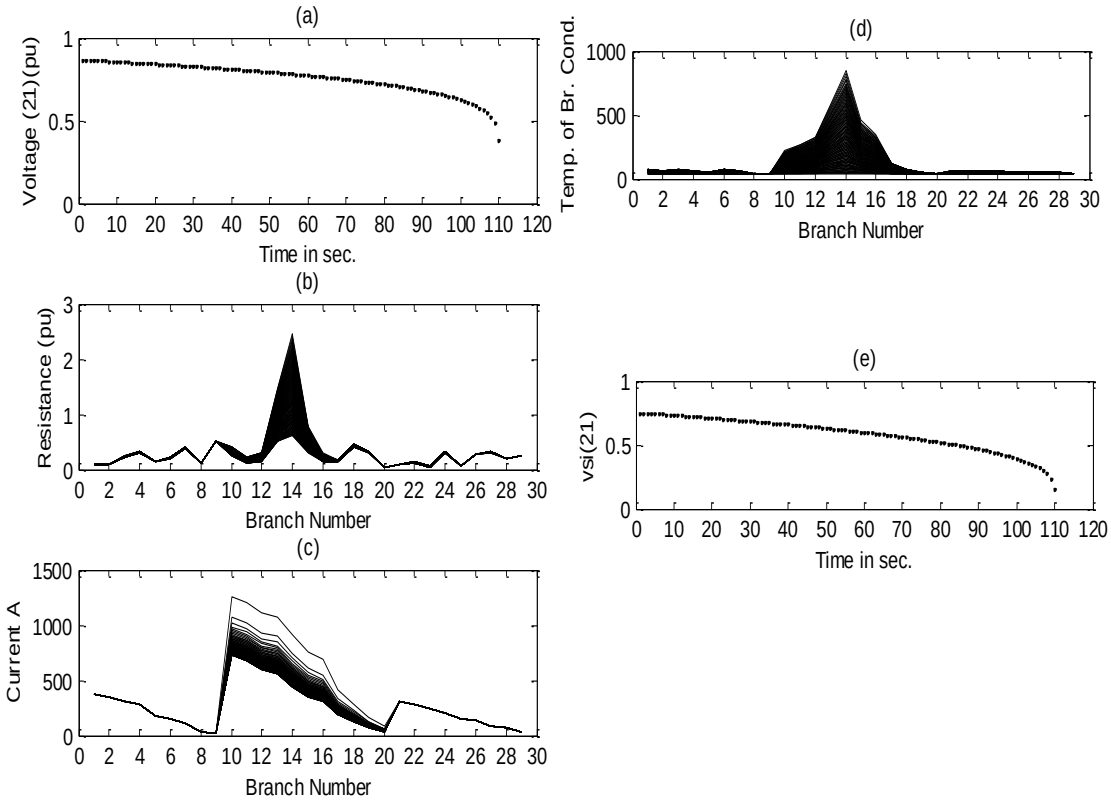

Fig. 4.3 Results for 30-node network. Fig.4.3 (a). The voltage (p.u.) of each branch. Fig 4.3 (b). The change in resistance of each branch after loading. The *VSI* of most sensitive node. Fig 4.3(c). Change in resistance of branch conductors with change in temperature. Fig 4.3(d) The change in temperature of each branch after loading. Fig 4.3(e) *VSI* of most sensitive node (21).

Suppose the 30-node distribution network under- consideration is protected by disc type induction inverse time over-current relays. These relays give the actuation signal to vacuum circuit breakers. The choice of inverse time properties and the time delay settings are done in such a way that the relay takes some time to actuate the tripping mechanism. The time delay depends upon the inverse time characteristics of and time delay multiplier. The formula and the constants used to compute the relay operating time are discussed in details by Gers and Holmes [48]. The IEC standard inverse relay is considered and the time dial setting is taken 1 in the following discussion. The other time delays added by the

auto-recloser and circuit barker are not considered. The pick-up current of the relay is set at 450A because the maximum expected current of the network is approximately 200A due to maximum demand of all nodes with constant power (CP) load modelling.

It is stated above that the growth of load at each node is in same proportion and up to the extent of voltage instability at most sensitive node is not possible. But a situation may arise if some fault is occurred at any point of the network and the severity of fault is such that it causes the voltage collapse prior to the protection system isolates the faulty part of the system.

In case of short circuit, the voltage collapse occurs within fraction of seconds or the protection system of the distribution network isolates the faulty portion within a very short time so that the heat generated in conductor does not dissipate in environment due to radiation and convection. During computation of temperature of each branch conductor in the above said conditions, the effect of q_{jjc}, q_{jjr} and q_{jjs} are neglected.

The significance of this study is that if the voltage collapse occurs in the distribution system, it can spread in the power system also and voltage collapse in a part of distribution system can disturb the power supply of the healthy portion of the distribution system. So this study and analysis of behavior of distribution system is helpful in design of protection system.

There are three main feeders of the 30-node distribution system F_1, F_2 and F_3 having nodes F_1=[1,2,3,4,5,6,7,8,9,10], F_2=[1,11,12,13,14,15,16,17,18,19,20,21] and F_3=[1,22,23,24,25,26,27,28,29,30]. Three situations are studied and analyzed i.e., for load suddenly increased (fault like situation in case of *VSI*) at any of the end nodes i.e. at node number 10, 21 or 30 of the network.

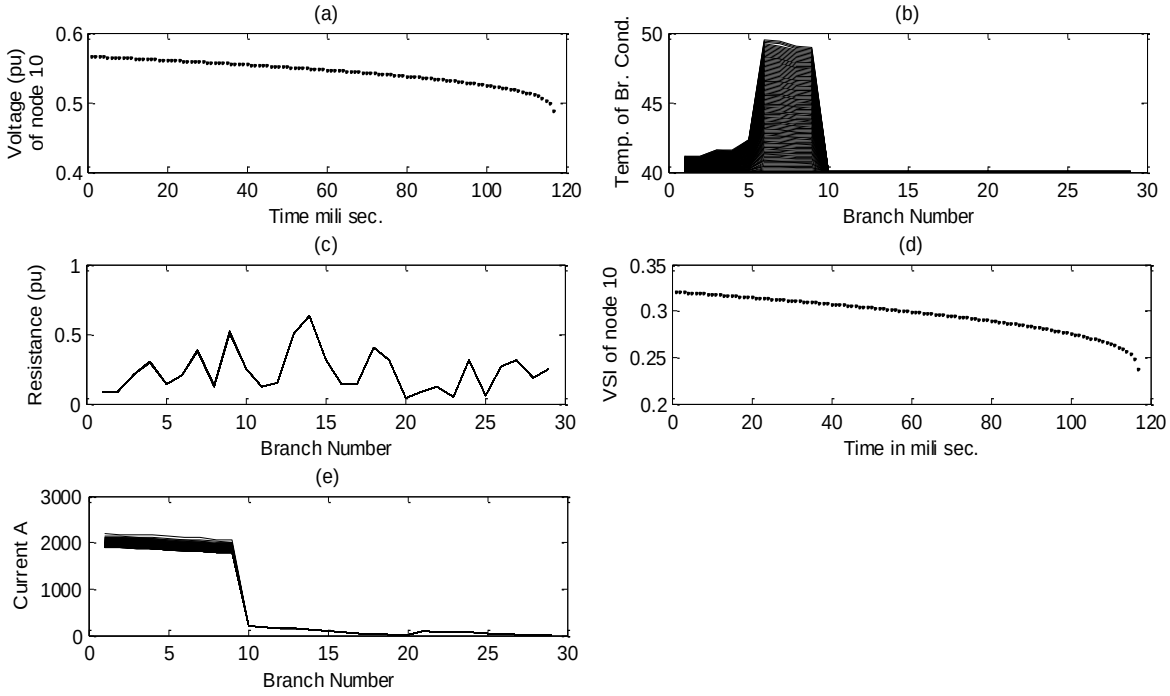

Fig. 4.4 The graphical representation of results for 30-node distribution network at time of voltage collapse when fault at node 10.

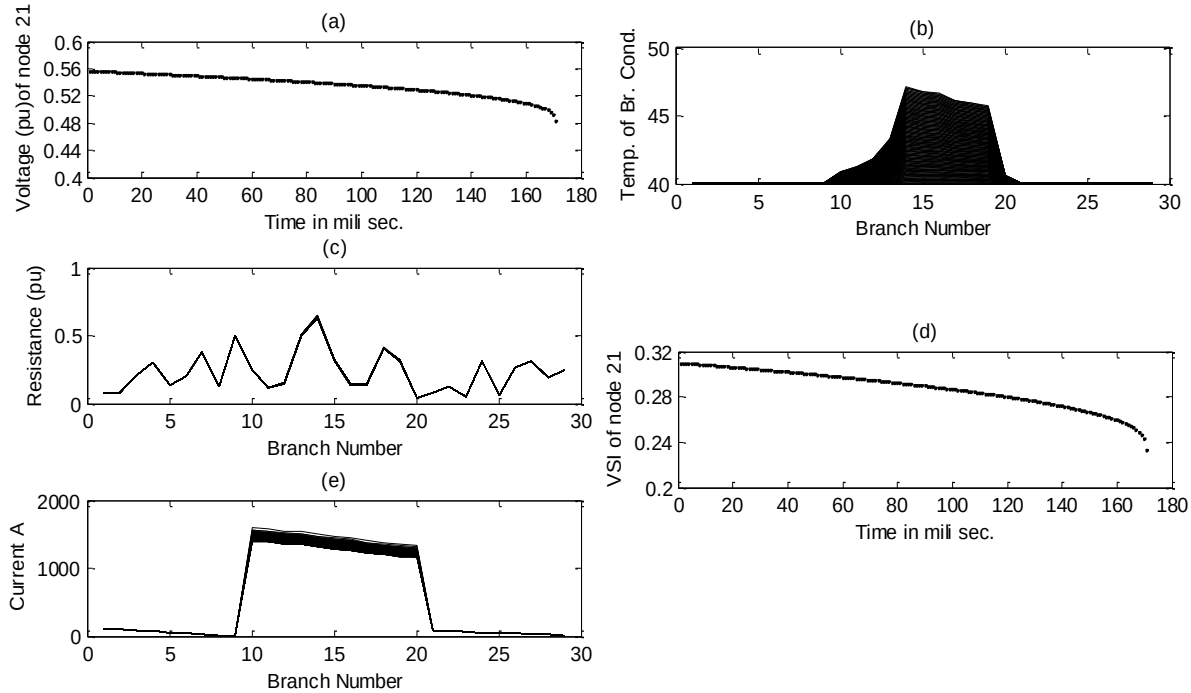

Fig. 4.5 The graphical representation of results for 30-node distribution network at time of voltage collapse when fault at node 21.

Table 4.4 The voltage stability index for each node and branch current, branch temperature for 11000kVA fault at node 10 for 30-node distribution network.

Node No.	Voltage Stability Index	Branch No.	Branch Current (Amp)	Temperature (□ C)
1	1	1	2191.1	41.135
2	0.91073	2	2181.8	41.125
3	0.86299	3	2172.2	41.585
4	0.70808	4	2162	41.569
5	0.5182	5	2128.2	42.351
6	0.44546	6	2116.4	49.604
7	0.35605	7	2103.8	49.48
8	0.21641	8	2067.9	49.138
9	0.17793	9	2060.3	49.068
10	0.063486	10	191.98	40.014
11	0.98697	11	178.25	40.017
12	0.9815	12	155.31	40.02
13	0.97594	13	146.11	40.029
14	0.95965	14	113.63	40.04
15	0.94497	15	90.248	40.027
16	0.93917	16	80.867	40.023
17	0.93689	17	47.995	40.012
18	0.93554	18	32.956	40.009
19	0.93284	19	18.838	40.007
20	0.93163	20	9.4191	40.003
21	0.93153	21	87.701	40.006
22	0.99801	22	78.601	40.005
23	0.99534	23	69.489	40.006
24	0.99445	24	55.815	40.006
25	0.99026	25	42.111	40.005
26	0.98963	26	37.542	40.005
27	0.98722	27	23.818	40.007
28	0.98565	28	19.239	40.007
29	0.9849	29	10.079	40.006
30	0.98437			

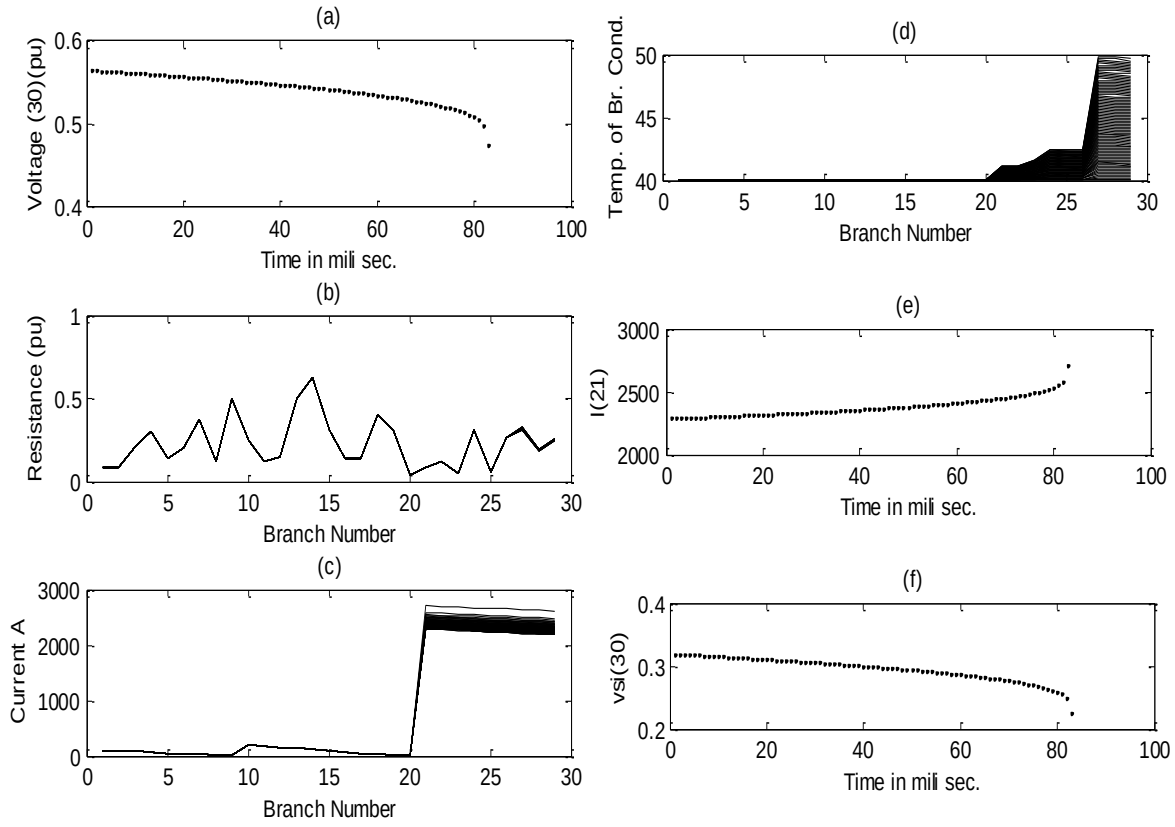

Fig. 4.6 The graphical representation of results for 30-node distribution network at time of voltage collapse when fault at node 30.

Table 4.5 The voltage stability index for each node and branch current, branch temperature for 7000 kVA fault at node 21 for 30-node distribution network.

Node No.	Voltage Stability Index	Branch No.	Current in Amp.	Temp. in deg. C
1	1	1	105.34	40.01
2	0.99761	2	96.242	40.009
3	0.99543	3	87.13	40.01
4	0.99062	4	77.996	40.009
5	0.98462	5	50.512	40.008
6	0.98296	6	41.342	40.015
7	0.98123	7	32.165	40.013
8	0.97871	8	9.1915	40.009
9	0.97846	9	4.5963	40.009
10	0.97798	10	1590.4	40.895
11	0.86046	11	1576	41.247
12	0.79996	12	1551.3	41.866
13	0.73145	13	1541.1	43.322
14	0.53291	14	1501.5	47.16
15	0.33834	15	1468.8	46.831
16	0.2588	16	1454.7	46.692
17	0.22743	17	1403.6	46.206
18	0.199	18	1379.4	45.984
19	0.12838	19	1354	45.76
20	0.085042	20	1335.5	40.62
21	0.079267	21	87.701	40.008
22	0.99801	22	78.601	40.008
23	0.99534	23	69.489	40.008
24	0.99445	24	55.815	40.009
25	0.99026	25	42.111	40.008
26	0.98963	26	37.542	40.007
27	0.98722	27	23.818	40.011
28	0.98565	28	19.239	40.01
29	0.9849	29	10.079	40.009
30	0.98437			

Table 4.6 The voltage stability index for each node and branch current, branch temperature for fault of 13500 kVA at node 30 for 30-node distribution network.

Node No.	Voltage Stability Index	Branch No.	Current in Amp.	Temp. in °C
1	1	1	105.34	40.005
2	0.99761	2	96.242	40.004
3	0.99543	3	87.13	40.005
4	0.99062	4	77.996	40.004
5	0.98462	5	50.512	40.004
6	0.98296	6	41.342	40.007
7	0.98123	7	32.165	40.006
8	0.97871	8	9.1915	40.004
9	0.97847	9	4.5963	40.004
10	0.97798	10	191.98	40.01
11	0.98697	11	178.25	40.012
12	0.9815	12	155.31	40.014
13	0.97594	13	146.11	40.021
14	0.95966	14	113.63	40.028
15	0.94498	15	90.248	40.019
16	0.93917	16	80.867	40.016
17	0.93689	17	47.995	40.008
18	0.93554	18	32.956	40.006
19	0.93284	19	18.838	40.005
20	0.93163	20	9.4191	40.002
21	0.93153	21	2707.6	41.168
22	0.90819	22	2698.3	41.159
23	0.77914	23	2688.4	41.637
24	0.73217	24	2673.4	42.506
25	0.48294	25	2656.4	42.471
26	0.43949	26	2650.6	42.459
27	0.27632	27	2631	50.016
28	0.14226	28	2623.5	49.954
29	0.082893	29	2606.9	49.822
30	0.029054			

4.6.1 Voltage stability limit for constant power load:

The kVA load at each end node i.e. at node number 10, 21 and 30 is increased to check the voltage stability limit and the loadability limit. In this study it is considered that initially the distribution network is supplying load equal to the maximum demand of all the loads. Figure 4.4, Fig. 4.5 and Fig. 4.6 respectively show the graphical representation of results at time of voltage collapse when fault are at node 10, node 21 and node 30 with constant power load. Table 4.4, Table 4.5 and Table 4.6 show the results of voltage stability index, branch current and branch temperature for faults at node 10, node 21 and node 30 for constant load modelling.

Figure 4.6 shows the graphical representation of results at time of voltage collapse when fault is at node 30. Table 4.6 shows the voltage stability index for each node and branch current, branch temperature for critical loading at node 30. Figure 4.5 shows the graphical representation of results at time of voltage collapse when fault is at node 21. Table 4.6 shows the voltage stability index for each node and branch current, branch temperature for critical loading at node 21.

Table 4.4 shows the voltage stability index for each node and branch current, branch temperature for critical loading at node 10. Figure 4.4 shows the graphical representation of results at the time of voltage collapse when fault is at node 10. Fig. 4.5 shows the graphical representation of results at time of voltage collapse when fault is at node 30. Table 4.6 shows the voltage stability index for each node and branch current, branch temperature for critical loading at node 30. Table 4.7 shows the information about the most sensitive node, the most sensitive branch, the highest branch current in each case of fault, time taken for voltage

collapse, actuating time of relay *VSI* and *LLI* in each case of loading. The case of each end node is taken separately.

4.6.2 Voltage stability limit for practical type load:

The practical distribution network supplies various types of loads. At each node the type and its percentage are considered as follows. Battery Charge (2%) + Fluorescent lamps (11%) + AC (8%) + Resistance space heating (5%) + Pump, fans and other motors (18%) + CFL (5%) + Incandescent lamp (6%) + Small motors (25%) + Large motors (20%). The values of load exponents are given in Satyanarayana ***et al.*** [17]. The results are shown in Table 4.7. The load added is considered as the short circuit so its load model is like the resistive load.

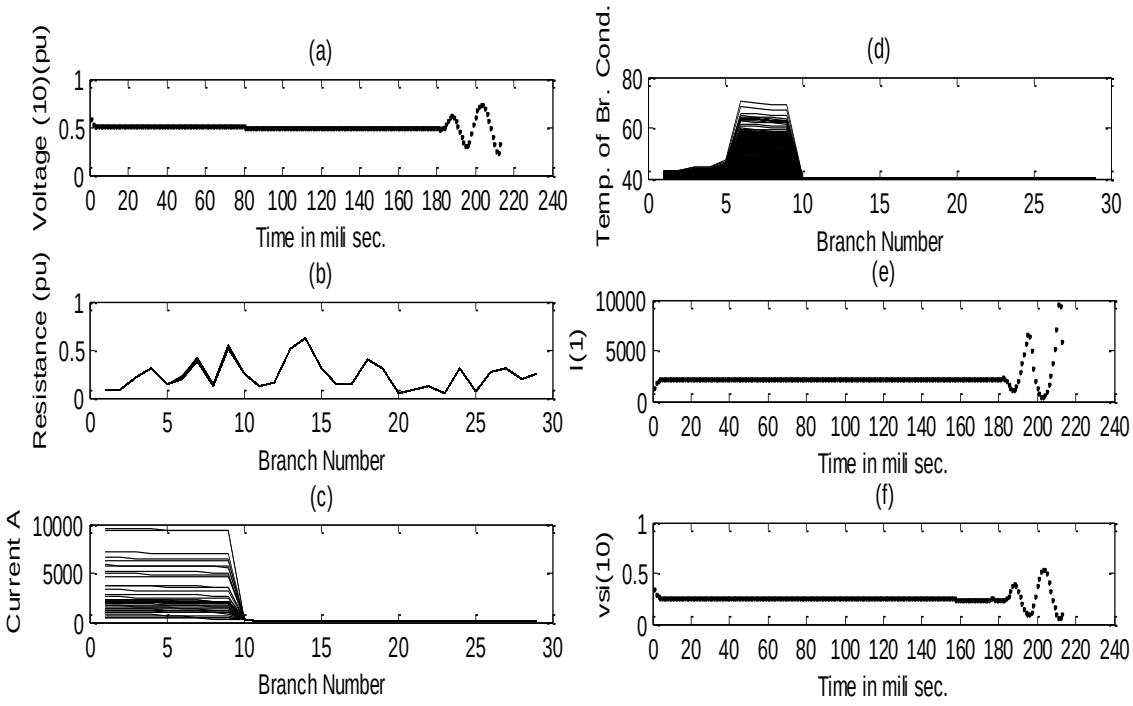

Fig. 4.7 The graphical representation of results for 30-node distribution network at time of voltage collapse when fault at node 10 with practical load modelling.

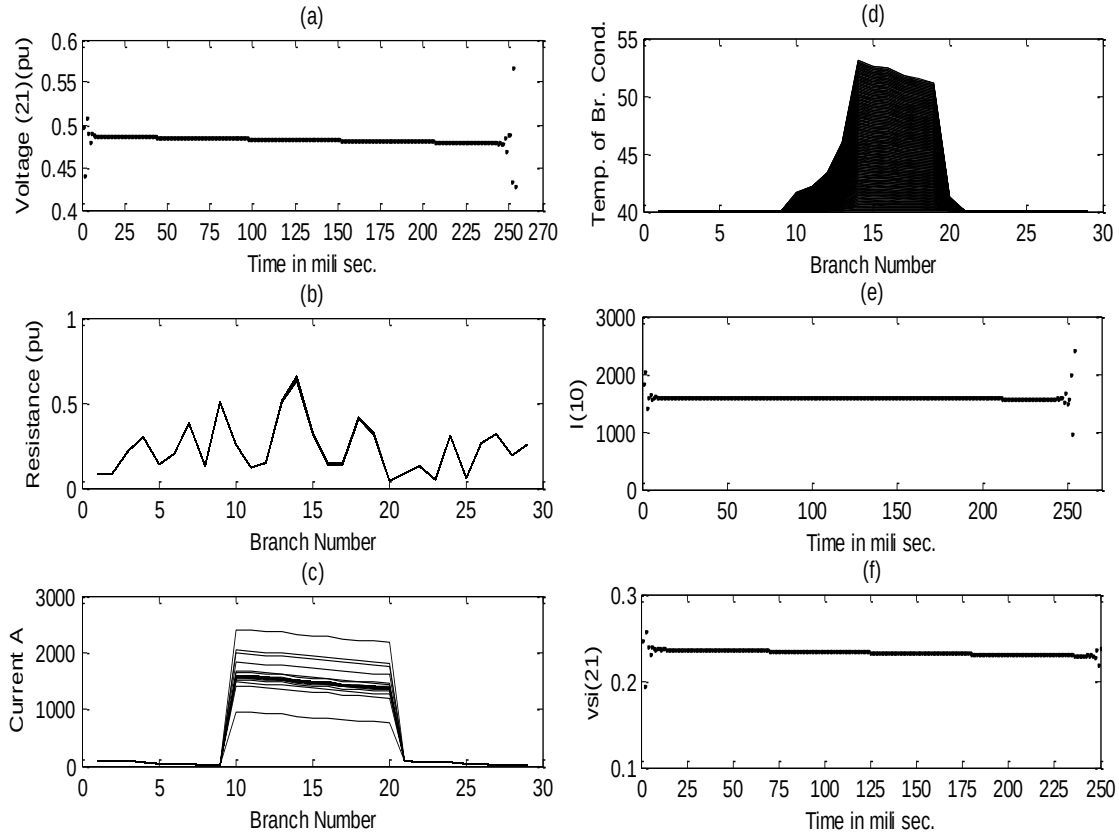

Fig. 4.8 The graphical representation of results for 30-node distribution network at time of voltage collapse when fault at node 21 with practical load modelling.

The value of loads, added at the end nodes in case of constant power load as well as practical load are the minimum values at which the voltage collapse can occur, at slightly lower values of load the protection system will actuate before the voltage collapse.

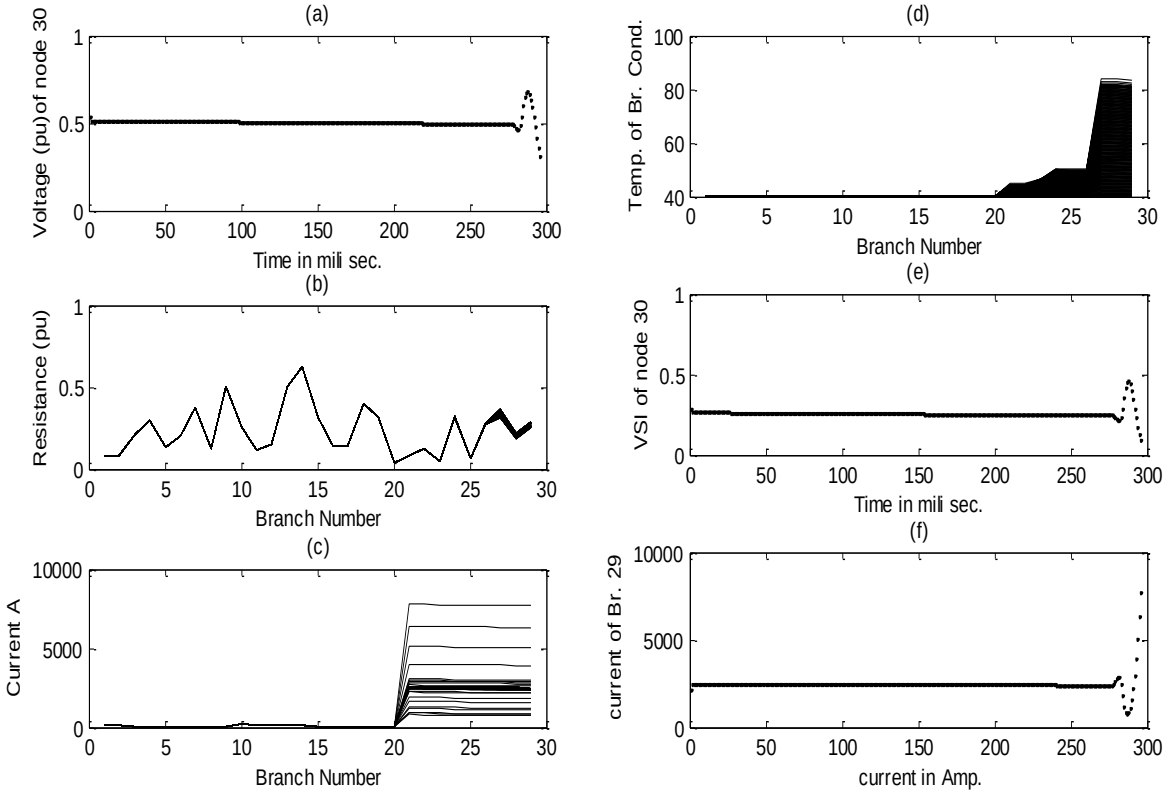

Fig. 4.9 The graphical representation of results for 30-node distribution network at time of voltage collapse when fault at node 30 with practical load modelling.

There is a worth noting difference between the voltage stability behavior of the network having constant power load and the practical load. The practical load constitutes the voltage dependent loads but in constant power load the power demand remains same irrespective to the voltage level, so the voltage of most sensitive node in case of constant power load sinks continuously and voltage collapse occurs as shown in Fig. 4.4 (a) but when the loads and the short circuit at the end node are voltage dependent, near the point of voltage collapse the voltage of most sensitive node starts oscillate and finally voltage collapse occurs. This phenomenon is shown graphically in Fig. 4.7, Fig. 4.8 and Fig. 4.9 each of which show (a) voltage of most sensitive node, (b) change in branch resistance (p.u.), (c) branch current in ampere, (d) branch temperature in □C, (e) voltage stability

index of most sensitive node and (f) highest branch current for faults at node 10, node 21 and node 30 respectively for practical load modelling. The oscillations are observed at the end of curve of *VSI*, voltage of most sensitive node and branch current. The reason of oscillations is that when the voltage of most sensitive node sinks the power demand of the loads reduces, this causes the voltage to cover up. But the temperature of the connecting branch is increasing. The load demand increases and consequently voltage sinks, after each oscillation. The dip in the voltage is more because of the higher temperature and resistance of the connecting branch.

4.7. Voltage stability limit and Line loadability limit for different ambient conditions:

All the loading conditions discussed above are computed with the same set of constants related to weather and ambient temperature conditions. These constants have a vital importance in computation of *VSI* and *LLI*. But the most prominent parameters are ambient temperature and wind velocity. To show their effect on the voltage stability limit and line loadability limit, the *VSI* and *LLI* are computed for relatively low ambient temperature and high wind velocity. The results are shown in Table 4.8.

Table 4.7 The values of *VSI* and *LLI* for loading at different end nodes for 30-node distribution network.

Node no.	*VSI* (Constant Power load)					*LLI* (Constant Power Load)		
	Value of load added (kVA)	*VSI* of most sensitive node	Time (sec)	Max. Branch current (A).	Relay actuating time (sec)	Value of load added (kVA)	*LLI* of most sensitive branch	Time (minutes)
10	11000	0.2332 node(10)	0.11	2191 Branch (1)	0.29	980	0.00737 Branch (6)	60
21	7000	0.2215 node(21)	0.17	1550 Branch (10)	0.33	210	0.00557 Branch (14)	60
30	13500	0.2384 node(30)	0.08	2550 Branch (1)	0.26	1170	0.005842 Branch (27)	60
Node no.	Value of load added in kW	*VSI* (Practical type load)				*LLI* (Practical type load)		
10	45000	0.07721 node(13)	.2	2146* Branch (1)	.3	1020	0.002337 Branch (6)	60
21	35000	0.06410 node(21)	0.25	1583 Branch (10)	0.33	250	0.0090907 Branch (14)	60
30	53000	0.078561 node(30)	0.23	2200 Branch (21)	0.28	1210	0.0041789 Branch (27)	60
* For practical type load the value current in first branch shown in the table prevails during the oscillations otherwise its value is comparatively low as shown in Fig. 6 so the over current protection system will not respond and chances of voltage collapse are very high in this case.								

Table 4.8 The values of *VSI* and *LLI* at different ambient temperature and wind velocities for 30-node distribution network.

Value of T_a and v	*VSI*			*LLI*		
	λ load multiplier	*VSI* of most sensitive node(13)	Time (sec)	λ load multiplier	*LLI* of most sensitive branch(14)	Time (minutes)
20□C and 3m/sec.	8.5	0.037621	150ms	1.95	0.001401	60
20□C and 1m/sec.	8.3	0.0091001	200ms	1.51	0.0029268	60
40□C and 3m/sec	8.2	0.012375	181ms	1.57	0.0096922	60
Accept the changes shown in this table for T_a and v the other constants have values for all the calculations in this paper i.e. Q_{jjse}=1100, H_e=1000, H_c=72.5, Z_c=139, Z_1=90, α=0.5, ε =0.5, φ=90, T_a=40, v=1.						

4.8. Line loadability limit:

It is previously discussed that the loadability of the distribution network is related to steady state operation. So to check the loadability limit for the loading condition under consideration, the network is loaded for the duration of one hour because within this time

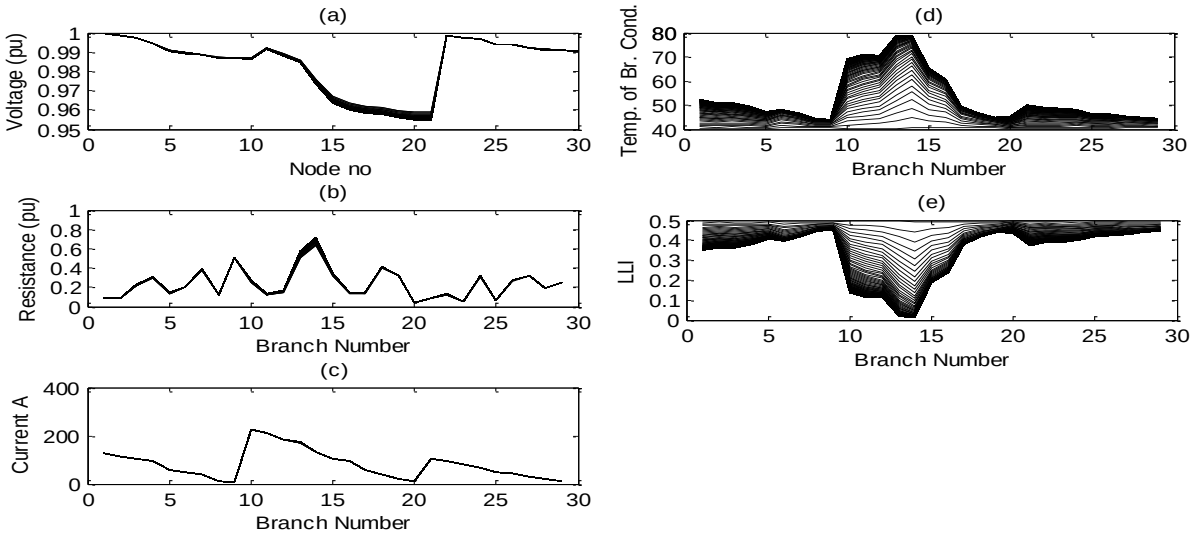

Fig. 4.10 The graphical representation of results for 30-node distribution network at time of maximum loadability limit when load of all nodes is increased with practical load modelling.

Table 4.9 The line loadability index for each branch current with different type of loading for 30-node distribution network.

Br no	*LLI* at λ=1.2 with practical load modelling	*LLI* with 1020 kVA load added at node 10 with practical load modelling	*LLI* with 250 kVA load added at node 21 with practical load modelling	*LLI* with 1210 kVA load added at node 30 with practical load modelling
1	0.34867	0.21038	0.37595	0.37595
2	0.36349	0.23146	0.38613	0.38613
3	0.3638	0.20413	0.38709	0.38709
4	0.37898	0.2283	0.39753	0.39753
5	0.40875	0.24512	0.41895	0.41895
6	0.39549	0.002337	0.41242	0.41242
7	0.41729	0.066052	0.42746	0.42746
8	0.44764	0.20051	0.44845	0.44845
9	0.44964	0.22332	0.44985	0.44985
10	0.13877	0.23502	0.17857	0.23443
11	0.11513	0.21965	0.15368	0.21965
12	0.11628	0.22154	0.14442	0.22154
13	0.017111	0.15776	0.047778	0.15776
14	0.01419	0.15767	0.0090907	0.15767
15	0.18604	0.2708	0.15694	0.2708
16	0.24074	0.3074	0.20603	0.3074
17	0.37873	0.40103	0.33896	0.40103
18	0.41685	0.42722	0.38151	0.42722
19	0.43944	0.4428	0.41188	0.4428
20	0.436	0.4362	0.43102	0.4362
21	0.37628	0.39485	0.39491	0.21179
22	0.38794	0.40295	0.40295	0.2322
23	0.39129	0.406	0.406	0.20505
24	0.40112	0.41367	0.41367	0.17466
25	0.4188	0.42589	0.42589	0.21887
26	0.42356	0.42919	0.42919	0.23254
27	0.43219	0.43775	0.43775	0.0041789
28	0.43851	0.44213	0.44213	0.036779
29	0.44708	0.44807	0.44807	0.097357

the operating temperature of branch conductors is get to be stabilized. The study of loadability limits can be significant in follow cases:

(i) In the planning stage it can be computed that how much load growth can be catered by the network.

(ii) Sometimes a situation may arise if the neighboring feeder has outage and a part of load has to be supplied by the network under consideration, it can be computed that how much load can be added to a node without violating the safe operating limits etc.

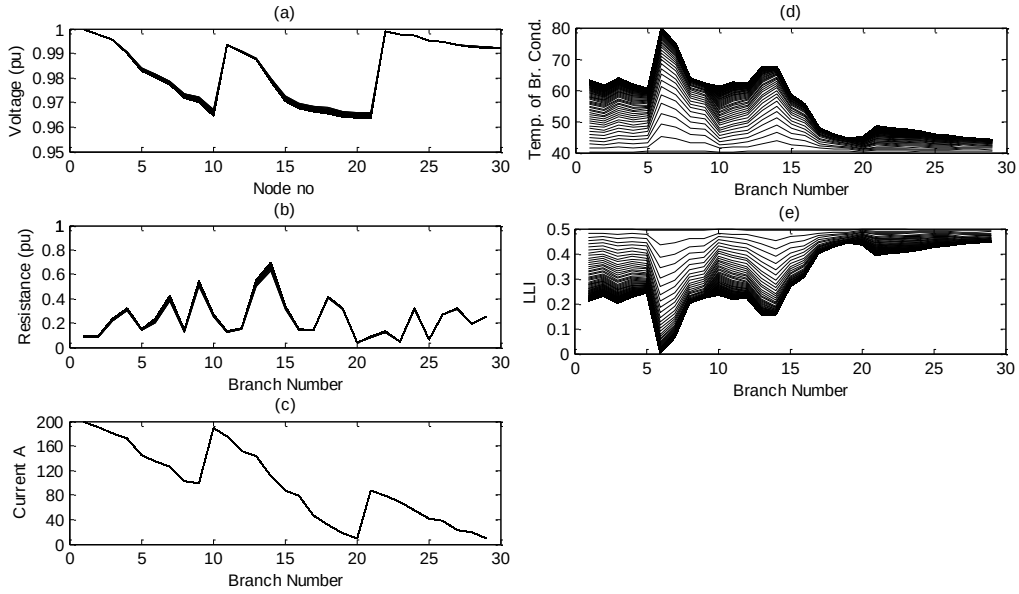

Fig. 4.11 The graphical representation of results for 30-node distribution network at time of maximum loadability limit when load is added at node 10 with practical load modelling.

Same types of loading conditions are studied for line loadability limits those are studied for voltage stability limits. Figure 4.2 shows the *VSI* of each node, resistance of each branch, current in each branch, *LLI* of each branch and real power losses in each branch at normal load. The loadability limit of the network is checked by computing the *LLI* for each

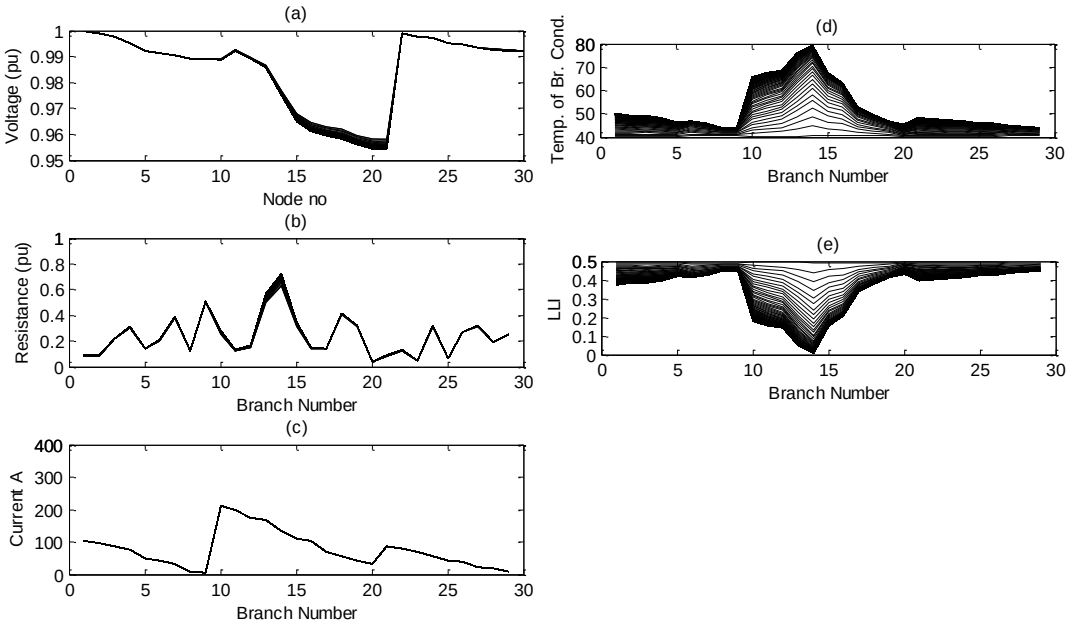

Fig. 4.12 The graphical representation of results at time of maximum loadability limit when load is added at node 21 with practical load modelling.

branch. Figure 4.9 shows node voltage, branch resistance, branch current, branch temperature and Line loadability index for the loadability limit occurred at λ=1.2. For above discussed loading, the values of *LLI* for each branch are also shown in tabulated form in Table 4.9. The results for end node loading with practical load modelling are also shown in Table 4.9. Table 4.7 shows the maximum load that can be added at node 10, node 21 and node 30 and respective line loadability index of most sensitive branch for constant power load and practical load modelling. Figure 4.11, Fig. 4.12 and Fig. 4.13 show the graphical results of end node loading for practical load modelling.

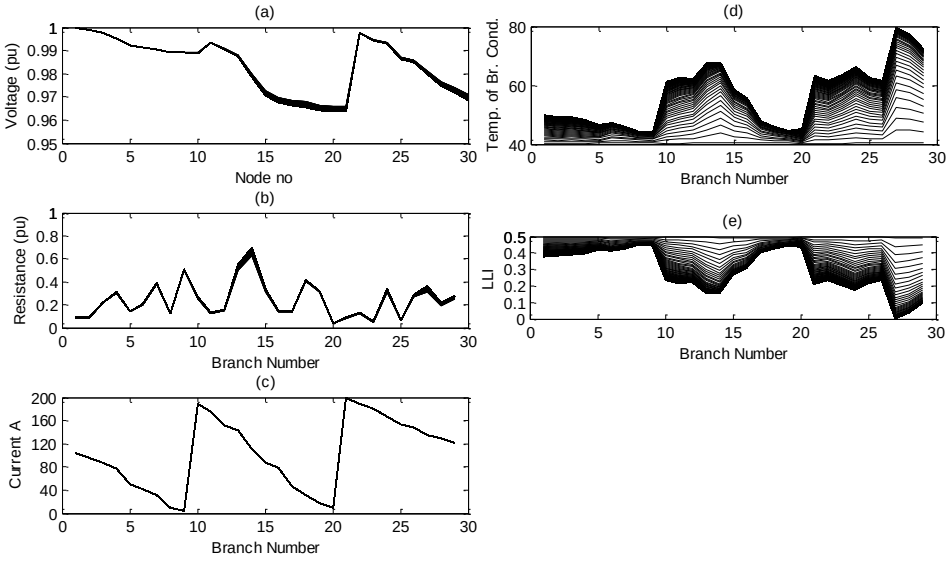

Fig. 4.13 The graphical representation of results for 30-node distribution network at time of maximum loadability limit when load is added at node 30 with practical load modelling.

4.9. Conclusion:

The proposed method in this chapter is a step ahead the previous research in the field of voltage stability studies and line loadability studies. With the incorporation of change in resistance of the branch conductors due to change in temperature makes the results more realistic and near to the practical conditions. The ability of proposed *VSI* and *LLI* to consider the effect of weather and ambient conditions has not been incorporated in any previous methods. Other novelties of the proposed *VSI* and *LLI* are that the voltage stability and line loadability of the distribution network are discussed in context of time and protection system.

CHAPTER 5

OPTIMAL CONDUCTOR SIZE SELECTION FOR RADIAL ELECTRIC POWER DISTRIBUTION NETWORKS

5.1 Introduction:

In transmission and distribution networks line conductors is the most important part. The conductors are major component of the capital investment. Variable cost of distribution network depends upon the losses. The losses in distribution network are dependent on the conductor size. Even the critical loading limit of distribution network also depends upon the conductor size. For the enhancement of critical loading the optimal conductor sizes selection for each branch is utmost necessary. The voltage stability limit of the distribution networks can also be improved by optimal conductor placement. The fault bearing capacity and reliability are governed by the conductor size. The rigorous literature survey is shown in **Section 2.4** of **Chapter** 2. From the literature survey following gaps of previous research are identified.

Sivanagaraju ***et al.*** [57] proposed that the voltage of each node is to be checked against the minimum acceptable node voltage. Suppose an end node or a node nearby end node violate the condition, according to their approach conductor size of the branch feeding to this node has to be upgraded. But practically it is observed that the branches at the end node are least responsible in voltage drop. So such upgradation of conductor is neither economically nor technically justified. The term load factor is also used in different way by the authors of this paper.

In the method proposed by Kaur and Sharma [58] the method adopted for computation of voltage at each node was not clear because voltage at the nodes common for different routes would be different. The value, which would be the correct one, was not discussed. In a situation when the conductor placed in some branches were of the maximum size available in inventory and the receiving-end nodes of these branches violate the maximum voltage drop, the method suggested would upgrade the next branch where the upgradation was possible but this very branch might or might not be the right candidate branch for conductor upgradation. The term load factor has been misunderstood by the authors because it is the ratio of average load to the maximum load for a pre specified period of time. So the maximum load would have to be served by the feeder for at least a minimum period of time. So the conductor sizes selected must be able to bear the peak load of the network. In their example of 123-node network, the proposed conductor sizes near the substation node would not be able to take that much load current.

The current carrying capacity of the conductor is not a constant parameter for a particular conductor, because the environment conditions and the heat generated in the conductor due to the current through it made the considerable change in the current carrying capacity. This fact has not been incorporated in any of the reported works.

In 11kV or of higher voltage feeders, the connected loads were generally not the single load rather they were the group of load in the consumer premises or loads connected to 11kV/440V transformer. Usually these were not switched on simultaneously. Hence a load contribution factor was observed. Contribution factor was defined by Gonen [59]. In conductor size selection, the effect of load contribution factor should be incorporated.

A procedure for optimal conductor size selection has been proposed in this chapter. The limitations of previous methods are removed in the proposed method.

5.2 Problem formulation:

The problem of conductor size selection for radial distribution system is solved by incorporating the effect of change in conductor resistance with the change in temperature due to heat losses in the conductor. By incorporating this effect, the value of real power losses computed will be exact. The economical choice of conductor size also depends on the cost of energy and power. Hence the choice will be more practical and correct. The constraints of at least minimum allowable voltage at each node of the network and the loadability limit of the branch conductors are considered. The loadability limit is related to the steady state temperature and the maximum allowable temperature of the branch conductor. The conductor selection by putting this as constraint will be more practical than simply considering its current carrying capacity, which is specified in the manufacturer's data sheet.

5.3 Objective Function:

The objective function consists of cost of the conductor for each branch, cost of its scrap value at the end of the plan period, cost of the energy losses and the cost of power. The effect of improvement of load contribution factor, load factor and effect of escalation of cost of energy and power with the time are incorporated.

$$\text{Min. } F_{jj,k} = CL_{(jj,k)} + CC_{jj,k} \qquad (5.1)$$

$CL_{(jj,k)}$ is the cost related to energy losses in branch-jj with k type of conductor.

$$CL_{(jj,k)} = \sum_{pp=1}^{n} \left[\frac{Loss_{(jj,k,pp)} \left[K_p \ 1+\Delta K_p \ ^{pp} + 8760 K_e Lsf_{(pp)} \ 1+\Delta K_p \ ^{pp} \right]}{1+dr \ ^{pp}} \right] \quad (5.2)$$

$$\mathrm{CC}_{(\mathrm{jj,k})} = \left[\mathrm{Cost}_{(\mathrm{k})} \mathrm{l}_{(\mathrm{jj})} - \ \mathrm{Scrap}_{(\mathrm{k})} \mathrm{l}_{(\mathrm{jj})} \right] \quad (5.3)$$

Branch Real power loss of branch jj

$$Loss_{(jj,k,pp)} = \left(\sum_{m=K+1}^{N} \frac{P_{(m,pp)}^2 + Q_{(m,pp)}^2}{V_{(m,pp)}^2} \right) R_{jj} \quad (5.4)$$

Total real power loss of the network for pp th year

$$= \sum_{jj=1}^{N-1} \left[\left(\sum_{m=K+1}^{N} \frac{P_{(m,pp)}^2 + Q_{(m,pp)}^2}{V_{(m,pp)}^2} \right) R_{jj} \right] \quad (5.5)$$

$$P_{(m,pp)} = F_c (1+\Delta F_c)^{pp} P_{(m,pp=1)} \quad (5.6)$$

$$Q_{(m,pp)} = F_c (1+\Delta F_c)^{pp} Q_{(m,pp=1)} \quad (5.7)$$

5.4 Constraints:

The objective function represented in Eq. 5.1 is minimized within the constraints of at least minimum allowable voltage at end nodes and line loadability index of each branch should be at least more than zero. But normally the minimum value of the line loadability index should be quite more than one for safe and reliable operation.

(i) Minimum allowable voltage at end nodes: It is considered that the minimum voltage level has to be maintained at the end nodes while optimal conductors for each branch are

selected. The procedure adopted is such that at first the economical conductor sizes are selected for each branch of the network. After that the voltage at the end nodes is checked if any of the end nodes violates the minimum limit, the branches at the route from substation to that very end node are identified. Then conductor size of that branch is upgraded, which has maximum voltage drop per kilometer. If the situation arises that the conductor of the candidate branch is the highest size available in inventory, the branch having next highest voltage drop per kilometer is considered and so on.

(ii) Line Loadability Index: Current carrying capacity of the conductor is constrained by the thermal limits of the conductor. Commonly 80□C is considered the maximum temperature for steady state loading of the overhead conductors. Beyond this temperature the tensile strength of the conductor reduces considerably and the conductor gets elongated permanently. To avoid the permanent loss of the strength and deformation of the conductor, the loading of the conductors should be within this limit and this limit is the loadability limit of the overhead conductors. It is discussed comprehensively in **Section 4.1.2 of Chapter 4**.

Let the maximum operating temperature $T_{jj(max)}$ of the branch-jj's conductor is 80□C.

The actual operating temperature of branch jj is T_{jj} .

$$\text{Line Loadability Index } (LLI) = \frac{T_{jj\ \max} - T_{jj}}{T_{jj\ \max}} \qquad (5.7)$$

The procedure to compute conductor temperature had been discussed in Le ***et al.*** [47] and comprehensively in IEEE Std. 738™-2006 [46] with associated definitions and tables of various constants and variables. However, the procedure to compute conductor temperature is discussed in brief in **Section 4.2 of Chapter 4**.

In all the previously reported work current carrying capacity of the conductors is taken as one of the constraints but taking *LLI* as the constraint is one step ahead of the reported work. A conductor may take more current in cold and windy region compared to in hot and still air.

The Line loadability index of each branch should be more than the minimum pre-defined limit for safe steady state operation of the network. After considering the voltage constraint if some branch violates the minimum *LLI* limit then the conductor of that very branch is up graded till its *LLI* is more than the minimum value.

5.5 Procedural steps for optimal conductor size selection:

1) Run the load-flow program using zero resistance, zero reactance of each branch and 1p.u. each node voltage. Select the conductor sizes according to their current carrying capacities. The load-flow method proposed in **Chapter 3** is used here.
2) Run the load-flow program, compute objective function and upgrade the conductor size if possible.
3) Run the load-flow program, compute objective function and upgrade or reduce the conductor size if possible to minimize the value of the objective function. Repeat this step till most economical conductor sizes are selected.
4) Run the load-flow program, apply the constraints and change the conductor size to avoid any violation of the constraints.
5) Print the results.

More detailed procedure has been presented in the flow chart as shown in Fig. 5.1.

5.6 Values of various parameters used:

While computing the conductor temperature and Line loadability index the value of various parameters related to environmental conditions and physical position of the line are shown below.

Q_{jjse} =1100

H_e =1000

H_c =72.5

Z_c =139

Z_1 =90

α =0.5

ε =0.5

φ =90

T_a =40

v =1.

The objective function is computed with the following values of various variables.

K_p =Rs. 5000/kW

K_e = Rs. 4.5/ kWh

ΔK_p =0.5%.

ΔK_e =0.5%.

pp=10 years.

$Lsf = 0.8Lf^2 + 0.2Lf$

Lf = 0.5

ΔLf : 1%.

F_c = Load contribution factor = 0.4 for Example 5.1 and 0.2 for Example 5.2.

ΔF_c =1%.

$Cost_{(k)}$ = Rs.130/kg/km.

$Scrap_{(k)}$ 20% of $Cost_{(k)}$.

dr= 2.15.

Reactance = 0.38ohm/km. For 123-node network as is used in Kaur and Sharma [58].

The conductor sizes available in inventory are enlisted in Table G2 (**Appendix-G**). These are the same sizes used by Kaur and Sharma [58].

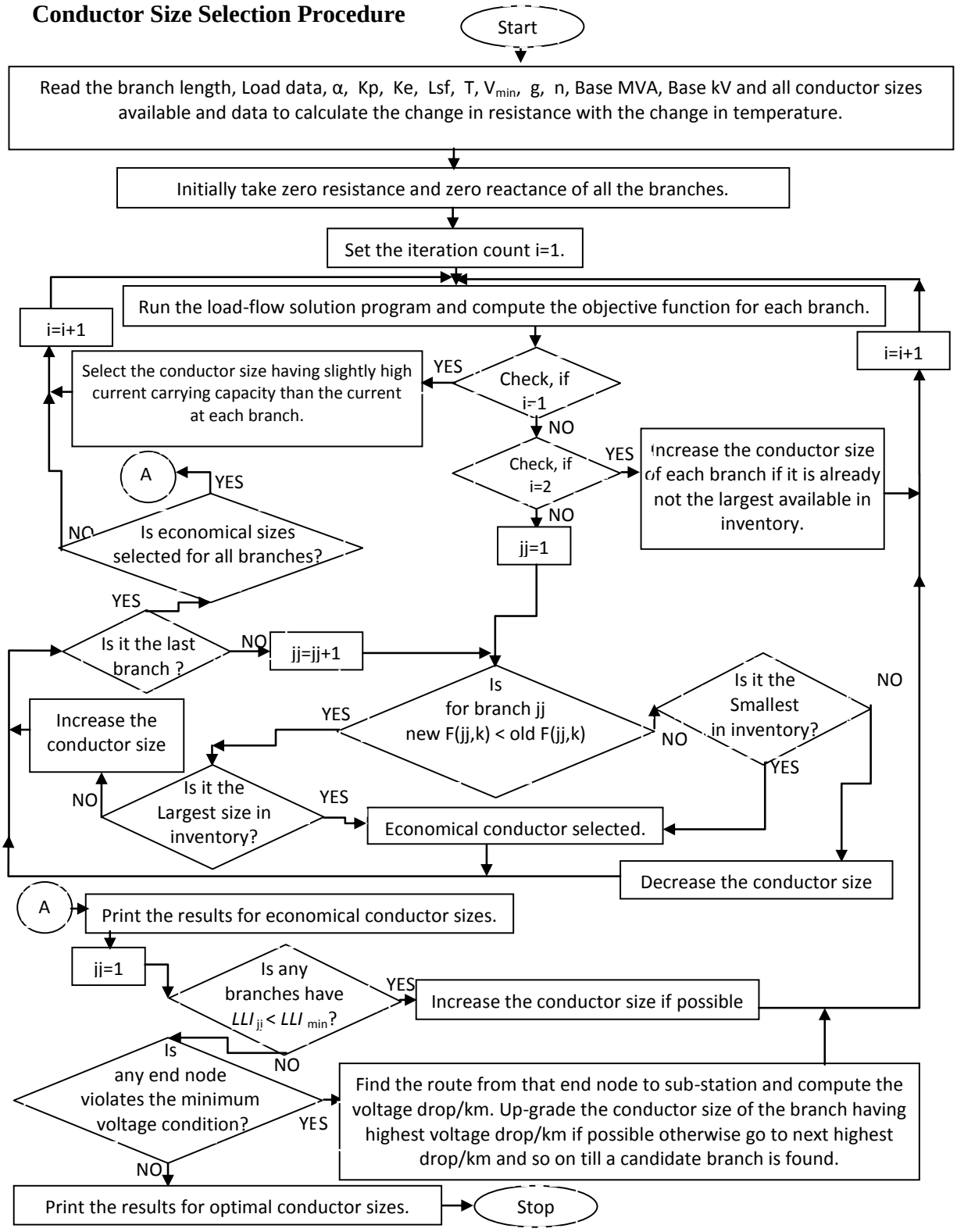

Fig. 5.1 Flow Chart showing the procedural steps for optimal conductor size selection.

5.7 Examples:

To show the goodness of the proposed approach two examples of the radial power distribution networks are considered. First example is the 123-node radial distribution network. Its single line diagram, line data and load data are available in Kaur and Sharma [58]. The single line diagram is also shown in Fig. 5.2. The line data, load data and conductor sizes available in inventory are given in Table G 1 and Table G 2 (**Appendix-G**).

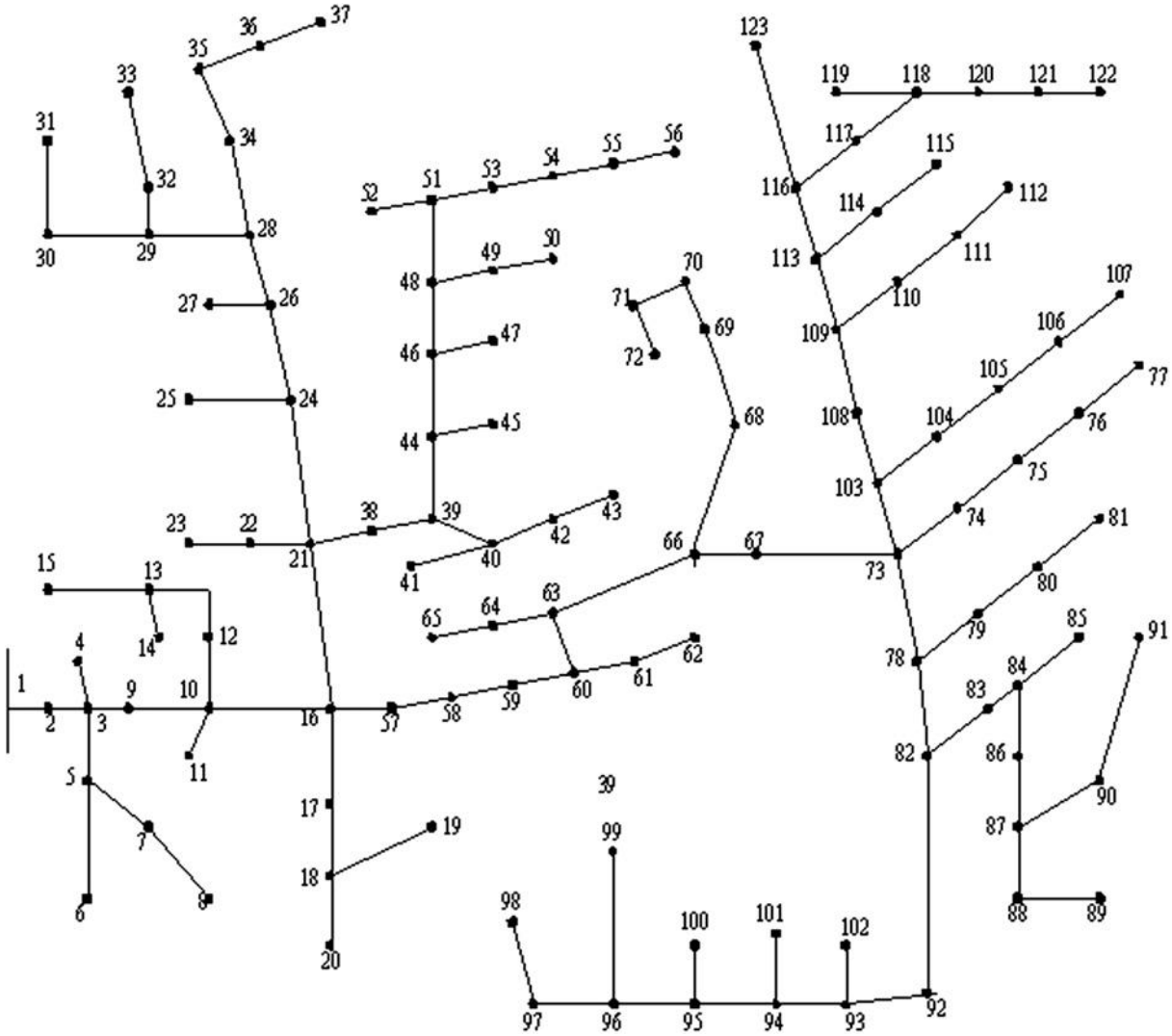

Fig. 5.2 Single-line diagram of 123-node radial distribution network [58].

The results are compared for proposed method and the existing approach regarding node voltage, branch temperature, branch wise cost, branch losses, branch current and branch wise conductor sizes. For the existing method the same conductor sizes are taken those are proposed in original work. Same inventory availability is considered. The results shown in Fig. 5.3, Table 5.1, Table 5.2, Table 5.3 and Table 5.4 reveal that for same available conductor sizes, the conductor sizes selected by proposed approach are more economical and the system is comparatively more reliable on the basis of technical aspects like node voltage, branch current, branch temperature and branch losses. The total cost for the plan period and real power losses for existing method is 6.1064×10^5 rupees and 31.454 kW respectively. The total cost for the plan period and real power losses for existing method is 2.8036×10^5 rupees and 19.207 kW respectively.

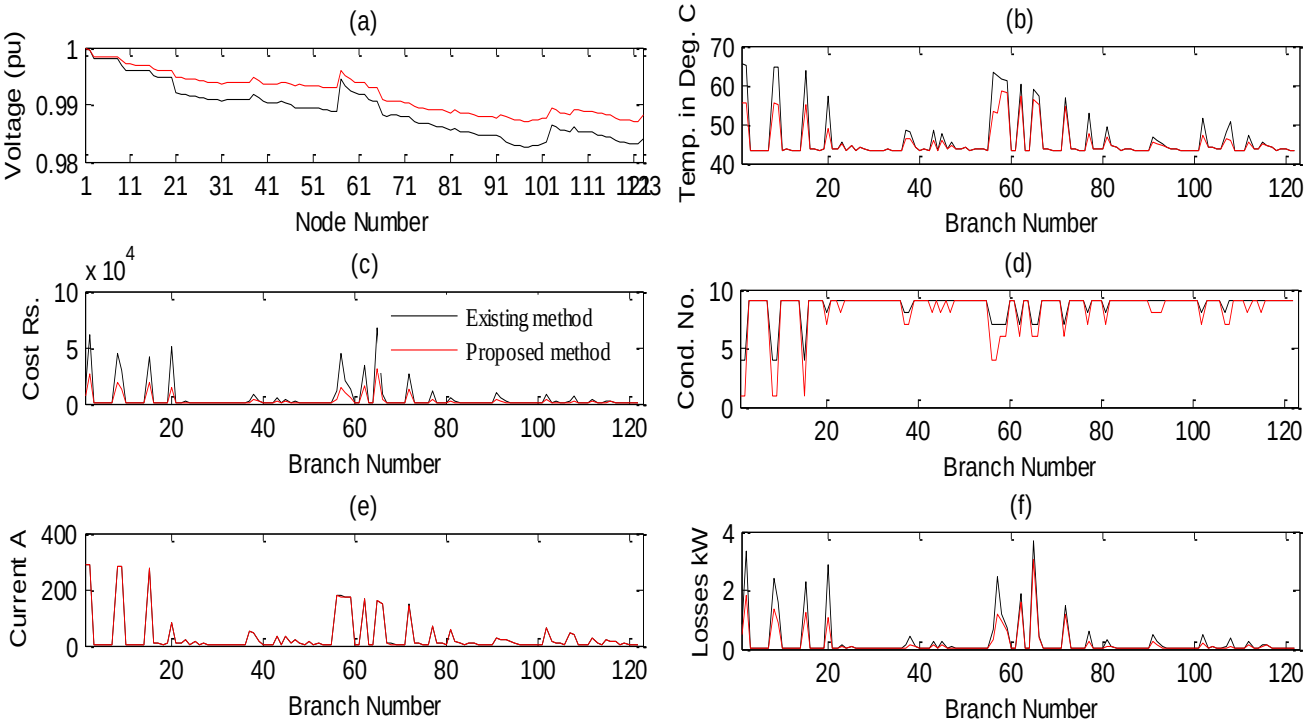

Fig. 5.3 The results for 123-node distribution network. Fig. 5.3 (a) comparison of node voltage (p.u.). Fig. 5.3 (b) comparison of branch Temperature. Fig. 5.3 (c) comparison of cost function. Fig. 5.3 (d) comparison of conductor sizes. Fig. 5.3 (e) comparison of branch current. Fig. 5.3 (f) comparison of branch losses.

Table 5.1 The results of node voltage, conductor no, cost function and loadability index for conductor size selected by Kaur and Sharma [58] for 123-node distribution network.

Node No.	Node Voltage magnitude (p.u.)	Branch no.	Cond. No.	Cost Function	Line loadability index
1	1	1	4	15355	0.18406
2	0.99961	2	4	61168	0.18512
3	0.99804	3	9	239.17	0.45745
4	0.99803	4	9	366.31	0.45711
5	0.99799	5	9	272.92	0.45745
6	0.99799	6	9	452.05	0.45737
7	0.99796	7	9	342.77	0.45743
8	0.99794	8	4	44759	0.19147
9	0.99688	9	4	29369	0.19549
10	0.99611	10	9	308.47	0.45743
11	0.9961	11	9	381.69	0.45633
12	0.99603	12	9	661.03	0.45681
13	0.99592	13	9	343.5	0.45742
14	0.99591	14	9	345.1	0.4574
15	0.9959	15	4	42251	0.20575
16	0.99498	16	9	434.64	0.45225
17	0.99487	17	9	257.67	0.45334
18	0.99481	18	9	483.16	0.4574
19	0.99478	19	9	209.49	0.45497
20	0.99476	20	8	50796	0.28659
21	0.99205	21	9	576.53	0.45426
22	0.99191	22	9	671.63	0.45507
23	0.99175	23	9	2844.5	0.42994
24	0.99154	24	9	799.5	0.45692
25	0.99142	25	9	1379.9	0.44336
26	0.99124	26	9	823.6	0.457
27	0.99113	27	9	897.18	0.45101
28	0.99102	28	9	657.41	0.45571
29	0.99087	29	9	421.08	0.45689
30	0.99081	30	9	723.32	0.45718
31	0.99072	31	9	317.76	0.45729
32	0.99084	32	9	411.72	0.45743
33	0.99083	33	9	331.37	0.45646
34	0.99096	34	9	471.34	0.45675
35	0.99088	35	9	513.36	0.45711
36	0.99081	36	9	289	0.45718
37	0.99078	37	8	2296.3	0.3935
38	0.99184	38	8	8102.7	0.39729
39	0.9911	39	9	2531.2	0.44887
40	0.99049	40	9	457.64	0.45691

41	0.99042	41	9	414.77	0.45645
42	0.99041	42	9	489.08	0.45698
43	0.99033	43	9	4965.7	0.39493
44	0.99046	44	9	449.66	0.45739
45	0.99043	45	9	4358.6	0.4031
46	0.98986	46	9	1514.4	0.4518
47	0.98948	47	9	1681.2	0.43358
48	0.98955	48	9	452.76	0.4544
49	0.98944	49	9	498.85	0.45644
50	0.98934	50	9	958.41	0.44907
51	0.98932	51	9	212.6	0.45728
52	0.9893	52	9	690.91	0.4527
53	0.98914	53	9	470.06	0.4557
54	0.98904	54	9	424.04	0.45633
55	0.98895	55	9	348.48	0.45735
56	0.98893	56	7	11474	0.21184
57	0.99461	57	7	44033	0.22134
58	0.99314	58	7	20954	0.2322
59	0.99243	59	7	12938	0.23479
60	0.99198	60	9	434.02	0.45673
61	0.99191	61	9	389.59	0.45728
62	0.99187	62	7	34109	0.24718
63	0.99078	63	9	384.43	0.45687
64	0.99072	64	9	344.64	0.45741
65	0.9907	65	7	66774	0.26447
66	0.98833	66	7	7902.7	0.28506
67	0.98802	67	9	591.07	0.45406
68	0.98818	68	9	338.67	0.45552
69	0.9881	69	9	521.05	0.45703
70	0.98803	70	9	601.71	0.45728
71	0.98797	71	9	445.61	0.45743
72	0.98796	72	7	26517	0.29179
73	0.98698	73	9	585.65	0.45214
74	0.98683	74	9	579.42	0.45493
75	0.98669	75	9	503.41	0.45683
76	0.98661	76	9	397.56	0.45718
77	0.98656	77	8	11395	0.34216
78	0.98619	78	9	811.13	0.45207
79	0.98598	79	9	919.9	0.45316
80	0.98575	80	9	721.97	0.45596
81	0.98559	81	8	5479.1	0.38115
82	0.98573	82	9	2242.6	0.44306
83	0.98525	83	9	355.4	0.45002
84	0.98516	84	9	309.67	0.45741
85	0.98514	85	9	1151.5	0.45386
86	0.98487	86	9	967.68	0.45517

87	0.98464	87	9	361.5	0.45718
88	0.9846	88	9	343.68	0.45742
89	0.98458	89	9	994.13	0.45709
90	0.98451	90	9	648.34	0.45745
91	0.9845	91	9	9319.1	0.417
92	0.9843	92	9	4613.4	0.42734
93	0.9835	93	9	1902.7	0.43862
94	0.98312	94	9	850.18	0.44926
95	0.98291	95	9	516.5	0.45429
96	0.98279	96	9	545.47	0.45591
97	0.98267	97	9	296.5	0.45705
98	0.98263	98	9	382.75	0.45736
99	0.98276	99	9	484.11	0.45661
100	0.98283	100	9	344.31	0.45689
101	0.98307	101	9	261	0.45702
102	0.98347	102	8	8956.1	0.35771
103	0.98631	103	9	1030	0.44937
104	0.98606	104	9	1841	0.45072
105	0.98561	105	9	719.75	0.45394
106	0.98543	106	9	1389.9	0.45619
107	0.98514	107	8	2078	0.3996
108	0.98612	108	9	6872.4	0.3693
109	0.98536	109	9	360.82	0.45664
110	0.98529	110	9	494.57	0.45692
111	0.98522	111	9	963.15	0.45742
112	0.98517	112	9	4327.7	0.40882
113	0.98474	113	9	455.76	0.45521
114	0.98463	114	9	1022.7	0.45605
115	0.98441	115	9	2771.4	0.43317
116	0.98423	116	9	2898.8	0.44023
117	0.98363	117	9	1253.6	0.4479
118	0.98333	118	9	788.58	0.45743
119	0.9833	119	9	329.36	0.45314
120	0.98325	120	9	988.22	0.4557
121	0.98302	121	9	446.55	0.45742
122	0.983	122	9	1371	0.45743
123	0.98417				
Total cost based on total cost of power, energy loss and cost of conductor for plan period = 6.1064×10^5 rupees.					

Table 5.2 The results of branch current, branch operating temperature and branch losses for conductor size selected by Kaur and Sharma [58] for 123-node distribution network.

Branch No.	Branch current	Branch operating temp.	Branch losses
1	287.3	65.275	0.8371
2	286.7	65.19	3.3335
3	0.48391	43.404	3.7853×10^{-005}
4	2.562	43.431	0.001516
5	0.31313	43.404	1.8114×10^{-005}
6	1.338	43.411	0.00053743
7	0.71738	43.405	0.00011885
8	283.12	64.682	2.4339
9	280.83	64.361	1.5946
10	0.71301	43.405	0.00010566
11	4.6267	43.494	0.0044505
12	3.5144	43.455	0.0048496
13	0.83866	43.406	0.00016243
14	1.0555	43.408	0.00025726
15	274.87	63.54	2.285
16	9.9211	43.82	0.013659
17	8.8246	43.733	0.007202
18	1.0567	43.408	0.00036097
19	6.8541	43.602	0.0043427
20	84.084	57.073	2.8824
21	7.78	43.659	0.013991
22	6.7202	43.594	0.013567
23	22.745	45.604	0.14453
24	3.2036	43.447	0.0049779
25	16.307	44.531	0.061662
26	2.938	43.44	0.0043859
27	11.036	43.919	0.030996
28	5.7518	43.543	0.010701
29	3.2861	43.449	0.0027435
30	2.317	43.426	0.0024796
31	1.7777	43.417	0.0006568
32	0.77415	43.406	0.00016608
33	4.3438	43.483	0.0034869
34	3.6558	43.46	0.0037043
35	2.5806	43.431	0.0021533
36	2.2939	43.425	0.00097218
37	50.093	48.52	0.12028
38	48.415	48.217	0.42086
39	12.736	44.091	0.097631
40	3.2298	43.447	0.0028912
41	4.3602	43.484	0.0043916
42	3.0178	43.442	0.0027344

43	34.16	48.406	0.27445
44	1.1473	43.409	0.0003952
45	31.877	47.752	0.23842
46	10.336	43.856	0.049424
47	21.197	45.313	0.083589
48	7.6035	43.648	0.01069
49	4.3877	43.485	0.0053365
50	12.583	44.074	0.036651
51	1.8666	43.418	0.00048277
52	9.479	43.784	0.020778
53	5.7625	43.544	0.0076722
54	4.625	43.494	0.0049413
55	1.4076	43.412	0.00045758
56	179.86	63.053	0.64633
57	176.21	62.293	2.4748
58	171.91	61.424	1.1743
59	170.87	61.217	0.72457
60	3.7177	43.462	0.0035116
61	1.856	43.418	0.00087508
62	165.78	60.225	1.9031
63	3.3493	43.451	0.0025909
64	0.99792	43.407	0.00022997
65	158.36	58.843	3.7033
66	148.96	57.195	0.4344
67	8.016	43.675	0.014853
68	6.0611	43.559	0.0059418
69	2.8409	43.437	0.0026097
70	1.8403	43.418	0.0013297
71	0.71888	43.405	0.00015515
72	145.74	56.657	1.4526
73	10.02	43.828	0.018576
74	6.9106	43.605	0.01214
75	3.4555	43.454	0.0035852
76	2.3037	43.426	0.0013482
77	68.746	52.628	0.63221
78	10.087	43.834	0.02589
79	9.0099	43.747	0.026278
80	5.3267	43.523	0.010488
81	55.201	49.508	0.29316
82	16.476	44.555	0.10072
83	11.851	43.998	0.013001
84	0.9228	43.407	0.00017699
85	8.2518	43.692	0.029908
86	6.5788	43.586	0.019003
87	2.3083	43.426	0.0012305
88	0.86562	43.406	0.00017304

89	2.6548	43.433	0.0043948
90	0.34628	43.404	5.2611×10^{-005}
91	27.543	46.64	0.49638
92	23.791	45.813	0.23737
93	18.84	44.911	0.090665
94	12.442	44.059	0.032251
95	7.7362	43.657	0.01245
96	5.4063	43.527	0.0081033
97	2.7697	43.436	0.0014174
98	1.3587	43.411	0.00046892
99	4.0121	43.471	0.0044618
100	3.2771	43.449	0.0022324
101	2.8713	43.438	0.0013329
102	63.714	51.383	0.49149
103	12.356	44.05	0.038876
104	11.279	43.942	0.064758
105	8.1543	43.685	0.018445
106	4.9024	43.505	0.017767
107	47.36	48.032	0.10732
108	40.446	50.456	0.3876
109	3.9308	43.469	0.0032121
110	3.1927	43.446	0.0030606
111	0.90893	43.407	0.0005342
112	30.172	47.294	0.23457
113	6.5218	43.583	0.0088459
114	5.1657	43.516	0.014179
115	21.377	45.346	0.13817
116	18.017	44.781	0.13562
117	13.431	44.168	0.050126
118	0.73385	43.406	0.00028604
119	9.0333	43.749	0.009434
120	5.7742	43.544	0.016177
121	0.83811	43.406	0.00021088
122	0.71588	43.405	0.00047339
Total real power losses 31.454 kW			

Table 5.3 The results of node voltage, conductor no, cost function and loadability index for conductor size selected by proposed method for 123-node distribution network.

Node No.	Node Voltage (p.u.)	Branch no.	Cond. No.	Cost Function	Line loadability index
1	1	1	1	6598.4	0.30534
2	0.9997	2	1	26326	0.30583
3	0.99851	3	9	238.86	0.45745
4	0.9985	4	9	353.53	0.45711
5	0.99846	5	9	272.77	0.45745
6	0.99845	6	9	447.52	0.45737
7	0.99843	7	9	341.77	0.45743
8	0.99841	8	1	19444	0.30871
9	0.99762	9	1	12835	0.31053
10	0.99704	10	9	307.58	0.45743
11	0.99702	11	9	344.12	0.45633
12	0.99696	12	9	620.09	0.45681
13	0.99685	13	9	342.13	0.45742
14	0.99683	14	9	342.93	0.4574
15	0.99683	15	1	18766	0.31519
16	0.99618	16	9	319.27	0.45226
17	0.99607	17	9	196.84	0.45335
18	0.996	18	9	480.11	0.4574
19	0.99598	19	9	172.81	0.45498
20	0.99595	20	7	14077	0.3905
21	0.99479	21	9	458	0.45427
22	0.99464	22	9	556.68	0.45508
23	0.99448	23	8	1423.2	0.43878
24	0.99451	24	9	757.3	0.45692
25	0.99439	25	9	857.21	0.44344
26	0.99421	26	9	786.42	0.45701
27	0.99409	27	9	634.45	0.45105
28	0.99399	28	9	566.7	0.45572
29	0.99384	29	9	397.82	0.45689
30	0.99377	30	9	702.3	0.45718
31	0.99369	31	9	312.19	0.45729
32	0.99381	32	9	410.31	0.45743
33	0.99379	33	9	301.82	0.45647
34	0.99392	34	9	439.95	0.45676
35	0.99384	35	9	495.11	0.45711
36	0.99378	36	9	280.76	0.45718
37	0.99374	37	7	977.48	0.42116
38	0.99469	38	7	3567.4	0.42227
39	0.99432	39	9	1703.3	0.44892
40	0.99372	40	9	433.12	0.45691
41	0.99365	41	9	377.53	0.45646

42	0.99364	42	9	465.89	0.45698
43	0.99357	43	8	1832.2	0.42426
44	0.99398	44	9	446.3	0.45739
45	0.99395	45	8	1681.5	0.42765
46	0.99365	46	9	1094.8	0.45185
47	0.99327	47	8	894.05	0.44032
48	0.99348	48	9	361.97	0.45442
49	0.99337	49	9	453.53	0.45645
50	0.99327	50	9	647.14	0.44914
51	0.99325	51	9	208.5	0.45728
52	0.99323	52	9	514.45	0.45274
53	0.99308	53	9	404.9	0.45572
54	0.99297	54	9	382.07	0.45634
55	0.99289	55	9	344.59	0.45736
56	0.99286	56	4	3880.7	0.33658
57	0.99594	57	4	15087	0.34039
58	0.995	58	6	9754.1	0.27134
59	0.99437	59	6	6031.8	0.27341
60	0.99398	60	9	404.31	0.45673
61	0.99391	61	9	382.19	0.45728
62	0.99387	62	6	16026	0.28331
63	0.99293	63	9	362.5	0.45687
64	0.99287	64	9	342.7	0.45741
65	0.99285	65	6	31764	0.29713
66	0.99077	66	6	3826.2	0.31361
67	0.99051	67	9	465.3	0.45408
68	0.99063	68	9	288.35	0.45553
69	0.99055	69	9	498.95	0.45703
70	0.99048	70	9	590.45	0.45728
71	0.99042	71	9	444.3	0.45743
72	0.9904	72	6	12924	0.319
73	0.98958	73	9	428.31	0.45217
74	0.98944	74	9	476.59	0.45495
75	0.9893	75	9	473.05	0.45683
76	0.98922	76	9	386.14	0.45718
77	0.98917	77	7	3656.8	0.40632
78	0.98921	78	9	591.65	0.45211
79	0.989	79	9	697.14	0.45319
80	0.98877	80	9	633.06	0.45597
81	0.98862	81	7	2125	0.41758
82	0.98899	82	9	1388.3	0.44316
83	0.9885	83	9	245.13	0.45007
84	0.98842	84	9	308.17	0.45741
85	0.9884	85	9	897.8	0.45388
86	0.98813	86	9	806.51	0.45519
87	0.9879	87	9	351.07	0.45718

88	0.98786	88	9	342.21	0.45742
89	0.98784	89	9	956.86	0.45709
90	0.98777	90	9	647.9	0.45745
91	0.98776	91	8	3987.4	0.43343
92	0.9882	92	8	2218.9	0.43772
93	0.98777	93	8	1126.1	0.44243
94	0.98756	94	9	575.99	0.44933
95	0.98736	95	9	410.65	0.45432
96	0.98723	96	9	476.58	0.45593
97	0.98711	97	9	284.45	0.45706
98	0.98707	98	9	378.76	0.45736
99	0.9872	99	9	446.18	0.45662
100	0.98727	100	9	325.33	0.4569
101	0.98751	101	9	249.67	0.45703
102	0.98773	102	7	3058.9	0.41079
103	0.98927	103	9	700.45	0.44942
104	0.98902	104	9	1292.1	0.45076
105	0.98856	105	9	563.41	0.45396
106	0.98838	106	9	1239.3	0.4562
107	0.9881	107	7	935.21	0.42295
108	0.98917	108	7	2098.3	0.427
109	0.98897	109	9	333.56	0.45665
110	0.98891	110	9	468.6	0.45692
111	0.98883	111	9	958.61	0.45742
112	0.98878	112	8	1733.1	0.43002
113	0.98863	113	9	380.64	0.45523
114	0.98853	114	9	902.29	0.45606
115	0.98831	115	8	1462.4	0.44015
116	0.98835	116	9	1746.5	0.44038
117	0.98776	117	9	827.74	0.44798
118	0.98746	118	9	786.15	0.45743
119	0.98743	119	9	249.21	0.45318
120	0.98738	120	9	850.78	0.45571
121	0.98716	121	9	444.76	0.45742
122	0.98714	122	9	1367	0.45743
123	0.9883				
Total cost based on total cost of power, energy loss and cost of conductor for plan period = 2.8036×10^5 rupees.					

Table 5.4 The results of branch current, branch operating temperature and branch losses for conductor size selected by proposed method for 123-node distribution network.

Branch No.	Branch current	Branch operating temperature	Branch losses
1	286.4	55.573	0.46559
2	285.8	55.534	1.8544
3	0.48368	43.404	3.7817×10^{-005}
4	2.5608	43.431	0.0015145
5	0.31298	43.404	1.8097×10^{-005}
6	1.3373	43.411	0.00053693
7	0.71705	43.405	0.00011873
8	282.23	55.303	1.3551
9	279.93	55.158	0.8883
10	0.71235	43.405	0.00010546
11	4.6224	43.494	0.0044423
12	3.5111	43.455	0.0048405
13	0.83788	43.406	0.00016212
14	1.0545	43.408	0.00025678
15	273.98	54.784	1.2747
16	9.9092	43.819	0.013626
17	8.814	43.732	0.0071847
18	1.0554	43.408	0.00036011
19	6.8459	43.602	0.0043322
20	83.801	48.76	1.1006
21	7.7585	43.658	0.013914
22	6.7017	43.593	0.013493
23	22.677	44.898	0.072979
24	3.1941	43.446	0.0049483
25	16.258	44.525	0.061293
26	2.9292	43.44	0.0043598
27	11.003	43.916	0.030811
28	5.7347	43.542	0.010638
29	3.2763	43.449	0.0027271
30	2.31	43.426	0.0024648
31	1.7723	43.417	0.00065289
32	0.77184	43.406	0.00016509
33	4.3308	43.483	0.0034661
34	3.6448	43.459	0.0036822
35	2.5729	43.431	0.0021404
36	2.287	43.425	0.00096638
37	49.91	46.307	0.046899
38	48.236	46.219	0.16422
39	12.694	44.086	0.096996
40	3.2193	43.447	0.0028725
41	4.3461	43.483	0.0043631
42	3.008	43.442	0.0027167
43	34.027	46.059	0.13751

44	1.1433	43.409	0.0003924
45	31.752	45.788	0.11962
46	10.297	43.852	0.049046
47	21.113	44.775	0.042151
48	7.5734	43.646	0.010606
49	4.3703	43.484	0.0052943
50	12.533	44.069	0.036361
51	1.8592	43.418	0.00047895
52	9.4414	43.781	0.020614
53	5.7396	43.543	0.0076115
54	4.6067	43.493	0.0049022
55	1.4021	43.412	0.00045396
56	179.27	53.073	0.31234
57	175.62	52.769	1.1977
58	171.33	58.292	0.96554
59	170.29	58.127	0.59582
60	3.7102	43.461	0.0034974
61	1.8523	43.418	0.00087156
62	165.21	57.335	1.5658
63	3.342	43.45	0.0025797
64	0.99576	43.407	0.00022898
65	157.81	56.23	3.0495
66	148.44	54.912	0.35806
67	7.9962	43.674	0.01478
68	6.0461	43.558	0.0059125
69	2.8339	43.437	0.0025968
70	1.8358	43.417	0.0013231
71	0.71711	43.405	0.00015438
72	145.22	54.48	1.1977
73	9.9933	43.826	0.018478
74	6.8923	43.604	0.012076
75	3.4464	43.453	0.0035663
76	2.2976	43.426	0.0013411
77	68.492	47.495	0.24394
78	10.057	43.832	0.025731
79	8.9824	43.745	0.026118
80	5.3105	43.523	0.010424
81	54.989	46.594	0.11398
82	16.421	44.547	0.10006
83	11.812	43.994	0.012915
84	0.91976	43.407	0.00017582
85	8.2246	43.69	0.029711
86	6.5571	43.585	0.018877
87	2.3007	43.426	0.0012224
88	0.86276	43.406	0.0001719
89	2.646	43.433	0.0043659

90	0.34513	43.404	5.2265×10^{-005}
91	27.422	45.326	0.24939
92	23.685	44.982	0.11945
93	18.755	44.606	0.045709
94	12.386	44.053	0.031961
95	7.7014	43.654	0.012339
96	5.382	43.526	0.0080304
97	2.7572	43.435	0.0014047
98	1.3525	43.411	0.00046471
99	3.994	43.471	0.0044217
100	3.2623	43.448	0.0022123
101	2.8589	43.438	0.0013214
102	63.482	47.137	0.19026
103	12.319	44.046	0.038644
104	11.245	43.939	0.06437
105	8.1299	43.683	0.018335
106	4.8877	43.504	0.01766
107	47.177	46.164	0.041882
108	40.284	45.84	0.076254
109	3.9165	43.468	0.0031887
110	3.181	43.446	0.0030382
111	0.90561	43.407	0.0005303
112	30.048	45.598	0.11775
113	6.4961	43.582	0.0087763
114	5.1454	43.515	0.014068
115	21.287	44.788	0.069638
116	17.942	44.77	0.13448
117	13.374	44.161	0.049707
118	0.73078	43.405	0.00028365
119	8.9955	43.746	0.0093551
120	5.75	43.543	0.016042
121	0.8346	43.406	0.00020911
122	0.71289	43.405	0.00046944
Real power losses =19.207 kW			

Second example is a 32-node branched radial distribution network as shown in Fig. 5.4. The line data and load data are available in Sivanagaraju [57], which has been shown in **Appendix-F**. The results regarding node voltage, branch conductor temperature, branch wise losses, branch wise current, branch wise cost and branch wise conductor type selected are shown in Fig. 5.5, Table 5.5, Table 5.6, Table 5.7 and Table 5.8. The results of all the

aspects of the distribution network are batter with the proposed approach than the existing. The total cost for the plan period and real power losses for existing method is 5.2543×10^5 rupees and 33.214 kW respectively. The total cost for the plan period and real power losses for proposed method is 4.85954×10^5 rupees and 32.64 kW respectively.

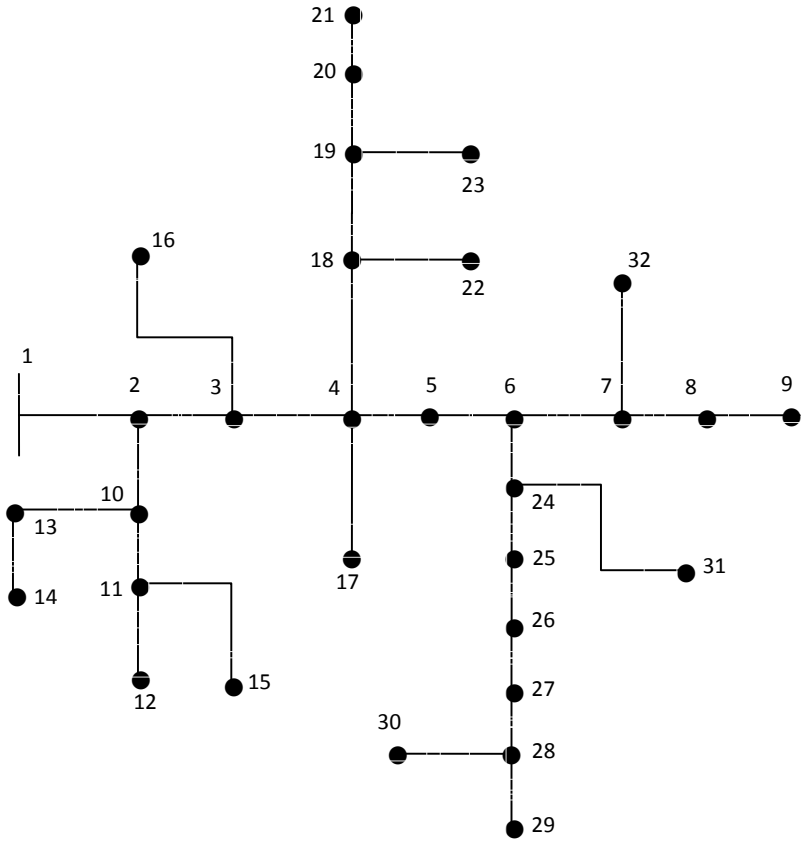

Fig. 5.4 Single-line diagram of 32-node radial power distribution network.

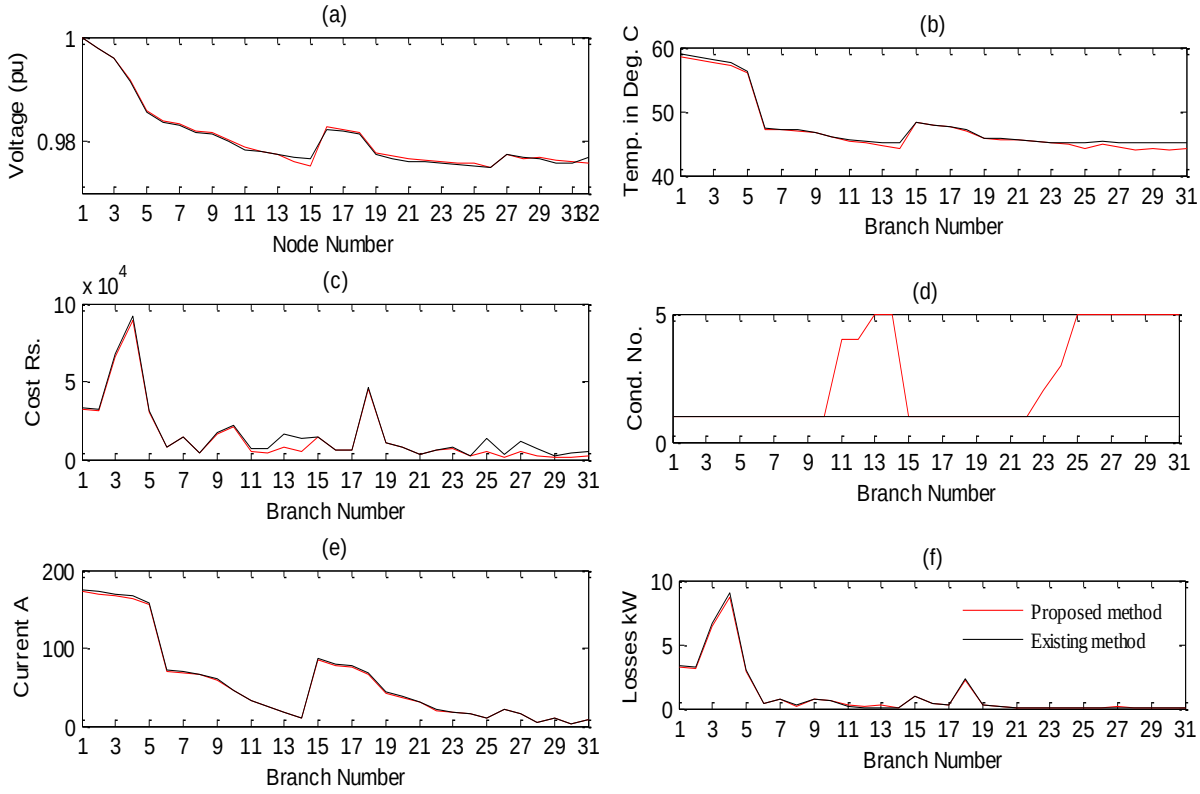

Fig. 5.5 The results for 32 node distribution network. Fig. 5.5 (a) comparison of node voltage (p.u.). Fig. 5.5 (b) comparison of br. Temperature. Fig. 5.5 (c) comparison of cost function. Fig. 5.5 (d) comparison of conductor sizes. Fig. 5.5 (e) comparison of branch current. Fig. 5.5 (f) comparison of branch losses.

Table 5.5 The results of 32-node network for node voltage, conductor no, cost function and loadability index for conductor size selected by Sivanagaraju [57].

Node No.	Node Voltage magnitude (p.u.)	Branch no.	Cond. No.	Cost Function	Line loadability index
1	1	1	1	33298	0.26343
2	0.99792	2	1	32389	0.26898
3	0.99588	3	1	67715	0.27443
4	0.99156	4	1	91846	0.27982
5	0.98563	5	1	30867	0.29546
6	0.98357	6	1	7852.2	0.40838
7	0.98291	7	1	14395	0.40974
8	0.98169	8	1	4630.2	0.41185
9	0.98131	9	1	16961	0.41673
10	0.97992	10	1	21538	0.42488
11	0.97831	11	1	7464.4	0.43091
12	0.97787	12	1	7042.3	0.43312
13	0.97751	13	1	16805	0.43479
14	0.97688	14	1	13467	0.43615
15	0.9766	15	1	14917	0.39515
16	0.98231	16	1	5998.4	0.40156
17	0.98181	17	1	5785.9	0.40397
18	0.98132	18	1	46392	0.41173
19	0.97743	19	1	11102	0.4264
20	0.97663	20	1	8179.3	0.42888
21	0.97608	21	1	3063.2	0.4315
22	0.97591	22	1	5686.2	0.43426
23	0.97567	23	1	8386.6	0.43486
24	0.97535	24	1	2754.8	0.43537
25	0.97527	25	1	13468	0.43614
26	0.97498	26	1	2868.6	0.43394
27	0.9773	27	1	11844	0.43538
28	0.97692	28	1	6663.9	0.4365
29	0.97655	29	1	2693.5	0.43614
30	0.97585	30	1	3983.1	0.43662
31	0.97583	31	1	5370.3	0.43625
32	0.97678				
Total cost based on total cost of power, energy loss and cost of conductor for plan period = 5.2543 x10^5 rupees.					

Table 5.6 The results of 32-node network for branch current, branch operating temperature and branch losses for conductor size selected by Sivanagaraju [57].

Branch No.	Branch current	Branch operating temperature	Branch losses
1	175.18	58.926	3.3224
2	172.44	58.482	3.2145
3	169.7	58.045	6.6832
4	166.95	57.615	9.012
5	158.65	56.363	2.9709
6	71.79	47.33	0.42833
7	70.042	47.221	0.76417
8	67.264	47.052	0.23477
9	60.316	46.662	0.75403
10	46.4	46.009	0.66776
11	32.461	45.527	0.1305
12	25.489	45.351	0.080407
13	18.514	45.216	0.106
14	9.7742	45.108	0.024612
15	86.862	48.388	0.98355
16	79.921	47.875	0.36568
17	77.143	47.682	0.34047
18	67.416	47.061	2.3585
19	43.327	45.888	0.3104
20	37.742	45.69	0.18387
21	30.756	45.48	0.048806
22	20.975	45.259	0.045359
23	18.179	45.211	0.051103
24	15.383	45.17	0.012195
25	9.7904	45.109	0.024693
26	22.331	45.285	0.02571
27	15.354	45.17	0.052244
28	5.5855	45.08	0.0040182
29	9.7817	45.108	0.0049299
30	2.7948	45.07	0.00060359
31	8.7393	45.1	0.00787
Total real power loss = 33.214 kW			

Table 5.7 The results of 32-node network for node voltage, conductor no, cost function and loadability index for conductor size selected by proposed method.

Node No.	Node Voltage magnitude (p.u.)	Branch no.	Cond. No.	Cost Function	Line loadability index
1	1	1	1	33311	0.26331
2	0.99792	2	1	32402	0.26886
3	0.99588	3	1	67743	0.27432
4	0.99155	4	1	91883	0.2797
5	0.98563	5	1	30879	0.29536
6	0.98357	6	1	7854.7	0.40834
7	0.9829	7	1	14399	0.40971
8	0.98169	8	1	4631.6	0.41182
9	0.9813	9	1	16967	0.4167
10	0.97991	10	1	21544	0.42486
11	0.97831	11	3	5931.6	0.43229
12	0.97771	12	4	4548.7	0.43692
13	0.97713	13	4	9771.4	0.441
14	0.97606	14	5	5043.5	0.44817
15	0.97541	15	1	14920	0.39512
16	0.98231	16	1	5999.5	0.40153
17	0.9818	17	1	5787	0.40395
18	0.98131	18	1	46400	0.41171
19	0.97742	19	1	11102	0.42639
20	0.97662	20	1	8179.4	0.42887
21	0.97608	21	1	3063.3	0.43149
22	0.9759	22	1	5686.2	0.43425
23	0.97566	23	1	8386.6	0.43485
24	0.97535	24	1	2754.8	0.43537
25	0.97526	25	1	13468	0.43613
26	0.97498	26	5	1535.7	0.43913
27	0.97712	27	5	5124.2	0.44503
28	0.97624	28	5	2311.5	0.44961
29	0.97644	29	5	1008.6	0.44817
30	0.97577	30	5	1341.3	0.45014
31	0.97572	31	5	1967.2	0.4486
32	0.97583				
Total cost based on total cost of power, energy loss and cost of conductor for plan period = 4.8595×10^5 rupees					

Table 5.8 The results 32-node network for branch current, branch operating temperature and branch losses for conductor size selected by proposed method.

Branch No.	Branch current	Branch operating temperature	Branch losses
1	175.21	58.935	3.3239
2	172.48	58.491	3.2161
3	169.74	58.054	6.6865
4	166.99	57.624	9.0164
5	158.69	56.371	2.9724
6	71.814	47.333	0.42862
7	70.066	47.223	0.76471
8	67.288	47.055	0.23495
9	60.34	46.664	0.75465
10	46.424	46.011	0.66846
11	32.485	45.417	0.19446
12	25.512	45.047	0.16068
13	18.534	44.72	0.21176
14	9.7861	44.146	0.073994
15	86.876	48.391	0.98387
16	79.935	47.877	0.36581
17	77.157	47.684	0.34059
18	67.43	47.063	2.3594
19	43.329	45.889	0.31042
20	37.743	45.691	0.18388
21	30.757	45.481	0.048809
22	20.975	45.26	0.04536
23	18.18	45.212	0.051104
24	15.383	45.171	0.012196
25	9.7904	45.109	0.024693
26	22.343	44.87	0.077347
27	15.365	44.398	0.15702
28	5.5862	44.031	0.01205
29	9.7826	44.146	0.014788
30	2.7952	43.989	0.0018099
31	8.7478	44.112	0.023647
Total real power loss = 32.64 kW			

5.8 Effect of environmental conditions on Choice of conductor:

The current carrying capacity of electrical conductors depends upon the conductor material, dimensions of the conductors and the environmental conditions. Here

environmental conditions, means ambient temperature and wind velocity and direction of wind. The temperature of conductor is a function of heat generated in conductor due to ohmic losses minus heat dissipated in surroundings. Heat dissipation mainly depends upon ambient temperature and wind velocity and wind direction. It is found that the conductor size may be lower for same power distribution for low ambient temperature and high wind region than the high temperature and low wind region. The proposed algorithm is applied for conductor size selection of 32-node system of second example for different ambient temperature and wind velocity conditions. Results shown in Table 5.9 reveal that the conductors selected at low temperature and high wind, are smaller for some branches.

5.9 Effect of load modelling on choice of conductor:

Constant power load is considered as the hardest type of load and for same load, the current is highest in constant power load. In practice loads in distribution network are not only constant power loads. Actual loads are combination of different kinds of loads. Different kinds of load models are discussed in **Chapter 3**. To show the effect of load modelling on the conductor size selection, practical load model is considered that is a combination of Battery Charge (2%) + Fluorescent lamps (11%) + AC (8%) + resistance space heating (5%) + Pump, fans and other motors (18%) + CFL (5%) + Incandescent lamp (6%) + Small motors (25%) + Large motors (20%). In Table 5.10 conductor sizes selected for the branches of 32-node distribution network are shown. It reveals that for some branches the optimal choice is smaller diameter conductor as compared to the optimal conductors selected for constant power load.

Table 5.9 The branch conductors selected for 32-node network at different environmental conditions.

Br. No.	Cond. Size for T_a =15 and v =3	Cond. Size for T_a =40 and v =1	Cond. Size for practical load modelling
1	1	1	1
2	1	1	1
3	1	1	1
4	1	1	1
5	1	1	1
6	2	1	2
7	2	1	2
8	2	1	2
9	1	1	2
10	4	1	3
11	5	2	4
12	5	4	5
13	5	5	5
14	5	5	5
15	1	1	1
16	1	1	1
17	1	1	1
18	1	1	1
19	3	1	1
20	4	1	2
21	4	1	3
22	5	1	5
23	5	1	5
24	5	1	5
25	5	1	5
26	5	5	5
27	5	5	5
28	5	5	5
29	5	5	5
30	5	5	5
31	5	5	5

5.10 Enhancement of Line Loadability and voltage stability of radial distribution network by optimal conductor size selection:

As it is discussed in the introduction part of this chapter, the loadability and voltage stability of distribution network can be improved by optimal conductor size selection. To investigate the effect of optimal conductor size selection on loadability of radial distribution network, a 30-node network is in Fig. 4.1 in **Chapter 4** is selected as a test system. The results of line loadability index and voltage stability index are investigated in **Chapter 4** before optimal conductor size selection. The results regarding loadability index, branch current, branch losses, branch temperature and cost function for base load and original network are shown in Table 5.10 and results for node voltage (p.u.) and voltage stability index for base load and original 30-node network are shown in Table 5.11. The results regarding loadability index, branch current, branch losses, branch temperature and cost function after optimal conductor size selection for 30-node network are shown in Table 5.12 and results for node voltage (p.u.) and voltage stability index after optimal conductor size selection for 30-node network are shown in Table 5.13. Figure 5.6 depicts the improvement in various parameters of 30-node network after optimal conductor size selection. Black curve is for before optimal conductor size selection and red curve for after optimal conductor size selection.

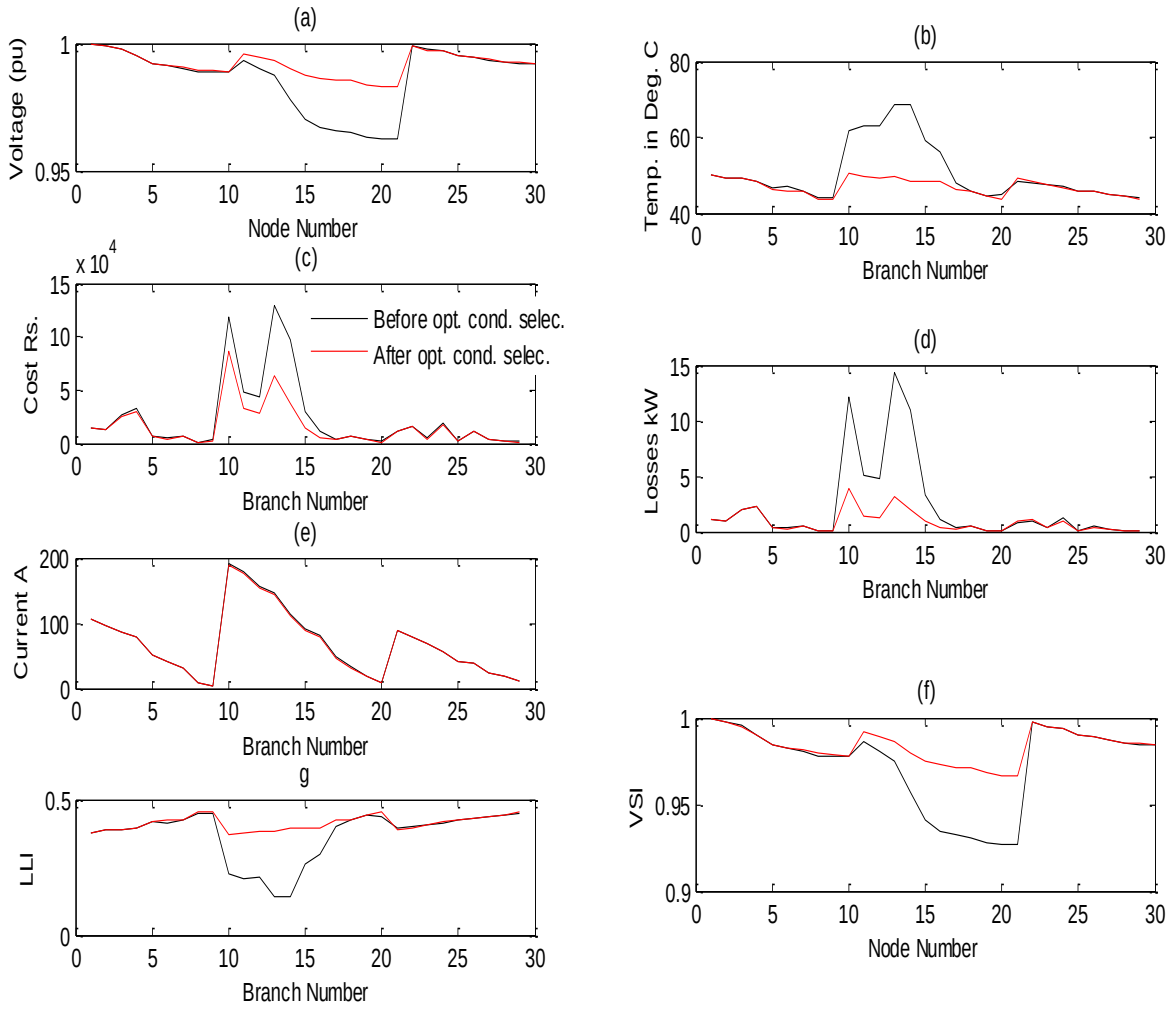

Fig. 5.6 Comparison of various parameters i.e. Fig. 5.6 (a) comparison of node voltage (p. u.) Fig. 5.6 (b) comparison of branch temperature Fig. 5.6 (c) comparison of cost function of each branch Fig. 5.6 (d) comparison of real power losses in each branch Fig. 5.6 (e) comparison of line loadability index Fig. 5.6 (f) comparison of voltage stability index of 30-node network after optimal conductor size selection. Black curve is for before optimal conductor size selection and red curve for after optimal conductor size selection.

Table 5.10 The results of loadability index, branch current, branch losses, branch temperature and cost function for base 30-node network.

Br. No.	*LLI*	Current	Losses	Temperature	Cost function
1	0.37533	105.36	1.1643	49.974	15115
2	0.38557	96.26	0.96899	49.155	13469
3	0.38647	87.147	2.0377	49.083	26739
4	0.397	78.013	2.2715	48.24	32493
5	0.41859	50.523	0.43289	46.513	7582.8
6	0.4118	41.352	0.42731	47.056	5014.8
7	0.42707	32.172	0.48282	45.834	6720.1
8	0.44842	9.1937	0.01306	44.126	994.05
9	0.44984	4.5974	0.013058	44.013	3646
10	0.22627	192.32	12.139	61.898	1.1819×10^5
11	0.21042	178.59	5.0196	63.167	47636
12	0.21125	155.64	4.7529	63.1	44340
13	0.14355	146.43	14.374	68.516	1.291×10^5
14	0.14093	113.9	10.931	68.726	96523
15	0.25998	90.472	3.3373	59.202	30330
16	0.29874	81.069	1.1663	56.101	10799
17	0.39803	48.116	0.39933	48.158	4337.1
18	0.4258	33.04	0.54336	45.936	7407.1
19	0.44233	18.886	0.13802	44.614	3373
20	0.43617	9.443	0.0045943	45.106	2690.7
21	0.39431	87.709	0.80246	48.455	12065
22	0.4027	78.609	0.96452	47.784	16083
23	0.40573	69.496	0.29968	47.542	4750.7
24	0.41341	55.821	1.2028	46.927	19079
25	0.42572	42.117	0.13645	45.942	2938.5
26	0.42905	37.547	0.46588	45.676	11617
27	0.4376	23.821	0.2199	44.992	4062.8
28	0.44202	19.242	0.085979	44.638	2050.4
29	0.44804	10.081	0.031407	44.157	2032.6

Table 5.11 The results of node voltage magnitude (p.u.) and voltage stability index for base 30-node network.

Node No.	Voltage magnitude (p.u.)	*VSI*
1	1	1
2	0.99878	0.99755
3	0.99766	0.99532
4	0.99519	0.9904
5	0.99211	0.98428
6	0.99126	0.98259
7	0.99036	0.98082
8	0.98906	0.97825
9	0.98894	0.978
10	0.98869	0.97752
11	0.9931	0.98626
12	0.99018	0.98045
13	0.98718	0.97453
14	0.97819	0.95686
15	0.96997	0.94084
16	0.96679	0.93469
17	0.96555	0.93229
18	0.96483	0.9309
19	0.9634	0.92814
20	0.96277	0.92692
21	0.96271	0.92681
22	0.99898	0.99797
23	0.99762	0.99525
24	0.99716	0.99434
25	0.99502	0.99007
26	0.9947	0.98943
27	0.99347	0.98698
28	0.99267	0.98539
29	0.99228	0.98463
30	0.99201	0.98409

Table 5.12 The results of conductor size, loadability index, branch current, branch losses, branch temperature and cost function for 30-node network after optimal conductor size selection.

Br. No.	Conductor code[Table E2]	*LLI*	Current	Losses	Temp.	Cost function
1	3	0.40147	105.19	0.55785	47.882	16993
2	4	0.40307	96.091	0.57769	47.755	13063
3	5	0.40088	86.985	1.3542	47.93	35438
4	6	0.40338	77.861	1.8901	47.73	31856
5	7	0.42082	50.416	0.34545	46.334	7113.7
6	7	0.42646	41.261	0.168	45.883	4472.3
7	8	0.42714	32.101	0.48142	45.829	6708.4
8	8	0.44843	9.1734	0.013023	44.126	993.73
9	8	0.44984	4.5873	0.013021	44.013	3645.7
10	1	0.37008	189.29	3.9304	50.393	85783
11	1	0.377	175.6	1.3503	49.84	32444
12	1	0.38735	152.75	1.0187	49.012	29650
13	1	0.39108	143.6	2.2484	48.714	71610
14	2	0.40113	111.48	1.3066	47.91	48813
15	4	0.40709	88.489	0.61166	47.433	15398
16	6	0.40215	79.284	0.35941	47.828	5949
17	7	0.42303	47.047	0.15032	46.158	3368.1
18	8	0.42684	32.305	0.52011	45.852	7211.2
19	8	0.44267	18.466	0.13214	44.587	3323.4
20	8	0.4484	9.2334	0.013194	44.128	995.17
21	5	0.40041	87.674	0.63996	47.967	16568
22	6	0.40276	78.575	0.9626	47.779	16076
23	7	0.40541	69.463	0.29942	47.567	4433.4
24	7	0.41698	55.79	0.96247	46.642	17662
25	7	0.426	42.091	0.10928	45.92	2831.3
26	7	0.42844	37.523	0.37318	45.725	11359
27	8	0.4376	23.806	0.21995	44.992	4063.3
28	8	0.44202	19.23	0.086	44.638	2050.6
29	8	0.44804	10.074	0.031414	44.157	2032.7

Table 5.13 The results of node voltage magnitude (p.u.) and voltage stability index for 30-node network after optimal conductor size selection.

Node No.	Voltage magnitude (p.u.)	*VSI*
1	1	1
2	0.99918	0.99836
3	0.99834	0.99669
4	0.99644	0.99288
5	0.9937	0.98744
6	0.99297	0.986
7	0.99254	0.98514
8	0.99125	0.98258
9	0.99113	0.98233
10	0.99088	0.98185
11	0.99613	0.99227
12	0.99469	0.98941
13	0.99344	0.98693
14	0.99051	0.98111
15	0.9885	0.97713
16	0.98754	0.97523
17	0.98703	0.97422
18	0.98669	0.97355
19	0.9853	0.97083
20	0.98469	0.96961
21	0.98457	0.96937
22	0.99911	0.99821
23	0.99773	0.99546
24	0.99727	0.99454
25	0.99544	0.99089
26	0.99516	0.99034
27	0.9941	0.98824
28	0.99331	0.98666
29	0.99292	0.98589
30	0.99265	0.98536

To investigate the improvement in line loadability and voltage stability of the radial distribution network after optimal conductor size selection, 30-node test network is selected subjected to end node loading for constant power load and practical load modelling. The results for line loadability comparison are shown in Table 5.14, which

reveals that loadability is considerably improved for each loading condition after optimal conductor size selection. Effect of optimal conductor size selection on voltage stability of the 30-node test network is investigated. Table 5.15 shows that the network is capable to withstand more sever faults at each end node. So voltage stability of test network is improved after optimal conductor size selection.

Table 5.14 The results of line loadability index for base network and after optimal conductor selection when end nodes are heavily loaded for constant power load and practical load for 30-node distribution network.

LLI (Constant Power Load)			*LLI* (Constant Power Load)		
Value of load added in kVA	Value of load added in kVA	Time in minutes	Value of load added in kVA	Value of load added in kVA	Time in minutes
980	0.00737 Branch (6)	60	1080	0.0095133 Branch (7)	60
210	0.00557 Branch (14)	60	1080	0.0039981 Branch (18)	60
1170	0.005842 Branch (27)	60	1190	0.0039872 Branch (27)	60
LLI (Practical type load)			*LLI* (Practical type load)		
1020	0.002337 Branch (6)	60	1120	0.0016416 Branch (7)	60
250	0.0090907 Branch (14)	60	1120	0.0035192 Branch (18)	60
1210	0.0041789 Branch (27)	60	1230	0.004382 Branch (27)	60

Table 5.15 The results of voltage stability index for base network and after optimal conductor selection when fault at end nodes for constant power load and practical load for 30-node distribution network.

Node no.	*VSI* (Constant Power load) Without optimal conductor size selection					*VSI* (Constant Power load) With optimal conductor size selection				
	Value of load added in kVA	*VSI* of most sensitive node	Time in sec.	Max. Branch current (A).	Relay actuating time in sec.	Value of load added in kVA	*VSI* of most sensitive node	Time in sec.	Max. Branch current (A).	Relay actuating time in sec.
10	11000	0.2332 node(10)	0.11	2191 Branch (1)	0.29	13000	0.0129 node(10)	0.068	2658 Branch (1)	0.267
21	7000	0.2215 node(21)	0.17	1550 Branch (10)	0.33	14100	0.1517 node(21)	0.099	2842 Branch (10)	0.257
30	13500	0.2384 node(30)	0.08	2550 Branch (1)	0.26	14500	0.1223 node(30)	0.098	2714 Branch (21)	0.256
Node no.	Value of load added in kW	*VSI* (Practical type load) Without optimal conductor size selection				Value of load added in kW	*VSI* (Practical type load) With optimal conductor size selection			
10	45000	0.07721 node(10)	.2	2146* Branch (1)	0.3	53000	0.0693 node (10)	0.18	2518 Branch (1)	0.27
21	35000	0.06410 node(21)	0.25	1583 Branch (10)	0.33	60000	0.03428 node(21)	0.167	2662 Branch (10)	0.257
30	53000	0.078561 node(30)	0.23	2200 Branch (21)	0.28	59000	0.04843 node(30)	0.17	2754 Branch (21)	0.253

5.11 Conclusion: The algorithm proposed in this chapter selects the most economical and technically more reliable conductor sizes for the branches of the radial distribution network. The constraints applied are more practical that leads to selection of more practical conductor sizes. As the change in various parameters with time like cost of energy and power, load factor, load contribution factor, practical load modelling etc. are incorporated to make the conductor selection more reliable. Enhancement of critical loading and voltage stability under fault conditions due to optimal conductor size selection is comprehensively discussed. The results give more practical insight of the various parameters of network i.e. node voltage, branch temperature, branch current etc.

CHAPTER 6

OPTIMAL CAPACITOR SIZE SELECTION FOR RADIAL ELECTRIC POWER DISTRIBUTION NETWORKS

6.1 Introduction:

Distribution networks used to supply the lagging power factor loads. Due to low power factor more total power has to be supplied for the required active power. This leads to higher power and energy losses and for existing installed distribution capacity, less active power can be supplied. In present days when the prices of energy are shooting up day by day, the power utilities are concentrating on power factor improvement to reduce the difference between active power and total power. The extent of power factor improvement is governed by economical benefits. Detailed literature survey regarding the topic of optimal capacitor placement is discussed in **Section 2.5** (**Chapter 2**).

In this chapter a new approach for optimal capacitor placement is proposed and it is investigated that the critical loading and voltage stability of distribution network can be increased by proper placement of shunt capacitors. Measure of loadability and voltage stability is taken the loadability index and voltage stability index proposed in **Chapter 4**. Line loadability index and voltage stability index are discussed in **Chapter 4**. For selection of optimal capacitor sizes, node-wise reactive power compensation is carried out. The locations and sizes of shunt capacitors for reactive power compensation are selected on the basis of economic benefits in the form of reduced energy losses and reduction of cost of

power of the distribution network under consideration within the voltage and power factor constraints.

6.2 Problem formulation:

A capacitor generates more economical benefits when it is placed near to the load causing low power factor. So in the proposed method the reactive power compensation is dealt according to the reactive power demand at each node. The capacitor placement is also more economical when capacitor is placed at a node, which has highest value of sum of power losses from substation to the node under-consideration.

Shunt capacitors available in standard sizes, hence before taking the decision of capacitor placement at a node, it should be ensured that the reactive power demand at that node is more than or equal to the minimum capacitor size available in inventory. Capacitor placement at a node is justified if the economic benefits are more than or equal to the cost of capacitor placement within the constraint that the node power factor should not exceed unity.

Let at m th node, a load is connected of total power

$$S_m = P_m + jQ_m \tag{6.1}$$

The existing power factor of the load at m th node is $\cos\phi_{1m}$ where

$$\cos\phi_{1m} = \frac{P_m}{\sqrt{P_m^{\,2} + Q_m^{\,2}}} \tag{6.2}$$

Power factor after capacitor placement of m th node is $\cos\phi_{2m}$ where

$$\cos\phi_{2m} = \frac{P_m}{\sqrt{P_m^{\,2} + (Q_m - Q_{cm})^2}} \tag{6.3}$$

The reactive power demand at m th node is $(Q_m - Q_{cm})$.

So $(Q_m - Q_{cm}) \geq Q_c$ at the candidate node.

6.3 Economical selection of capacitor sizes:

A cost function is developed for economic analysis of capacitor placement. As stated above capacitor placement is justified if it generates equal or more economic benefits than its cost or in other words the cost function F_{cl} is minimized.

Cost function for each capacitor location is

$$F_{cl} = Q_{cl}C_c + \left(\sum_{b=l}^{ss} P_{Lb}C_e \right) time + \sum_{b=l}^{ss} P_{Lb}C_p \qquad (6.5)$$

Here $Q_{cl}C_c$ is cost of capacitor(s) at a location,

$\sum_{b=l}^{ss} P_{Lb}$ is the sum of real power losses from sub-station to the location where the capacitor is placed,

C_e is the cost of energy and

$\sum_{b=l}^{ss} P_{Lb}C_p$ is the cost of power, which includes the cost of generation transmission and distribution.

6.4 Constraints:

While minimizing the cost function, it should be less than unity (lagging). By maintaining this condition, the problems of over compensation and node voltage higher than the substation voltage are automatically avoided.

6.5 Fixed and Switched capacitors:

The value of fixed and switched capacitors for a network is determined by the chronological load curve. The fixed capacitors are installed to compensate the reactive

power demand at a load equal to the minimum on the chronological load curve of distribution networks.

If the data regarding the chronological load curve is not available, fixed capacitors are installed to compensate the reactive power demand for 25% of the rated load. Rest of the reactive power compensation is provided by switched capacitors.

6.6 Algorithm for optimal sizing and location of shunt capacitors for radial power distribution networks:

1. Read line data, data regarding branch conductor sizes, weather conditions, load data, required power factor, available capacitor sizes, cost of capacitor/kVAr, cost of energy, cost of power etc.
2. Run the load-flow solution program and find the real power losses, cost function and power factor at each node. Put 'don't try' flag on the nodes those do not fulfill $(Q_m - Q_{cm}) \geq Q_c$ condition.
3. Compute $\sum_{b=l}^{ss} P_{Lb}$ for each node and identify the node having maximum value of $\sum_{b=l}^{ss} P_{Lb}$.
4. Place a capacitor of minimum value at the node having maximum value of $\sum_{b=l}^{ss} P_{Lb}$ and again repeat Step 2.
5. Compare the cost function F_{cl} for the node under consideration for before capacitor placement and after capacitor placement.
6. If cost function F_{cl} is minimized with capacitor placement then keep it with the network. Go to Step 2.

7. If cost function is not minimized, revert back the last capacitor placement and put a ‘don’t try’ flag on this node for successive iterations. Go to step 2 if all the nodes do not have ‘don’t try’ flag.
8. When all the nodes have ‘don’t try’ flag, print the results.

6.7 Examples:

Two examples of radial distribution networks are considered to show the goodness and effectiveness of the proposed method. First example is considered to compare results of proposed method with existing method. Second example is considered to show the improvement in line loadability index and voltage stability index with capacitor placement. The line loadability index gives branch wise loading limit of system in steady operating conditions and the voltage stability index gives of system stability limit in fault conditions.

6.7 Example 6.1:

A 69-node electrical power distribution network is considered. Its line and load data has already been shown in **Appendix-C**. The results of existing method proposed by Das [100] are compared with the proposed method and presented in Table 6.1, Table 6.2 and Table 6.3. In Table 6.1 capacitor location and rating at various load conditions are shown for existing method and proposed method. Table 6.2 shows minimum voltage of 69-node network, real power losses, cost of energy losses and cost of capacitor placed for various loading conditions for existing method and proposed method. Table 6.3 shows the line power factor after capacitor placement for both methods. Comparison of results reveals that the minimum voltage at far end node and real power losses are almost comparable and there is a saving in total cost. The power factor correction is even better for the proposed

method for same capacitor step size (100 kVAr) and small capacitor step size (25 kVAr). So the proposed method is better than the existing one.

Table 6.1 The switching scheme of capacitors at different loads for 69-node distribution network.

Capacitor location and sizes for existing method [100]				
Location	Control setting			Optimal Size (kVAr)
	50%	100%	160%	
61	0	700	800	800
64	300	800	1200	1200
59	0	100	1100	1100
Capacitor location and sizes for proposed method				
49	100 F	100 F+100 S	100 F+100 S	100 F+100 S
50	100 F	100 F+100 S	100 F+100 S	100 F+100 S
59	0 F	0 F+0 S	0 F+100 S	0 F+100 S
61	400 F	400 F+400 S	400 F+1000 S	400 F+1000 S
64	0 F+0 S	0 F+100 S	0 F+200 S	0 F+200 S
11	0 F+0 S	0 F+100 S	0 F+100 S	0 F+100 S
12	0 F+0 S	0 F+100 S	0 F+100 S	0 F+100 S
21	0 F+0 S	0 F+0 S	0 F+100 S	0 F+100 S
'F' stands for fixed capacitor and 'S' switched capacitor.				

Table 6.2 Comparison of various parameters between existing and proposed method for 100kVAr step size for 69-node distribution network.

System parameter	Load Level existing method [100]			Load Level Proposed method.		
	50%	100%	160%	50%	100%	160%
Min. Voltage	0.96220	0.93693	0.90014	0.96327	0.92614	0.87938
Losses	40.48	156	460.45	39.39	158.94	428.63
Cost of Losses	4857.6	49233.6	41440.5	4726.8	50161	38576
Total cost with existing method [100]=95531.7$+9300$=104831.7$						
Total cost with proposed method=93463.8$+ 6000$=99463.8$						

Table 6.3 The line power factor for existing method and proposed method for 69-node distribution network.

Node No.	Line PF for existing method with 100kVAr step size	Line PF for proposed method for 100kVAr step size	Line PF for proposed method for 25kVAr step size
2	0.82482	0.95381	0.98066
3	0.82484	0.95381	0.98066
4	0.82599	0.962	0.98148
5	0.83035	0.97202	0.99298
6	0.82932	0.97142	0.99253
7	0.82826	0.97152	0.9926
8	0.8285	0.97552	0.99389
9	0.82638	0.9101	0.9872
10	0.82576	0.91414	0.98734
11	0.82615	0.92174	0.99134
12	0.83056	0.9198	0.98923
13	0.83693	0.90033	0.98437
14	0.83594	0.90146	0.98606
15	0.83547	0.90314	0.98796
16	0.83533	0.90293	0.98805
17	0.83517	0.91267	0.99146
18	0.82784	0.92409	0.98912
19	0.81536	0.94218	0.98449
20	0.81526	0.94218	0.98449
21	0.81487	0.9426	0.98489
22	0.81429	0.81419	0.90954
23	0.81382	0.81376	0.91691
24	0.81377	0.81378	0.91692
25	0.81376	0.81379	0.81379
26	0.81374	0.81376	0.81376
27	0.81373	0.81374	0.81374
28	0.78093	0.78087	0.92311
29	0.76598	0.7658	0.87317
30	0.72555	0.72536	0.72536
31	0.72554	0.72532	0.72532
32	0.7255	0.72535	0.72535
33	0.72539	0.72541	0.72541
34	0.65254	0.6527	0.6527
35	0.83205	0.83207	0.83207
36	0.82095	0.82119	0.98244
37	0.82217	0.82226	0.98006

38	0.82379	0.82394	0.97662
39	0.8238	0.82397	0.97664
40	0.8255	0.82572	0.96885
41	0.82832	0.82826	0.95468
42	0.82925	0.82922	0.95676
43	0.82926	0.82928	0.95682
44	0.83052	0.83055	0.9649
45	0.83055	0.83052	0.96487
46	0.83055	0.83055	0.9649
47	0.81106	0.92232	0.91619
48	0.81179	0.92177	0.91562
49	0.81386	0.93041	0.90318
50	0.81402	0.93185	0.90481
51	0.8181	0.8181	0.94426
52	0.8	0.8	0.8
53	0.82967	0.9953	0.99614
54	0.82938	0.99545	0.99627
55	0.82907	0.99626	0.99627
56	0.82873	0.99701	0.99625
57	0.82195	0.99652	0.99574
58	0.81835	0.99687	0.99611
59	0.81687	0.99708	0.99633
60	0.83192	0.99717	0.99638
61	0.814	0.99696	0.99616
62	0.87385	0.95219	0.99718
63	0.81447	0.96387	0.99833
64	0.81414	0.96373	0.99827
65	0.87276	0.81476	0.98376
66	0.81068	0.8107	0.8107
67	0.81068	0.81068	0.81068
68	0.81373	0.81383	0.988
69	0.81373	0.81373	0.98801

The formulation of proposed method is such that the value of reactive power compensation is applied according to the reactive power demand of particular load where the capacitor is to be placed. So the step size of capacitors or capacitor sizes available in inventory should be small so that most of the loads are to be compensated. Table 6.4 and Table 6.5 show the

results of 69-node power distribution network with capacitor step size 25 kVAr instead of 100kVAr used previously. By using smaller step size cost function is further minimized and system performance is improved as compared to previous attempt.

Table 6.4 The comparison of different parameter at various loads with existing method and proposed method for 69-node distribution network.

System parameter	Load Level existing method [100]			Proposed method.		
	50%	100%	160%	50%	100%	160%
Min. Voltage	0.96220	0.93693	0.90014	0.96569	0.92933	0.8814
Losses	40.48	156	460.45	35.39	147.33	404.33
Cost of Losses	4857.6	49233.6	41440.5	4247.3	46399	36390
Total cost with existing method [100]=95531.7$+9300$=104831.7$						
Total cost with proposed method=87036.3$+9300$=96336.3$						

Table 6.5 The switching scheme of capacitors at different loads for 69-node distribution network.

Switching scheme for λ=1.6			Switching scheme for λ=1			Switching scheme for λ=0.5	
Node no	Switched Capacitor kVAr	Fixed Capacitor kVAr	Node no	Switched Capacitor kVAr	Fixed Capacitor kVAr	Node no	Fixed Capacitor kVAr
7	25	0	7	25	0	8	25
8	50	25	8	25	25	11	50
9	25	0	11	50	50	12	50
10	25	0	12	50	50	21	25
11	100	50	16	25	0	48	25
12	100	50	17	25	0	49	125
16	25	0	18	25	0	50	125
17	50	0	21	50	25	59	25
18	50	0	45	25	0	61	425
21	100	25	46	25	0	64	75
24	25	0	48	25	25		
28	25	0	49	25	125		
29	25	0	50	25	125		
36	25	0	51	25	0		
37	25	0	59	25	25		
39	25	0	61	400	425		
40	25	0	64	75	75		
45	25	0	65	25	0		
46	25	0					
48	50	25					
49	25	125					
50	25	125					
51	25	0					
54	25	0					

55	25	0					
59	75	25					
61	825	425					
62	25	0					
64	175	75					
65	50	0					
68	25	0					
69	25	0					
Min. Voltage = 0.8814 Losses = 404.33kW Capacitor cost=9300$ Cost of losses =36390$ Total cost =48790$			Min. Voltage = 0.92933 Losses = 147.33kW Capacitor cost=5700$ Cost of losses =46399$ Total cost =53999$			Min. Voltage = 0.96569 Losses = 35.39kW Capacitor cost=2850$ Cost of losses =4247.3$ Total cost =8047.3$	
Total loss cost= 87036.3$ Total cost of capacitors=9300$ Value of cost function=96336.3$ Total installed capacitor= 3100kVAr							

6.7 Example 2:

Another example of 30-node power distribution network is considered. Line data and load data is shown in **Appendix-E** and single line diagram is shown in Fig.4.1 in **Chapter 4**.

The results of line loadability index and branch losses are shown in Table 6.6 without capacitor placement and with capacitor placement. The enhancement of line loadability limit and reduction of branch losses are observed after capacitor placement. Table 6.7 and Table 6.8 show the results for comparison of voltage stability index and node voltage, line power factor and node power factor respectively before capacitor placement and after capacitor placement. Figure 6.1 shows the results for various parameter of 30-node radial power distribution network for before capacitor placement and after capacitor placement. The parameters shown in red curve are for without capacitor placement and black curve

depicts quantities after capacitor placement. For Table 6.6 to Table 6.8 and in Fig. 6.1 the test network is under base load conditions.

Table 6.6 The results for *LLI* and branch losses before capacitor placement and after capacitor placement for 30-node distribution network.

Node No.	Fixed Cap.	Switched Cap.	Br. No.	*LLI* before cap. placement	*LLI* after cap. placement	Branch losses after capacitor placement	Branch losses before capacitor placement
1	0	0	1	0.4063	0.40492	0.44169	0.55727
2	0	0	2	0.40903	0.40444	0.44666	0.57744
3	0	0	3	0.40807	0.40292	1.0171	1.3534
4	0	0	4	0.41254	0.40365	1.3688	1.8899
5	0	60	5	0.42614	0.42084	0.23744	0.34544
6	0	45	6	0.42995	0.42648	0.11658	0.16799
7	0	45	7	0.43401	0.42714	0.33849	0.48142
8	0	90	8	0.44894	0.44843	0.0094745	0.013023
9	0	15	9	0.44997	0.44984	0.0094738	0.013021
10	0	15	10	0.38123	0.38003	3.0356	3.9188
11	15	0	11	0.38725	0.38639	1.0213	1.3465
12	0	0	12	0.39614	0.39592	0.73744	1.0161
13	0	0	13	0.39929	0.39935	1.5924	2.2428
14	0	75	14	0.40755	0.40674	0.8988	1.3043
15	0	75	15	0.41425	0.4084	0.41512	0.6114
16	0	45	16	0.41314	0.40242	0.24461	0.35938
17	0	120	17	0.42793	0.42305	0.10068	0.15031
18	15	45	18	0.43475	0.42685	0.34468	0.5201
19	15	45	19	0.44529	0.44267	0.086725	0.13214
20	0	45	20	0.44906	0.4484	0.0086638	0.013193
21	0	45	21	0.40513	0.40247	0.53702	0.63956
22	0	0	22	0.4088	0.40303	0.79057	0.96252
23	0	0	23	0.41191	0.40543	0.23933	0.29942
24	15	0	24	0.4221	0.417	0.72609	0.96247
25	15	0	25	0.42939	0.42601	0.077999	0.10928
26	0	15	26	0.43115	0.42846	0.26576	0.37318
27	15	15	27	0.44186	0.4376	0.14618	0.21995
28	0	15	28	0.44492	0.44202	0.055925	0.086
29	0	45	29	0.44885	0.44804	0.02015	0.031414
30	15	45					

Table 6.7 The results for *VSI* and node voltage (p.u.) before capacitor placement and after capacitor placement for 30-node distribution network.

Node No.	Voltage stability index after cap. placement	Voltage stability index before cap. placement	Node voltage after cap. placement	Node voltage before cap. placement
1	1	1	1	1
2	0.9987	0.99836	0.99935	0.99918
3	0.99737	0.99669	0.99869	0.99834
4	0.99431	0.99289	0.99715	0.99644
5	0.9899	0.98745	0.99493	0.9937
6	0.98874	0.986	0.99435	0.99297
7	0.98805	0.98514	0.99401	0.99254
8	0.98572	0.98258	0.99283	0.99125
9	0.9855	0.98234	0.99272	0.99113
10	0.98505	0.98185	0.9925	0.99088
11	0.99428	0.99228	0.99714	0.99613
12	0.99222	0.98942	0.9961	0.9947
13	0.99054	0.98694	0.99526	0.99345
14	0.98671	0.98113	0.99333	0.99052
15	0.98414	0.97715	0.99204	0.98851
16	0.98282	0.97525	0.99137	0.98755
17	0.98204	0.97424	0.99098	0.98704
18	0.98152	0.97357	0.99072	0.9867
19	0.97909	0.97085	0.98949	0.98532
20	0.97802	0.96964	0.98895	0.9847
21	0.97781	0.9694	0.98884	0.98458
22	0.99844	0.99821	0.99922	0.99911
23	0.99603	0.99546	0.99801	0.99773
24	0.99523	0.99455	0.99761	0.99727
25	0.99215	0.99089	0.99607	0.99544
26	0.99171	0.99034	0.99585	0.99516
27	0.99001	0.98824	0.99499	0.9941
28	0.98862	0.98666	0.99429	0.99331
29	0.98795	0.98589	0.99396	0.99292
30	0.9875	0.98536	0.99373	0.99265

Table 6.8 The results for Line power factor and Node power factor before capacitor placement and after capacitor placement for 30-node distribution network.

Node No	Line power Node power factor after cap. placement	Line power factor before cap. placement	Node power factor after cap. placement	Node power factor before cap. placement
1	0.90951	0.79982	0.8	0.8
2	0.91901	0.79988	0.8	0.8
3	0.92993	0.79989	0.8	0.8
4	0.94276	0.80002	0.89443	0.8
5	0.96472	0.80004	0.98287	0.8
6	0.95997	0.80002	0.98287	0.8
7	0.95205	0.80033	0.95783	0.8
8	0.93633	0.80003	0.93633	0.8
9	0.93634	0.80006	0.93633	0.8
10	0.91717	0.79878	0.8	0.8
11	0.92605	0.79955	0.8	0.8
12	0.94219	0.79961	0.8	0.8
13	0.94918	0.79907	0.90077	0.8
14	0.96131	0.79945	0.93633	0.8
15	0.96729	0.79986	0.98287	0.8
16	0.9653	0.8	0.95203	0.8
17	0.9734	0.80002	0.96265	0.8
18	0.97779	0.80036	0.97014	0.8
19	0.98287	0.80016	0.98287	0.8
20	0.98287	0.80003	0.98287	0.8
21	0.8887	0.79995	0.8	0.8
22	0.89847	0.80001	0.8	0.8
23	0.91055	0.80003	0.8	0.8
24	0.93432	0.8001	0.848	0.8
25	0.95738	0.80002	0.93633	0.8
26	0.95967	0.80006	0.89443	0.8
27	0.98534	0.8002	0.93633	0.8
28	0.99227	0.8001	0.98287	0.8
29	0.99768	0.80007	0.99768	0.8

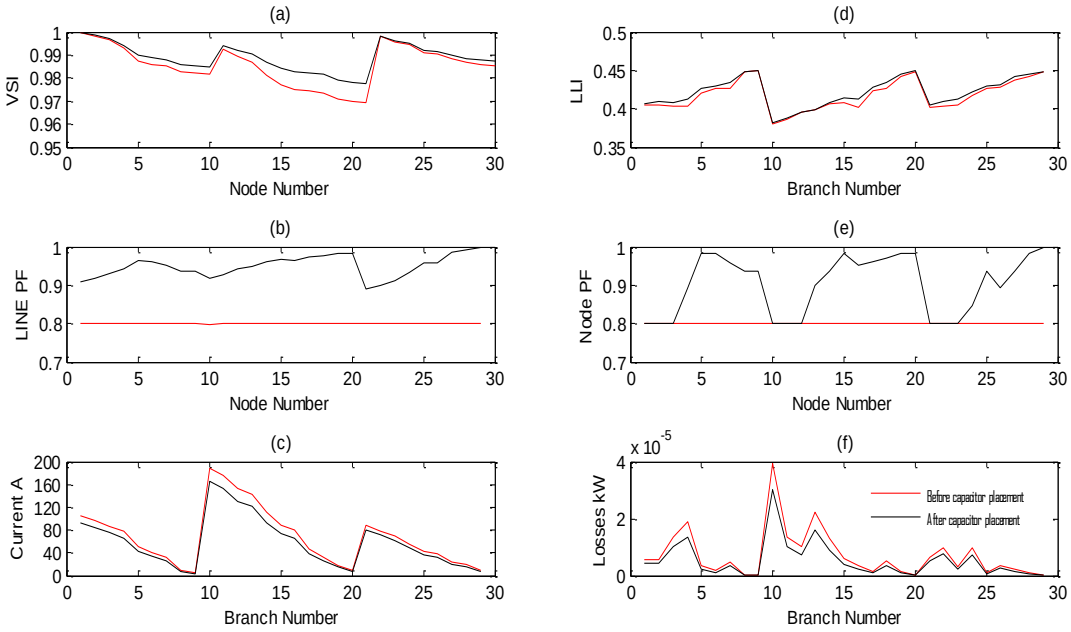

Fig. 6.1 Comparison of various parameters i.e. Fig. 5.6 (a) comparison of voltage stability index, Fig. 5.6 (b) comparison of line power factor, Fig. 5.6 (c) comparison of branch current Fig. 5.6 (d) comparison of Line loadability index Fig. 5.6 (e) comparison of node power factor, Fig. 5.6 (f) comparison of real power losses of each branch of 30-node network before and after capacitor placement black curve for after capacitor placement and red curve for before capacitor placement for 30-node distribution network.

6.8 Enhancement of line loadability and voltage stability after capacitor placement:

With shunt capacitor placement at or near the load terminal, there is a reduction in current from that node to substation so consequently there is a reduction in losses, temperature rise in branch conductors, improvement in voltage profile of nodes because voltage drop reduces due to reduction in current. The overall effect of capacitor placement in distribution network is that there is an enhancement in the line loadability and voltage stability. The effect of capacitor placement at normal load conditions is discussed in previous section. In this section the effect of capacitor placement under high load condition

and under fault conditions is investigated. The results for high load (up to loadability limit) at end nodes with constant power load and practical load are shown in Table 6.9.

In Table 6.10 the results of voltage stability index when fault at each end node for constant power load and practical load are shown. The results clearly indicate that there is an improvement in voltage stability after capacitor placement.

Table 6.9 The results of line loadability index for 30-node network (after optimal conductor size selection) with and without capacitor placement when end nodes are heavily loaded for constant power load and practical load.

LLI (Constant Power Load)			*LLI* (Constant Power Load)		
Value of load added in kVA	Value of load added in kVA	Time in minutes	Value of load added in kVA	Value of load added in kVA	Time in minutes
1130 (node 10)	0.00797 Branch (7)	60	1080 (node 10)	0.0095133 Branch (7)	60
1150 (node 21)	0.007952 Branch (18)	60	1080 (node 21)	0.0039981 Branch (18)	60
1240 (node 30)	0.004634 Branch (27)	60	1190 (node 30)	0.0039872	60
LLI (Practical type load)			*LLI* (Practical type load)		
1170 (node 10)	0.005976 Branch (7)	60	1120 (node 10)	0.0016416 Branch (7)	60
1190 (node 21)	0.004104 Branch (18)	60	1120 (node 21)	0.0035192 Branch (18)	60
1270 (node 30)	0.003760 Branch (27)	60	1230 (node 30)	0.004382 Branch (27)	60

Table 6.10 The results of voltage stability index for 30-node network (after optimal conductor selection) with and without capacitor placement when fault at end nodes for constant power load and practical load.

Node no.	*VSI* (Constant Power load) With optimal conductor size selection and with capacitor placement					*VSI* (Constant Power load) With optimal conductor size selection and without capacitor placement				
	Value of load added in kVA	*VSI* of most sensitive node	Time in sec.	Max. Branch current (A).	Relay actuating time in sec.	Value of load added in kVA	*VSI* of most sensitive node	Time in sec.	Max. Branch current (A).	Relay actuating time in sec.
10	13100	0.1632 node(10)	0.055	2614 Branch (1)	0.268	13000	0.0129 node(10)	0.068	2658 Branch (1)	0.267
21	14270	0.17078 node(21)	0.09	2807 Branch (10)	0.257	14100	0.1517 node(21)	0.099	2842 Branch (10)	0.257
30	14670	0.015066 node(30)	0.065	3121 Branch (21)	0.247	14500	0.1223 node(30)	0.098	2714 Branch (21)	0.256
Node no.	Value of load added in kW	*VSI* (Practical type load) Without optimal conductor size selection and with capacitor placement				Value of load added in kW	*VSI* (Practical type load) With optimal conductor size selection and without capacitor placement			
10	53200	0.06751 node(10)	0.17	2601 Branch (1)	0.268	53000	0.0693 node (10)	0.18	2518 Branch (1)	0.27
21	60300	0.08053 node(21)	0.141	2838 Branch (10)	0.257	60000	0.03428 node(21)	0.167	2662 Branch (10)	0.257
30	59300	0.1155 node(30)	0.17	2846 Branch (21)	0.257	59000	0.04843 node(30)	0.17	2754 Branch (21)	0.253

6.9 Conclusion:

A novel approach for optimal capacitor size selection and location is proposed. It is established with the support of tabulated results that the proposed approach better than the existing one. As multiple capacitor banks are placed at different locations, reliability of reactive power compensation is higher. Chances of over compensation are minimum with the proposed approach as with the variation of load at any particular node the value of switched capacitor would change accordingly. Maximum benefits of reactive power compensation are exploited from the installed capacity of capacitors. With the optimal

capacitor placement the improvement in line loadability and improvement in voltage stability are investigated and it is established with the help of tabulated results and graphical representation that the line loadability of the distribution networks and voltage stability of distribution networks can be improved by optimal capacitor placement.

CHAPTER 7

NETWORK RECONFIGURATION FOR RADIAL ELECTRIC POWER DISTRIBUTION NETWORKS

7.1 Introduction:

In previous chapters it has been discussed how to enhance the loadability limit and voltage stability limit of radial distribution networks by optimal conductor size selection and capacitor placement. In this chapter, it is discussed how the already installed capacity can be best utilized to increase the loadability limit and voltage stability limit by network reconfiguration. Detailed literature survey is discussed in **Section 2.6** (**Chapter 2**). In all the discussed reported work on network reconfiguration, the problem was dealt with lot of flexibility. But in practical distribution networks the chances of network reconfiguration are very limited because the distribution networks are erected in the residential, commercial, industrial areas etc. The feeders may or may not be touching each other and even some times the tie-lines cannot be stretched from any one point to another point due to various constraints. The application of optimization techniques is not justified in this case because it leads to only theoretical exercise. However, in spite of all these constraints, network reconfiguration is considered to optimize the available capacity of the distribution network.

In this chapter an attempt has been made to establish that the reconfiguration of networks can be carried out for load balancing during the seasonal change in load depicted by the chronological load curves of the feeders. None of the previous researchers had proposed this type of approach. Usually same type of loads are concentrated in particular

areas like the feeders dedicated to supply residential areas, the dominated loads are domestic and commercial, some feeders may be dominated with industrial loads, some with agriculture etc. By examining the chronological load curves, the possibilities of feeder reconfiguration can be identified.

7.2 Problem formulation:

The first step is to find the chances of network reconfiguration and the location of tie-switches, is to draw the annual chronological load curves of the candidate feeders or laterals. By examining the annual chronological load curves and the location of feeders, the position of tie lines, the switching scheme can be developed. While fixing the location of tie-lines and developing the switching schemes, the line loadability limits of the feeders or lateral should not be violated. For example only that much load should be shifted to some feeder from some other feeder so that the receiving feeder's current carrying capacity should not be violated. It is assumed for simplicity that the length and the type of conductor of tie-line is same as that branch which is disconnected by corresponding isolating switch.

7.3 Constraints:

At the time of reconfiguration procedure following points should be taken as constraints.

1. Only the practically possible locations of tie-lines should be considered. Because mostly it is not possible to set a tie-line to connect any two locations of the distribution network.
2. The line loadability index should be maximized.
3. Radial nature of the network should be maintained. When a tie line is connected, an isolator switch is opened to avoid mesh configuration.

4. Direction of flow of current through branches should be same as before reconfiguration. This is necessary because the conductor sizes of branches are selected according to the current through branches, if the direction of current is reversed, there are chances that a branch which was the last branch of a lateral becomes the first branch of lateral so it has to feed more loads so that the current carrying capacity can be violated.

7.4 Procedural Steps for network reconfiguration:

1. Draw the annual chronological load curve for each lateral from annual load data.
2. By approximation make the curves in discrete form.
3. Identify the locations of tie-lines between laterals or feeders which are practically possible.
4. Identify the most suitable options of tie-lines by computation of load-flow solution and line loadability index.
5. Develop the annual switching scheme for tie-lines from Step 4.
6. Print the results

7.5 Example:

An example of 30-node typical Indian radial distribution network is considered to illustrate the proposed procedure for network reconfiguration for enhancement of loadability of the radial distribution networks. Line data and load data is given in **Appendix-E**. Single line diagram of 30-node radial distribution network is shown in Fig. 7.1. The value of base voltage is 11kV and value of base power is 100 MVA. There are three laterals of distribution network. Lateral 1 is dedicated to serve industrial load. The industrial load is considered to be the agriculture based industry like cotton mills,

sugar mills and rice mills. Industrial load consists of 50% large industrial motors + 10% compact florescent lamp + 10% air conditioner + 20% small industrial motor load + 10% pump set and fan load.

Lateral 2 is dedicated to serve residential and commercial loads. The domestic and commercial load consists of 20% florescent lamps+ 15% incandescent lamp + 30% air conditioner load + 15% resistance space heater + 30% pump set and fan.

Lateral 3 is dedicated to serve agriculture load. Agriculture load consists of 95% pump set load + 5% incandescent lamp load. The load exponents for various loads are shown in

Chronological load curves, which are developed from the annual load data of the laterals, as shown in Fig. 7.2. Curve 1 depicts the domestic load. Domestic load is high in India during summer season (June to September). Curve 2 shows the monthly percentage load for agriculture load dominated in lateral. The agriculture load is high during paddy season from May to September. Curve 3 is for agriculture based industrial load, which is also a seasonal type of load. Figure 7.3 shows the approximated chronological load curves for 30-node radial distribution network. To improve the load factor the service utility encourages such industry to use more power in off-peak months. So the load on such feeders is high during winter season. Looking at the approximated chronological curves shown in Fig 7.3 it is evident that the load can be shifted seasonally from one lateral to another.

To show the benefits and effectiveness of network reconfiguration the 30-node test network is considered in its base form which means without optimal conductor size selection and without capacitor placement. All the possible options for reconfiguration are tried and the results of beneficial seasonal reconfigurations are shown. The comparison of

various parameters like minimum node voltage, minimum voltage stability index, minimum line loadability index and total real power losses of the network before and after reconfiguration are shown in Table 7.1. Table 7.1 also shows the status of tie-lines and isolator switches during each season. Table 7.2, Table 7.3 and Table 7.4 show the comparison of results regarding *LLI*, *VSI*, node voltage and branch power losses for 30-node distribution network from January to April, May to August and September to December respectively without optimal conductor size selection and capacitor placement. Same results are shown in graphical form with the help of Fig. 7.4, Fig. 7.5 and Fig. 7.6 respectively.

The beneficial reconfiguration options are searched through the proposed algorithm after optimal conductor size selection and capacitor placement. The optimal conductor sizes selected for 30-node test network are discussed in **Chapter 5** (Table 5.12). The values of total capacitors on in every season are shown in Table 7.9. The tie-lines and isolator switches status is shown in Table 7.5. The tie-lines' and isolator switches' status is same for January to April and September to December for base network and for network with optimal conductor size selection and capacitor placement. But for the duration of May to August in base network no reconfiguration is beneficial due to the fact that the conductors for lateral 2 are under size. But after optimal conductor size selection and capacitor placement during May to August, the reconfiguration is beneficial and the status of tie-line and isolator switch has been shown in Table 7.5. The detailed results are shown in tabular form from Table 7.6 to Table 7.9 and in graphical form in Fig. 7.7 to Fig. 7.9.

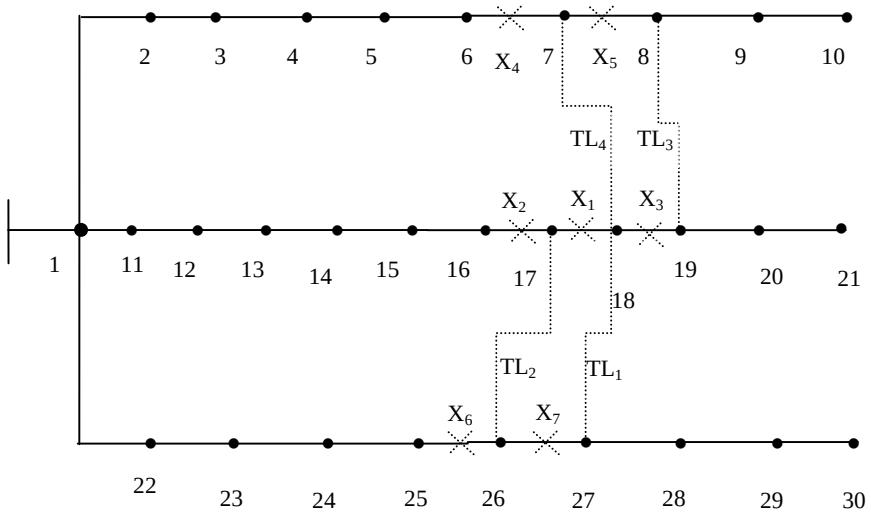

Fig. 7.1 The single line diagram of 30-node network

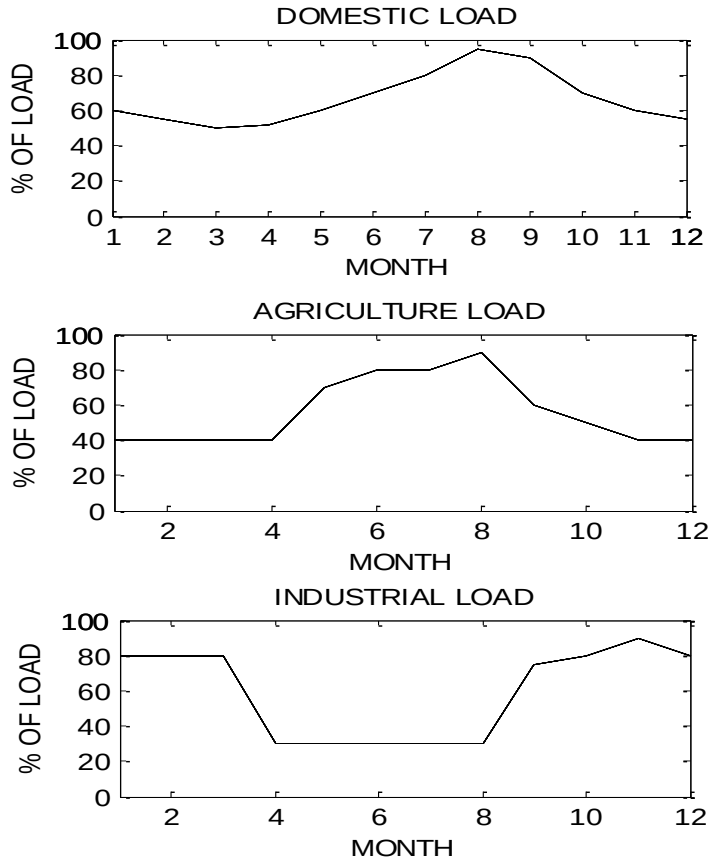

Fig. 7.2 The actual chronological load curves for 30-node network

Table 7.1 The switching scheme of tie-lines, isolator switches and comparison of result with and without network reconfiguration for 30-node distribution network.

Months	Isolator switch status	Tie-line status	Without Reconfiguration				With Reconfiguration			
			Min. Volt (p.u.)	Min. *LLI*	Min. *VSI*	Real Power Loss kW	Min. Volt. (p.u.)	Min. *LLI*	Min. *VSI*	Real Power Loss kW
Jan.-April	X_1 (Open)	TL_1 (Closed)	V_{21}= 0.9714	LLI_{13}= 0.2621	VSI_{21}= 0.94312	36.76	V_{18}= 0.98002	LLI_{13}= 0.33699	VSI_{18}= 0.96047	26.009
May-Aug.	Nil	Nil	V_{10}= 0.99016	LLI_{21}= 0.37967	VSI_{10}= 0.98041	13.422	Original configuration prevails			
Sep.-Dec.	(X_2 , X_3) Open	TL_2, TL_3 (closed)	V_{21} = 0.97098	LLI_{14}= 0.25954	VSI_{19} = 0.94281	35.872	V_{17} = 0.98326	LLI_{10}= 0.36463	VSI_{17}= 0.98326	22.51

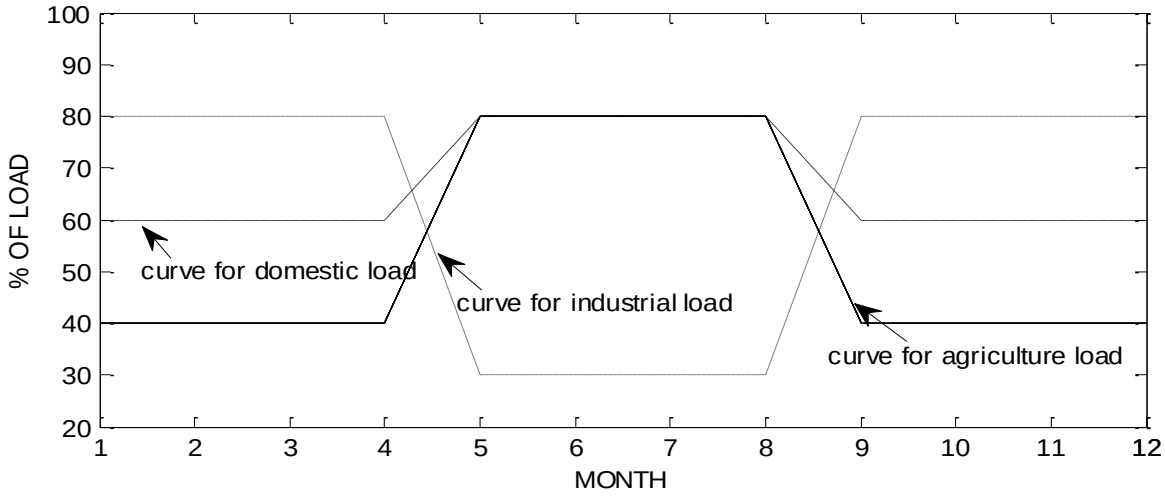

Fig. 7.3 The approximated chronological load curves for 30-node network

Table 7.2 The comparison of results regarding *LLI* and branch power losses for 30-node distribution network from January to April without optimal conductor size selection and capacitor placement.

Br. No.	*LLI* With Reconfiguration	*LLI* Without Reconfiguration	Power loss with reconfiguration	Power loss without reconfiguration
1	0.41026	0.4106	0.49938	0.49294
2	0.41465	0.41496	0.41611	0.41033
3	0.41641	0.41675	0.87444	0.86137
4	0.42093	0.42121	0.97614	0.96077
5	0.43185	0.43202	0.18649	0.18329
6	0.43374	0.43403	0.18357	0.18031
7	0.44029	0.44048	0.2079	0.20411
8	0.44949	0.44951	0.0056432	0.005539
9	0.45011	0.45011	0.0056431	0.0055378
10	0.34828	0.3072	5.0465	7.4198
11	0.34646	0.29877	2.0101	3.0582
12	0.35507	0.30078	1.7693	2.8883
13	0.33699	0.2621	5.0963	8.6608
14	0.3577	0.26298	3.2254	6.5682
15	0.40411	0.33391	0.80153	2.0306
16	0.4181	0.35729	0.24557	0.71281
17	0.44716	0.41788	0.023971	0.24732
18	0.43555	0.43503	0.32687	0.33853
19	0.4455	0.44533	0.083179	0.086122
20	0.43636	0.43635	0.0027712	0.002869
21	0.40448	0.42265	0.60905	0.26468
22	0.40879	0.42542	0.79093	0.31831
23	0.40905	0.42803	0.26973	0.098817
24	0.4111	0.4325	1.301	0.39628
25	0.41899	0.43656	0.19337	0.045008
26	0.42136	0.43766	0.74531	0.15369
27	0.44604	0.44612	0.073742	0.072486
28	0.44753	0.44758	0.028855	0.028361
29	0.44955	0.44956	0.010551	0.01037

Table 7.3 The comparison of results regarding node voltage magnitude (p.u.) and *VSI* for 30-node distribution network from January to April without optimal conductor size selection and capacitor placement.

Node No.	Node voltage magnitude (p. u.) With Reconfiguration	Node Voltage magnitude (p. u.) Without Reconfiguration	*VSI* With Reconfiguration	*VSI* Without Reconfiguration
1	1	1	1	1
2	0.9992	0.9992	0.9984	0.99841
3	0.99847	0.99848	0.99694	0.99696
4	0.99685	0.99687	0.99371	0.99376
5	0.99484	0.99487	0.9897	0.98977
6	0.99428	0.99432	0.98859	0.98867
7	0.99369	0.99374	0.98743	0.98752
8	0.99284	0.9929	0.98574	0.98584
9	0.99276	0.99282	0.98558	0.98568
10	0.9926	0.99266	0.98525	0.98537
11	0.99558	0.99463	0.99118	0.98929
12	0.99374	0.99235	0.98752	0.98476
13	0.99193	0.99003	0.98393	0.98017
14	0.98667	0.98312	0.97352	0.96652
15	0.9823	0.97681	0.96492	0.95416
16	0.98077	0.97435	0.96191	0.94935
17	0.98021	0.97338	0.96081	0.94747
18	0.98003	0.97281	0.96047	0.94637
19	0.99218	0.97169	0.98441	0.94418
20	0.99168	0.97119	0.98344	0.94321
21	0.99164	0.97114	0.98335	0.94312
22	0.99912	0.99942	0.99823	0.99884
23	0.99788	0.99864	0.99577	0.99727
24	0.99745	0.99837	0.9949	0.99675
25	0.99522	0.99715	0.99047	0.9943
26	0.99484	0.99696	0.9897	0.99393
27	0.99328	0.99625	0.9866	0.99252
28	0.99282	0.99579	0.98568	0.99161
29	0.99259	0.99557	0.98524	0.99116
30	0.99244	0.99542	0.98493	0.99086

Table 7.4 The results regarding *LLI*, *VSI*, node voltage and branch power losses for 30-node distribution network for May to August without optimal conductor size selection and capacitor placement.

Br. No.	*LLI* With reconfiguration	Power loss with reconfiguration	Node No.	Node voltage magnitude (p.u.) With Reconfiguration	*VSI* With Reconfiguration
1	0.38999	0.88473	1	1	1
2	0.39781	0.73593	2	0.99893	0.99787
3	0.39911	1.5455	3	0.99796	0.99593
4	0.40712	1.7225	4	0.99581	0.99164
5	0.42422	0.32815	5	0.99313	0.9863
6	0.42115	0.32335	6	0.99239	0.98483
7	0.43271	0.36554	7	0.99161	0.98329
8	0.44888	0.0098996	8	0.99048	0.98105
9	0.44995	0.0098966	9	0.99037	0.98084
10	0.42904	0.43132	10	0.99016	0.98041
11	0.43083	0.17687	11	0.99871	0.99743
12	0.43368	0.16633	12	0.99817	0.99634
13	0.43497	0.49232	13	0.99762	0.99524
14	0.43958	0.37122	14	0.99599	0.992
15	0.44356	0.11666	15	0.99452	0.98907
16	0.4449	0.041175	16	0.99394	0.98791
17	0.44841	0.014462	17	0.99371	0.98745
18	0.44942	0.019805	18	0.99357	0.98718
19	0.45002	0.005051	19	0.9933	0.98664
20	0.43664	0.00016848	20	0.99318	0.9864
21	0.37967	1.0815	21	0.99317	0.98638
22	0.39099	1.2985	22	0.99882	0.99764
23	0.39426	0.40333	23	0.99724	0.99448
24	0.40363	1.6174	24	0.99671	0.99343
25	0.42019	0.18321	25	0.99422	0.98848
26	0.42467	0.62523	26	0.99385	0.98774
27	0.43326	0.29504	27	0.99242	0.9849
28	0.4392	0.1153	28	0.99149	0.98306
29	0.44727	0.042089	29	0.99105	0.98217
				0.99073	0.98155

Table 7.5 The comparison of results regarding *LLI* and branch power losses for 30-node distribution network for September to December without optimal conductor size selection and capacitor placement.

Br. No.	*LLI* With Reconfiguration	*LLI* Without reconfiguration	Power Loss with reconfiguration	Power Loss without reconfiguration
1	0.4034	0.41488	0.62972	0.41177
2	0.40792	0.4185	0.54373	0.34316
3	0.40821	0.42037	1.1925	0.72106
4	0.41307	0.4241	1.4007	0.80505
5	0.42348	0.43361	0.34201	0.15385
6	0.41529	0.43664	0.38846	0.15139
7	0.42442	0.44205	0.53809	0.1715
8	0.44963	0.44964	0.004681	0.0046572
9	0.45014	0.45014	0.004681	0.0046572
10	0.36463	0.30568	4.1065	7.5078
11	0.36514	0.29704	1.602	3.0965
12	0.37563	0.29889	1.3479	2.9275
13	0.36473	0.25954	3.7857	8.783
14	0.38974	0.26026	2.1044	6.6647
15	0.42544	0.33229	0.43078	2.0591
16	0.43529	0.35604	0.11435	0.72245
17	0.43882	0.41754	0.087426	0.24991
18	0.44762	0.43491	0.059421	0.34099
19	0.44549	0.44529	0.083381	0.086761
20	0.43636	0.43635	0.0027778	0.0028903
21	0.41843	0.42997	0.34454	0.1263
22	0.42066	0.43129	0.45336	0.15204
23	0.42158	0.43377	0.15684	0.047223
24	0.42349	0.4374	0.77689	0.18959
25	0.42771	0.43934	0.11967	0.021559
26	0.43986	0.43987	0.073923	0.073649
27	0.44829	0.4483	0.034874	0.034745
28	0.44899	0.449	0.013649	0.013598
29	0.44995	0.44995	0.004992	0.0049738

Table 7.6 The comparison of results regarding *VSI* and node voltage for 30-node distribution network for September to December without optimal conductor size selection and capacitor placement.

Node No.	Node Voltage magnitude With reconfiguration	Node Voltage magnitude Without reconfiguration	*VSI* With Reconfiguration	*VSI* Without reconfiguration
1	1	1	1	1
2	0.9991	0.99927	0.9982	0.99855
3	0.99827	0.99861	0.99653	0.99722
4	0.99638	0.99714	0.99277	0.99429
5	0.99396	0.99531	0.98796	0.99064
6	0.9932	0.9948	0.98645	0.98963
7	0.99235	0.99427	0.98476	0.98858
8	0.99098	0.9935	0.98204	0.98704
9	0.99091	0.99343	0.9819	0.9869
10	0.99076	0.99328	0.9816	0.98661
11	0.99602	0.9946	0.99205	0.98922
12	0.99438	0.99231	0.98878	0.98468
13	0.9928	0.98998	0.98565	0.98005
14	0.98828	0.98302	0.97669	0.96632
15	0.98476	0.97667	0.96976	0.95389
16	0.98364	0.9742	0.96755	0.94906
17	0.98326	0.97323	0.9668	0.94717
18	0.99572	0.97266	0.99145	0.94607
19	0.99525	0.97153	0.99052	0.94387
20	0.99049	0.97103	0.98107	0.94289
21	0.99045	0.97098	0.98098	0.94281
22	0.99934	0.9996	0.99867	0.9992
23	0.9984	0.99906	0.99681	0.99812
24	0.99807	0.99888	0.99615	0.99775
25	0.99635	0.99803	0.99272	0.99606
26	0.99605	0.9979	0.99212	0.9958
27	0.99556	0.99741	0.99114	0.99483
28	0.99524	0.99709	0.99051	0.99419
29	0.99509	0.99694	0.9902	0.99389
30	0.99498	0.99683	0.98999	0.99367

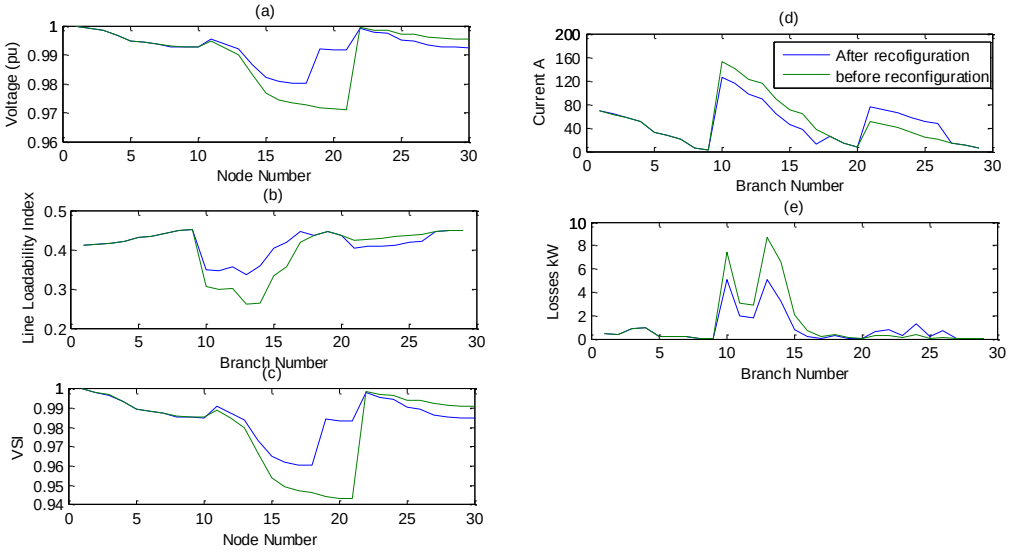

Fig. 7.4 The comparison of results from January to April without optimal conductor selection and without capacitor placement for 30-node distribution network. Fig. 7.4 (a) comparison of node voltage (p.u.), Fig. 7.4 (b) comparison of Line loadability index, Fig. 7.4 (c) comparison of voltage stability index, Fig. 7.4 (d) comparison of Branch current and Fig. 7.4 (d) comparison of branch losses

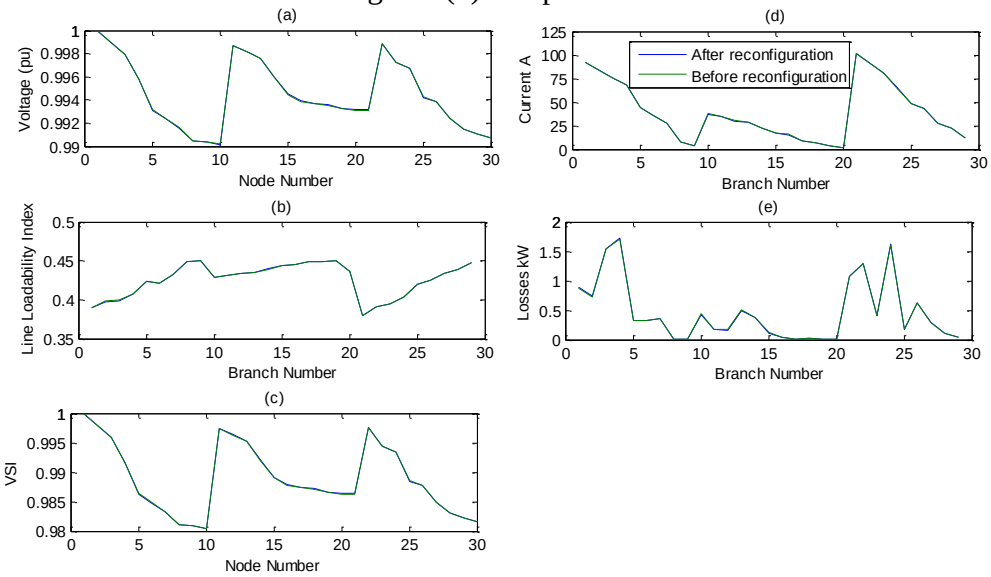

Fig. 7.5 The comparison of results from May to August without optimal conductor selection and without capacitor placement for 30-node distribution network. Fig. 7.5 (a) comparison of node voltage (p.u.), Fig. 7.5 (b) comparison of Line loadability index, Fig. 7.5 (c) comparison of voltage stability index, Fig. 7.5 (d) comparison of Branch current and Fig. 7.5 (d) comparison of branch losses

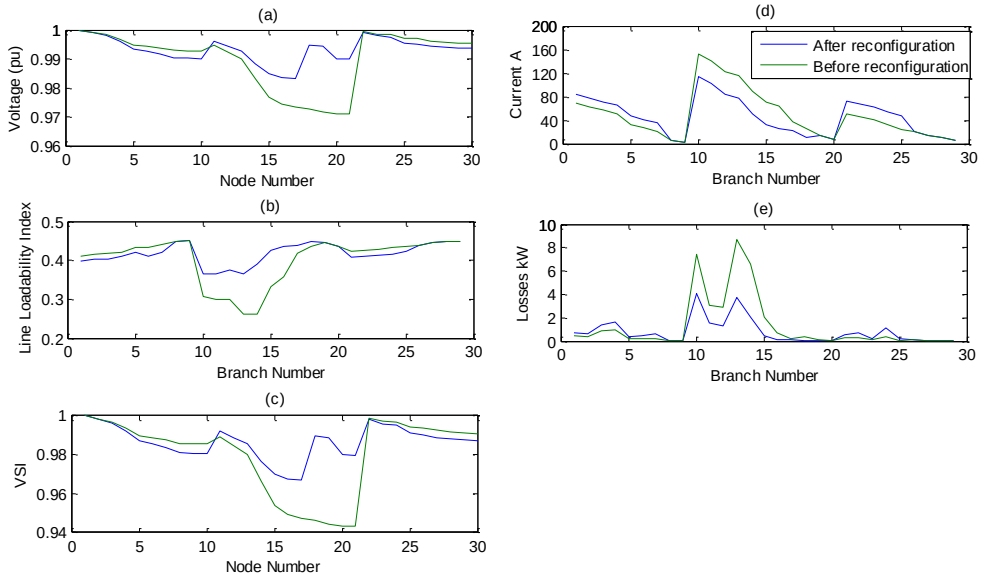

Fig. 7.6 The comparison of results from September to December without optimal conductor selection and without capacitor placement for 30-node distribution network. Fig. 7.6 (a) comparison of node voltage (p.u.), Fig. 7.6 (b) comparison of Line loadability index, Fig. 7.6 (c) comparison of voltage stability index, Fig. 7.6 (d) comparison of Branch current and Fig. 7.6 (d) comparison of branch losses

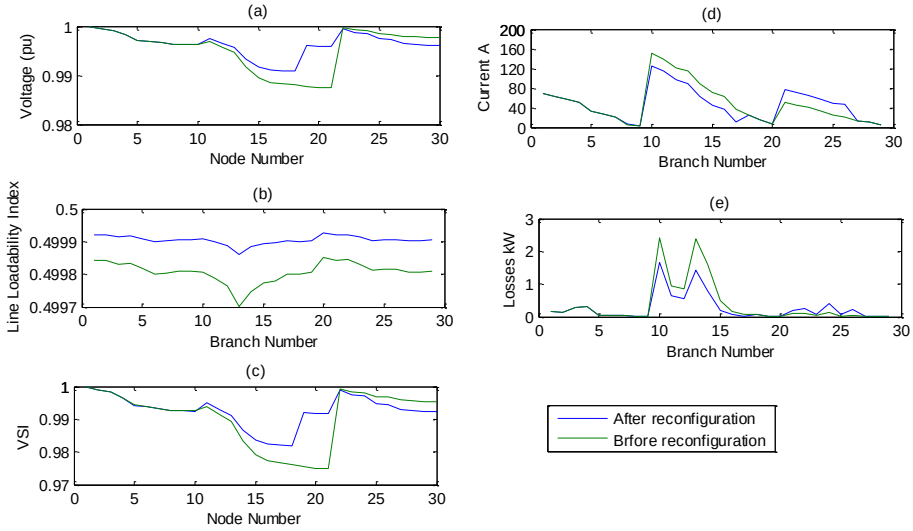

Fig. 7.7 The comparison of results from January to April with optimal conductor selection and with capacitor placement for 30-node distribution network. Fig. 7.7 (a) comparison of node voltage (p.u.), Fig. 7.7 (b) comparison of Line loadability index, Fig. 7.7 (c) comparison of voltage stability index, Fig. 7.7 (d) comparison of Branch current and Fig. 7.7 (d) comparison of branch losses

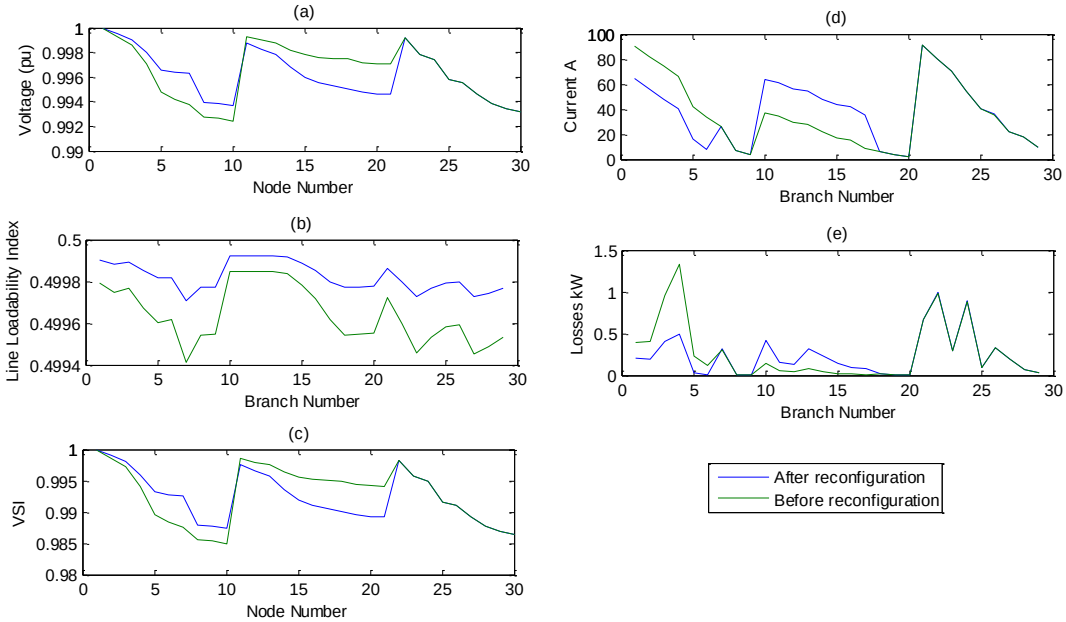

Fig. 7.8 The comparison of results from May to September with optimal conductor selection and with capacitor placement for 30-node distribution network. Fig. 7.8 (a) comparison of node voltage (p.u.), Fig. 7.8 (b) comparison of Line loadability index, Fig. 7.8 (c) comparison of voltage stability index, Fig. 7.8 (d) comparison of Branch current and Fig. 7.8 (d) comparison of branch losses

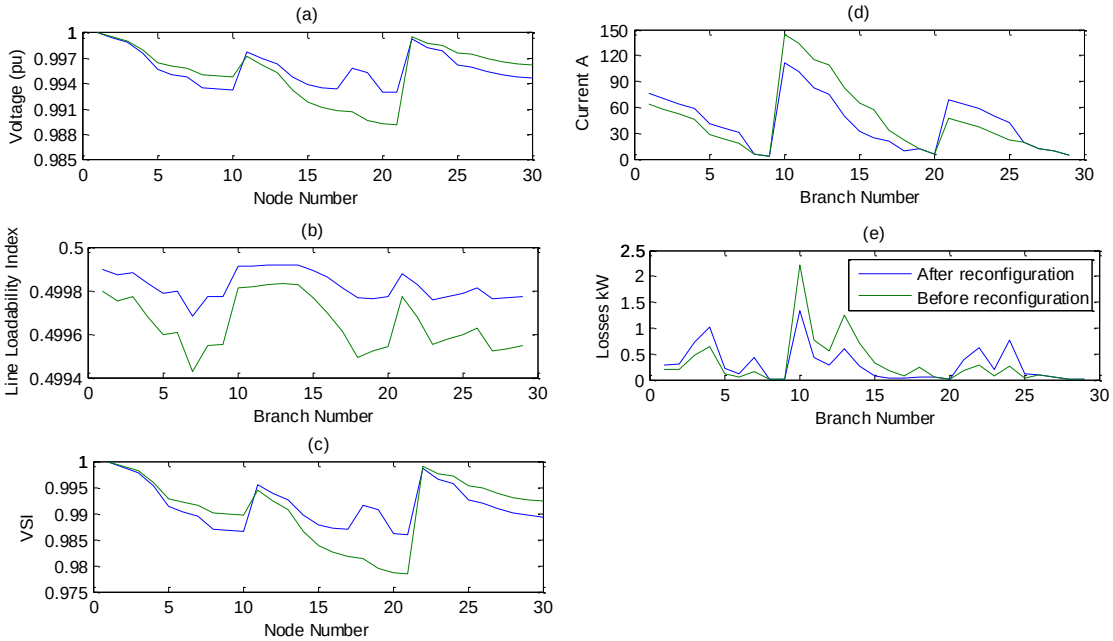

Fig. 7.9 The comparison of results from September to December with optimal conductor selection and with capacitor placement for 30-node distribution network. Fig. 7.8 (a) comparison of node voltage (p.u.), Fig. 7.8 (b) comparison of Line loadability index, Fig. 7.8 (c) comparison of voltage stability index, Fig. 7.8 (d) comparison of Branch current and Fig. 7.8 (d) comparison of branch losses

Table 7.7 The switching scheme of tie-lines, isolator switches and comparison of result with and without network reconfiguration with optimal conductor size selection and capacitor placement.

Months	Isolator switch status	Tie-line status	Without Reconfiguration				With Reconfiguration			
			Min. Volt. (p.u.)	Min. *LLI*	Min. *VSI*	Real Power Loss kW	Min. Volt. (p.u.)	Min. *LLI*	Min. *VSI*	Real Power Loss kW
Jan.-April	X_1 (Open)	TL_1 (Closed)	V_{21}= 0.98976	LLI_{18}= 0.49946	VSI_{21}= 0.97963	9.076	V_{18}= 0.99275	LLI_{18}= 0.49973	VSI_{21}= 0.98554	8.6633
May-Aug.	X_4 (Open)	TL_4 (closed)	V_{10}= 0.99245	LLI_1= 0.49941	VSI_{10}= 0.98496	7.7547	V_{30}= 0.99316	LLI_7= 0.49971	VSI_{30}= 0.98637	6.8485
Sep.-Dec.	(X_2 , X_3) (Open)	TL_2, TL_3 (closed)	V_{21} = 0.98916	LLI_7= 0.49943	VSI_{21}= 0.98597	9.1878	V_{21} = 0.99296	LLI_7= 0.49968	VSI_{21} = 0.98597	8.5019

Table 7.8 The comparison of results regarding *LLI* and branch power losses for 30-node distribution network for January to April with optimal conductor size selection and capacitor placement.

Br. No.	*LLI* With reconfiguration	*LLI* With reconfiguration	Power Loss with reconfiguration	Power Loss without reconfiguration
1	0.4999	0.4998	0.2223	0.22027
2	0.49988	0.49976	0.229	0.22674
3	0.49989	0.49978	0.53279	0.52711
4	0.49984	0.49969	0.73799	0.72966
5	0.4998	0.49961	0.1299	0.12833
6	0.49981	0.49962	0.061579	0.060815
7	0.49974	0.49948	0.169	0.16686
8	0.49977	0.49955	0.0040502	0.004001
9	0.49977	0.49955	0.0040508	0.004001
10	0.49991	0.49981	1.5413	2.1199
11	0.49991	0.49982	0.50998	0.7222
12	0.49992	0.49983	0.35472	0.53493
13	0.49992	0.49983	0.75112	1.1696
14	0.49992	0.49983	0.35239	0.64845
15	0.49989	0.49977	0.12826	0.29264
16	0.49986	0.49969	0.065579	0.17011
17	0.49982	0.49962	0.0073894	0.06611
18	0.49973	0.49946	0.21439	0.21542
19	0.49976	0.49952	0.054102	0.054361
20	0.49977	0.49954	0.0054107	0.0054364
21	0.49988	0.49977	0.38477	0.18505
22	0.49983	0.49968	0.61498	0.27456
23	0.49976	0.49955	0.20603	0.083953
24	0.49977	0.49958	0.76962	0.26062
25	0.49979	0.4996	0.10934	0.027851
26	0.49979	0.49961	0.42152	0.095959
27	0.49976	0.49952	0.053395	0.052802
28	0.49977	0.49953	0.020951	0.020716
29	0.49977	0.49955	0.007750	0.0076625

Table 7.9 The comparison of results regarding *VSI* and node voltage magnitude (p.u.) for 30-node distribution network for January to April with optimal conductor size selection and capacitor placement.

Node No.	Node voltage magnitude With reconfiguration	Node voltage Without reconfiguration	*VSI* With Reconfiguration	*VSI* Without reconfiguration
1	1	1	1	1
2	0.99949	0.99949	0.99898	0.99899
3	0.99897	0.99898	0.99795	0.99796
4	0.99779	0.99781	0.99559	0.99562
5	0.9961	0.99612	0.99222	0.99226
6	0.99566	0.99568	0.99134	0.99138
7	0.9954	0.99542	0.99082	0.99087
8	0.9946	0.99463	0.98923	0.98929
9	0.99453	0.99456	0.98909	0.98915
10	0.99438	0.99441	0.9888	0.98886
11	0.99764	0.99735	0.99529	0.99471
12	0.99678	0.99638	0.99358	0.99278
13	0.99607	0.99556	0.99216	0.99114
14	0.99445	0.99364	0.98893	0.98733
15	0.99346	0.99239	0.98696	0.98483
16	0.99304	0.99179	0.98612	0.98364
17	0.99282	0.99145	0.98569	0.98297
18	0.99275	0.99123	0.98554	0.98254
19	0.99403	0.99027	0.9881	0.98064
20	0.99361	0.98985	0.98726	0.9798
21	0.99352	0.98976	0.98709	0.97963
22	0.99935	0.99953	0.9987	0.99906
23	0.99829	0.99881	0.99659	0.99762
24	0.99792	0.99857	0.99585	0.99714
25	0.99634	0.99762	0.99269	0.99525
26	0.99607	0.99749	0.99216	0.99498
27	0.99499	0.99696	0.99001	0.99392
28	0.99457	0.99654	0.98917	0.99309
29	0.99437	0.99634	0.98877	0.99269
30	0.99423	0.9962	0.98848	0.9924

Table 7.10 The comparison of results regarding *LLI* and branch power losses for 30-node distribution network for May to August with optimal conductor size selection and capacitor placement.

Br. No.	*LLI* With reconfiguration	*LLI* With reconfiguration	Power loss with reconfiguration	Power loss without reconfiguration
1	0.4999	0.49979	0.20166	0.39839
2	0.49988	0.49975	0.19181	0.41075
3	0.49989	0.49977	0.40312	0.95677
4	0.49985	0.49967	0.48826	1.3275
5	0.49982	0.4996	0.034241	0.23603
6	0.49982	0.49962	0.0062261	0.11263
7	0.49971	0.49941	0.31627	0.31246
8	0.49977	0.49954	0.0072107	0.0071296
9	0.49977	0.49955	0.0072121	0.0071294
10	0.49992	0.49985	0.42483	0.14463
11	0.49992	0.49985	0.15641	0.050085
12	0.49992	0.49985	0.13388	0.037732
13	0.49992	0.49985	0.31339	0.083198
14	0.49992	0.49984	0.2362	0.0481
15	0.49989	0.49978	0.14402	0.02237
16	0.49985	0.49972	0.096623	0.013067
17	0.4998	0.49962	0.082772	0.0053415
18	0.49977	0.49954	0.019006	0.018833
19	0.49977	0.49955	0.0050932	0.0050454
20	0.49978	0.49955	0.00050933	0.00050455
21	0.49986	0.49972	0.67481	0.67127
22	0.4998	0.4996	0.98929	0.9836
23	0.49973	0.49946	0.29773	0.2959
24	0.49977	0.49953	0.89226	0.88618
25	0.49979	0.49958	0.097378	0.096675
26	0.4998	0.49959	0.33504	0.33254
27	0.49973	0.49945	0.19022	0.18873
28	0.49974	0.49949	0.074886	0.07429
29	0.49977	0.49953	0.02813	0.027897

Table 7.11 The comparison of results regarding *VSI* and node voltage magnitude (p.u.) for 30-node distribution network for May to August with optimal conductor size selection and capacitor placement.

Node No.	Node voltage magnitude (p.u.) With reconfiguration	Node Voltage magnitude (p.u.) Without reconfiguration	*VSI* With Reconfiguration	*VSI* Without reconfiguration
1	1	1	1	1
2	0.99951	0.99932	0.99901	0.99863
3	0.99902	0.99862	0.99805	0.99724
4	0.99799	0.99703	0.99598	0.99408
5	0.9966	0.99476	0.99322	0.98955
6	0.99637	0.99417	0.99276	0.98836
7	0.99629	0.99381	0.9926	0.98766
8	0.99394	0.99274	0.98792	0.98554
9	0.99384	0.99265	0.98772	0.98535
10	0.99365	0.99245	0.98734	0.98496
11	0.99877	0.99926	0.99754	0.99853
12	0.99829	0.99899	0.99659	0.99798
13	0.99786	0.99875	0.99572	0.9975
14	0.9968	0.99819	0.99362	0.99638
15	0.99598	0.99781	0.99198	0.99562
16	0.99553	0.99763	0.99107	0.99526
17	0.99526	0.99753	0.99055	0.99506
18	0.99501	0.99747	0.99005	0.99494
19	0.99475	0.9972	0.98952	0.99441
20	0.99463	0.99708	0.98928	0.99417
21	0.9946	0.99706	0.98924	0.99412
22	0.99916	0.99916	0.99831	0.99832
23	0.99785	0.99785	0.9957	0.99571
24	0.99742	0.99742	0.99484	0.99485
25	0.99577	0.99578	0.99155	0.99157
26	0.99553	0.99554	0.99107	0.9911
27	0.9946	0.99462	0.98923	0.98927
28	0.99382	0.99384	0.98767	0.98771
29	0.99343	0.99346	0.98691	0.98696
30	0.99316	0.99318	0.98637	0.98641

Table 7.12 The comparison of results regarding *LLI* and branch power losses for 30-node distribution network for September to December with optimal conductor size selection and capacitor placement.

Br. No.	*LLI* With reconfiguration	*LLI* Without reconfiguration	Power Loss with reconfiguration	Power Loss without reconfiguration
1	0.4999	0.4998	0.28444	0.20007
2	0.49987	0.49975	0.29969	0.20395
3	0.49988	0.49977	0.71644	0.46856
4	0.49983	0.49968	1.0259	0.63911
5	0.49979	0.4996	0.21922	0.1077
6	0.4998	0.49961	0.12157	0.052699
7	0.49968	0.49943	0.4206	0.15218
8	0.49977	0.49955	0.0040595	0.0039879
9	0.49977	0.49955	0.00406	0.0039878
10	0.49991	0.49981	1.3255	2.2168
11	0.49991	0.49982	0.43176	0.75799
12	0.49992	0.49983	0.29005	0.56575
13	0.49992	0.49983	0.603	1.2417
14	0.49992	0.49983	0.25509	0.70124
15	0.49989	0.49977	0.07632	0.31703
16	0.49986	0.4997	0.03299	0.1822
17	0.49981	0.49961	0.028902	0.071847
18	0.49977	0.49949	0.046866	0.23168
19	0.49976	0.49952	0.054163	0.054413
20	0.49977	0.49954	0.0054168	0.0054416
21	0.49988	0.49977	0.38357	0.18508
22	0.49983	0.49968	0.61291	0.27462
23	0.49976	0.49955	0.20527	0.083974
24	0.49977	0.49958	0.76633	0.26071
25	0.49979	0.4996	0.10878	0.027865
26	0.49981	0.49963	0.096946	0.096016
27	0.49976	0.49952	0.053347	0.052832
28	0.49977	0.49953	0.020932	0.020728
29	0.49977	0.49955	0.007743	0.007667

Table 7.13 The comparison of results regarding *VSI* and node voltage magnitude (p.u.) for 30-node distribution network for September to December with optimal conductor size selection and capacitor placement.

Node No.	Node Voltage magnitude (p.u.) With reconfiguration	Node Voltage magnitude (p.u.) Without reconfiguration	*VSI* With reconfiguration	*VSI* Without reconfiguration
1	1	1	1	1
2	0.99947	0.99954	0.99893	0.99908
3	0.99891	0.99907	0.99783	0.99813
4	0.99761	0.99799	0.99522	0.99598
5	0.99568	0.99644	0.99137	0.99289
6	0.99512	0.99604	0.99026	0.99209
7	0.99476	0.9958	0.98955	0.99162
8	0.99347	0.99503	0.98699	0.99008
9	0.9934	0.99495	0.98684	0.98994
10	0.99325	0.99481	0.98655	0.98965
11	0.99776	0.99722	0.99553	0.99444
12	0.99696	0.99619	0.99392	0.99239
13	0.9963	0.99531	0.99261	0.99064
14	0.9948	0.99326	0.98962	0.98657
15	0.99392	0.99189	0.98788	0.98384
16	0.99359	0.99124	0.98721	0.98255
17	0.99343	0.99089	0.98691	0.98186
18	0.99582	0.99066	0.99166	0.9814
19	0.99538	0.98967	0.99079	0.97945
20	0.99305	0.98925	0.98614	0.97861
21	0.99296	0.98916	0.98597	0.97844
22	0.99932	0.99953	0.99865	0.99906
23	0.99824	0.99881	0.99649	0.99761
24	0.99787	0.99857	0.99574	0.99714
25	0.99624	0.99762	0.9925	0.99525
26	0.99597	0.99749	0.99196	0.99498
27	0.99544	0.99696	0.99089	0.99392
28	0.99502	0.99654	0.99006	0.99309
29	0.99481	0.99634	0.98966	0.99269
30	0.99467	0.99619	0.98937	0.9924

Table 7.14 The value of capacitor (kVAr) at each node from January to December for 30-node distribution network.

Node No.	Value of capacitor in (kVAr) (January to April)	Value of capacitor in (kVAr) (May to August)	Value of capacitor in (kVAr) (September to December)
1	0	0	0
2	0	0	0
3	0	0	0
4	0	0	0
5	0	0	15
6	0	0	30
7	0	0	30
8	30	15	60
9	15	15	15
10	15	15	15
11	0	15	0
12	0	0	0
13	0	0	0
14	0	0	0
15	15	0	0
16	15	0	0
17	45	0	30
18	30	15	15
19	60	15	30
20	45	0	45
21	45	0	45
22	0	0	0
23	0	0	0
24	0	0	0
25	0	30	0
26	15	30	15
27	15	45	15
28	15	30	15
29	30	60	30
30	30	45	30

7.6 Conclusion:

From the above discussion it can be concluded that rather the chances for reconfiguration are very limited in case of distribution networks but it has great benefits in the form of reduced losses, increased line loadability, increased voltage stability, reduced branch current and improved voltage profile of the network after reconfiguration. Along with these benefits the reliability of supply is increased. At the time of outage, supply of some portion of network can be restored. Through network reconfiguration the already installed capacity can be best used. The line loadability and voltage stability of the distribution networks can be enhanced. The tabulated results and graphical represented that the critical loading and voltage stability of the 30-node test network has been improved. The proposed approach is novel no such approach in the field of network reconfiguration is reported so far.

CHAPTER 8

MAIN CONCLUSION AND FUTURE SCOPE OF WORK

The aim of this chapter is to give the overall conclusion of the thesis and to show the future scope of work. In this chapter the results and findings of each chapter are to be discussed.

8.1 Main conclusion:

A brief introduction of distribution networks, introduction of critical loading, objectives of research, scope of research and organization of research are discussed in **Chapter 1**. The detailed literature survey of load-flow solution for distribution networks, line loadability index and voltage stability index for radial distribution networks, optimal conductor size selection for radial distribution networks, optimal sizing and location of shunt capacitors for radial distribution networks and reconfiguration of distribution networks is discussed in **chapter 2**.

A new and efficient load-flow method is proposed in **chapter 3**. The algorithm of load-flow method is developed in such a way that it does not require the sequential numbering of node and branches. The nodes of each lateral are identified from the line data through the computer program and the load-flow is carried out by using these lateral arrays. The equations of load-flow solution are capable to take the effect of charging capacitances. So this load-flow solution method is very suitable for load-flow of distribution networks having capacitors installed at various nodes. Due to non-requirement of sequential node numbering and branch numbering this load-flow solution method is also very suitable for network reconfiguration. The efficiency and reliability of the proposed method is established by comparing the results of proposed method with the existing methods [17] and [21] for 69-node distribution network and 33-node distribution network respectively. It is observed that the cpu time and

memory requirement is quite less for the proposed method. The proposed load-flow method is used in this work for load-flow solution in subsequent chapters. The convergence of load-flow solution is also checked for various load models.

In **chapter 4** a new definition is proposed for line loadability index for radial distribution network. The line loadability index is related to the operating temperature of the branch conductors. The steady state of operating condition and the steady state critical loading condition of the distribution network are studied and analyzed through line loadability index. By the analysis of line loadability index the most sensitive branch of the distribution network and other weak branches can be identified. A voltage stability index is proposed in this chapter. The voltage stability index can be used to find the voltage stability limit of the distribution network under fault conditions. Most sensitive node of the network can be identified by voltage stability index. While computing the voltage stability index for each node of the distribution network the effect of change of resistance due to change of temperature is incorporated. Through line loadability index and voltage stability index the steady state conditions of the distribution network and the network conditions under the fault conditions can be analyzed. In **chapter 4** the line loadability analysis and voltage stability analysis is shown with the help of tabulated results and graphical representations. With the help of voltage stability index the minimum severity of fault can be computed for which there are chances of voltage collapse will occur, before the protection system of the distribution network will respond to clear the fault. With the help of line loadability index the maximum loading limit of the distribution network can be found.

In **chapter 5** a new method for optimal conductor size selection for radial distribution networks is proposed, and the enhancement of critical loading and enhancement of voltage stability is achieved by optimal conductor size selection. In the conductor size selection procedure the effect of change in resistance due to change in temperature caused by flow of current through conductor is incorporated.

To show the goodness and reliability of the proposed method the results of optimal conductor size selection for existing methods [57] and [58] are compared with the proposed method. The proposed method showed the better results in every respect. The enhancement in critical loading and improvement in voltage stability are shown with the help of tabulated results and graphical representations.

In **chapter 6** the optimal capacitor placement method is proposed. The power factor improvement is achieved by placing the optimal sizes of capacitors at nodes where the reactive power compensation is required. Almost all the methods discussed in literature survey used the line reactive power compensation but in proposed the reactive power compensation is achieved by node reactive power compensation. The comparison of results with the existing method [100] is shown in tabulated form and it is established that the proposed method for reactive power compensation by shunt capacitors is better than the proposed method, because with less capacitor cost higher economical benefits can be achieved. Even the power factor improvement is also better with the proposed method. It is also shown with the help of tabulated results and graphical representations that the enhancement of critical loading of radial distribution network and improvement of voltage stability of radial distribution network can be achieved by reactive power compensation.

In **chapter 7** the enhancement of critical loading and improvement in voltage stability is achieved through network reconfiguration of radial distribution network. The possibilities of network reconfiguration are identified through the investigation of chronological load curve. There is a seasonal change in load demand of different kind of consumers. So the load from a lateral having high load demand can be shifted to the lateral having low load demand. This procedure is applied to a typical distribution 30-node distribution network having three lateral dedicated to different types of loads. The enhancement of critical loading and improvement of voltage stability are shown with the help of

tabulated results and graphical representations. The proposed method is based on the practical constraints of network reconfiguration.

The enhancement of critical loading and improvement in voltage stability is achieved after each step i.e. optimal conductor size selection, capacitor placement and network reconfiguration.

8.2 Future scope of research:

After carrying out the extensive research work it realized that the present research work can be extended in following directions.

- In this work it is assumed that the distribution network is balanced so the research work can be extended for three phase unbalanced distribution networks. So load-flow solution method for unbalanced three phase distribution networks has to be developed.
- This work is oriented for radial distribution network in further research can be extended for the weakly meshed and meshed distribution networks.
- The network line loadability and voltage stability can be investigated in the environment of smart grid.
- In the present work the static load modelling is considered the effect of dynamic load modelling on critical loading of distribution network and voltage stability of distribution network can be investigated.

  The effect of online voltage controller can be incorporated in the investigations of critical loading and voltage stability studies.

References

[1] W. G. Tinney and C. E. Hart, "Power flow solutions by Newton's method," ***IEEE Transactions on Power Apparatus and Systems***, Volume 86, Number 11, pp. 1449–1457, 1967.

[2] B. Stott, and O. Alsac, "Fast decoupled load-flow," ***IEEE Transactions on Power Apparatus and Systems***, Volume 93, Number. 3, pp. 859–869, 1974.

[3] S. Iwamoto and Y. Tamura, "A load flow-calculation method for ill-conditioned power systems," ***IEEE Transactions on Power Apparatus and Systems***, Volume 100, Number 4, pp. 1736–1743, 1981.

[4] D. Rajicic and Y. Tamura, "A modification to fast decoupled power flow for network with high *R/X* Ratios," ***IEEE Transactions on Power Delivery***, Volume 3, Number 2, pp. 743–746, 1988.

[5] W. H. Kersting, "A method to the design and operation of a distribution system," ***IEEE Transactions on Power Apparatus and Systems***, Volume 103, Number 7, pp. 1945–1952, 1984.

[6] D. Shirmohammadi, H. W. Hong, A. Semlyen and G, X. Luo, "A compensation-based power-flow method for weakly meshed distribution and transmission networks," ***IEEE Transactions on Power Systems,*** Volume 3, Number 2, pp. 753–762, 1988.

[7] M. E. Baran and F. F. Wu, "Optimal sizing of capacitors placed on a radial distribution system," ***IEEE Transactions on Power Delivery***, Volume 4, Number 1, pp. 735–743, 1989.

[8] G. Renato Cespedes, "New method for the analysis of distribution networks," ***IEEE Transactions on Power Delivery***, Volume 5, Number 1, pp. 391–396, 1990.

[9] S. K. Goswami and S. K. Basu, "Direct solution of distribution systems", ***IEE Proceedings on Generation Transmission and Distribution***, Volume 138, Number 1, pp. 78–88, 1991.

[10] G. B. Jasmon and L. H. C. Lee, "Distribution network reduction for voltage stability Analysis and load-flow calculations," ***International journal of Electric Power and Energy System***, Volume 13, Number 1, pp. 9–13, 1991.

[11] D. Das, H. S. Nagi and D.P. Kothari, "Novel method for solving radial distribution networks," ***IEE Proceedings on Generation Transmission and Distribution***, Volume 141, Number 4, pp. 291–298, 1994.

[12] M. H. Haque, "Load flow-solution of distribution systems with voltage dependent load models," ***Electric Power Systems Research***, Volume 36, Number 3, pp. 151–156, 1996.

[13] S. Ghosh and D. Das, "Method for load solution of radial distribution networks," ***IEE Proceedings on Generation Transmission and Distribution***, Volume 146, Number 6, pp. 641–648, 1999.

[14] P. Aravindhababu, S. Ganapathy and K. R. Nayar, "A novel technique for the analysis of radial distribution systems," ***International Journal of Electrical Power and Energy Systems,*** Volume 23, Number 3, pp. 167-171, 2001.

[15] S.F. Mekhamer, S. A. Soliman, M. A. Mustafa and M. E. El-Hawary, "Load-flow solution of radial distribution feeders: a new contribution," ***Electrical Power and Energy Systems***, Volume 24, Number 5, pp. 701-707, 2002.

[16] U. Eminoglu, and M. H. Hocaoglu, “A new power flow method for radial distribution systems including voltage dependant load models,” ***Electric Power Systems Research***, Volume 76, Number 1-3, pp. 106-114, 2005.

[17] S. Satyanarayana, T. Ramana, S. Sivanagaraju and G. K. Rao, “An efficient load flow solution for radial distribution network including voltage dependent load models,” ***Electric Power Components and Systems***, Volume 35, Number 5, pp. 539-551, 2007.

[18] S. Ghosh and K. S. Sherpa, “ An efficient method for load-flow solution of radial distribution networks,” ***World Academy of Science, Engineering and Technology***, Volume 45, pp. 700-7008, 2008

[19] K. Nagaraju, S. Sivanagaraju, T. Ramana and P. V. Prasad, “A novel load-flow method for radial distribution systems for realistic loads,” ***Electric Power Components and Systems***, Volume 39, Number 2, pp. 128-141, 2011.

[20] M. E. Baran and F. F. Wu, “Optimal capacitor placement on radial distribution systems,” ***IEEE Transactions on Power Delivery***, Volume 4, Number 2, pp. 1401-1407, 1989.

[21] A. Hamouda and K. Zehar, “Improved algorithm for radial distribution networks load-flow solution,” ***International Journal of Electrical Power and Energy Systems***, Volume 33, Number 3, pp. 508-514, 2011.

[22] H. G. Kwatny, A. K. Pasrija, L. Y. Bahar, L, “Loss of steady state stability and voltage collapse in electric power systems,” ***Proceedings of IEEE Conference on Decision and control***, Dec. 1985, pp. 804-811, FL, Ft. Lauderdale.

[23] H. D. Chiang, I. Dobson, R. J. Thomas, J. S. Thorp, and L. Fekih-Ahmed, "On voltage collapse in electric power system," ***IEEE Transactions on Power Systems***, Volume 5, Number 2, May 1990, pp-601-611.

[24] N. Flatabo, R. Ognedal, and T. Carlsen, "Voltage stability condition in a power transmission system calculated by sensitivity methods," ***IEEE Trans*actions on *Power Systems***, Volume 5, Number 4, pp. 1286-1293, 1990.

[25] H.K. Clark, "New challenge: Voltage stability," ***IEEE Power Engineering Review***, Volume 10, Number 4, pp. 33-37, 1990.

[26] R. K. Gupta, Z. A. Alaywan, R. B. Stuart, and T. A. Reece, "Steady state voltage instability operations perspective," ***IEEE Transactions on Power Systems***, Volume 5, Number 4, pp. 1345-1351,1990.

[27] G. B. Jasmon and L. H. C. C Lee, "Stability of loadflow techniques for distribution voltage stability analysis," ***IEE Proceedings on Generation Transmission and Distribution***,, Volume 138, Number 6, pp. 479-484, 1991.

[28] D. J. Hill, G. Anderson and P. A. Lof, "Fast calculation of voltage stability index," ***IEEE Transactions on Power Systems***, Volume 7, Number 1, pp-54-64, 1992.

[29] M. J. H. Sterling, A. M. Chebbo and M. R. Irving, "Voltage collapse proximity indicator: behavior and implications," ***IEE Proceedings on Generation Transmission and Distribution***,, Volume 139, Number 3, pp. 341-352, 1992.

[30] F. Gubina, B. Strmcnik, "A simple approach to voltage stability assessment in radial networks," ***IEEE Transactions on Power Systems***, Volume12, Number 3, pp.1121-1128, 1997.

[31] Y. Y. Hong and C. H. Gau, "Voltage stability indicator for identification of the weakest bus/area in power systems," ***IEE Proceedings on Generation, Transmission and Distribution***,, Volume 141, Number 4, pp. 305-309, 1994.

[32] A. Mohamed and G. B. Jasmon, "A new clustering technique for power system voltage stability analysis," ***Electrical Machines and Power Systems***, Volume 23, Number 4, pp. 389-403, 1995.

[33] T. Van. Cutsem, C. Moisse, and R Mailhot, "Determination of secure operating limits with respect to voltage collapse," ***IEEE Transactions on Power Systems***, Volume14, Number 1, pp. 327–335, 1999.

[34] M. Moghavvemi and M. O. Faruque, "Power system security and voltage collapse: a line outage based indicator for prediction," ***Electric Power and Energy Systems***, Volume 21, Number 6, pp. 455-461, 1999.

[35] M. Moghavvemi and M.O. Faruque, "Technique for assessment of voltage stability in ill-conditioned radial distribution network," ***IEEE Power Engineering Review***. Volume 21, Number 1, pp. 58–60, 2001.

[36] M. Chakravorty and D. Das, "Voltage stability analysis of radial distribution networks," ***Electric Power and Energy Systems***, Volume 23, Number 2, pp.129-135, 2001.

[37] M. H. Haque, "On-line monitoring of maximum permissible loading of a power system within the voltage stability limit," ***IEE Proceedings on Generation, Transmission and Distribution***, Volume 150, Number 1, pp. 107-112, 2003.

[38] A. Chaturvedi, K. Prasad and R. Ranjan, "A new voltage stability index for radial distribution network," ***International Journal of Power and Energy Systems***, Volume 26, Number 1, pp.83-88, 2006.

[39] Y. Kataoka, M. Watanabe, S. Iwamoto, "A new voltage stability index considering voltage limits," ***IEEE PES Power System Conference and Exposition***, November 2006, pp. 1878-1883, Atlanta, GA.

[40] U. Eminoglu, M. H. Hocaoglu, "A voltage stability index for radial distribution networks," ***42nd International Universities Power Engineering Conference***, September 2007, pp. 408 – 413, Brighton.

[41] Y. Juan, L. Wenyuan and Y. Wei, "Letter to the Editor: A new line loadability index for radial distribution systems," ***Electric Power Components and Systems***, Volume 36, Number 11, pp. 1245—1252, 2008.

[42] M. M. Hamada, M. A.A. Wahab and N. G. A. Hemdan, "Simple and efficient method for steady-state voltage stability assessment of radial distribution systems," ***Electric Power Systems Research***, Volume 80, Number 2, pp. 152-160, 2010.

[43] X. Y. Chen, D. M. Zhao and X. Zhang, "A novel voltage stability prediction index based on wide area measurement," ***Power and Energy engineering conference, Asia-Pacific***, pp. 1-4, 28-31 march 2010, Chengdu.

[44] S. Sakthivel, D. Mary, "Voltage stability limit improvement by static VAR compensator (SVC) under line outage contingencies through particle swarm optimization algorithm," ***International Review of Electrical Engineering***, Volume 4, Number 2, pp. 766-771, 2011.

[45] M. Hosseini, "Voltage stability analysis and contingency ranking in power systems using neural network," ***International Review of Electrical Engineering***, Volume 3, Number 5, pp. 776-781, 2010.

[46] IEEE Power Engineering Society, "IEEE Std 738™-2006 IEEE standard for calculating the current-temperature of bare overhead conductors," ***Institute of Electrical and Electronics Engineers, Inc. USA***, 2007

[47] T. L. Le, M. Negnevitsky and M. Piekutowski, "Expert system application for the loading capability assessment of transmission lines," ***IEEE Transactions on Power Systems***, Volume 10, Number 4, pp. 1805-1812, 1995.

[48] J. M. Gers., E. J. Holmes, "Protection of electricity distribution networks," ***The institution of electrical engineers, United kingdom, London***, 2004.

[49] A. W. Funk Houser, "A method for determining economical ACSR conductor sizes for distribution systems," ***AIEE Transactions on Power Apparatus and systems***, Volume 74, pp. 479-483, 1955.

[50] M. Ponnavaiko & K.S.P. Rao, "An approach to optimal distribution system planning through conductor gradation," ***IEEE Transactions on Power Apparatus and Systems***, Volume 101, Number 6, pp. 1735–1742, 1982.

[51] W. C. Kiran & R. B. Adler, "A distribution system cost model and its application to optimal conductor sizing," ***IEEE Transactions on Power Apparatus and Systems***, Volume 101, Number 2, pp. 271–275, 1982.

[52] P.S. Nagendra Rao, "An extremely simple method of determining optimal conductor selection for radial distribution feeders," ***IEEE Transactions on Power Apparatus and Systems***, Volume 104, Number 6, pp. 1439–42, 1985.

[53] H. N. Tram, D. L. Wall, “Optimal conductor selection in planning radial distribution systems,” ***IEEE Transactions on Power Systems***, Volume 3, Number 1, 200–206, 1988.

[54] G. J. Anders, “Parameters affecting economic selection of cable sizes”, ***IEEE Transactions on Power Delivery***, Volume8, Number 3, pp.1661-1667, 1993.

[55] S. Leppert, A. Allen, “Conductor life cycle cost analysis,” ***Proceedings of Rural Electric Power Conference***, 1995, C 2.1–2.8.

[56] Z. Wang, H. Liu, D. C. Yu, X. Wang, H. Song, “A practical approach to the conductor size selection in planning radial distribution systems,” ***IEEE Transactions on Power Delivery***, Volume 15, Number 1, 350–354, 2000.

[57] S. Sivanagaraju, N. Sreenivasulu, M. Vijayakumar, and T. Ramana, “Optimal conductor selection for radial distribution systems,” ***Electric Power Systems Research***, Volume 63, Number 2, pp. 95–103, 2002.

[58] D. Kaur and J. D. Sharma, “Optimal conductor sizing in radial distribution systems planning,” ***Electrical Power and Energy Systems***, Volume 30, Number 4, 261–271, 2008.

[59] T. Gonen, “Electric power distribution system engineering,” ***McGraw-Hill. Inc. United States of America***, 1986.

[60] R. F. Cook, “Calculating loss reduction afforded by shunt capacitor application,” ***IEEE Transactions on Power Apparatus and Systems***, Volume 83, PP. 1227-1230, 1964.

[61] H. Duran, “Optimum Number, location and size of shunt capacitors in radial distribution feeders: a dynamic programming approach,” ***IEEE Transactions on Power Apparatus and Systems***, Volume 87, Number 9, pp. 1769–1774, 1968.

[62] R. F. Cook, “Optimizing the applications of shunt capacitors for reactive volt–ampere control and loss reduction,” ***AIEE Transactions Part III,*** Volume 80, Number 8, pp. 1961–1969, 1961.

[63] N.E. Chang, “Locating shunt capacitors on primary feeders for voltage control and loss reduction,” ***IEEE Transactions on Power Apparatus and Systems***, Volume 88, Number 10, pp. 1574–1577, 1969.

[64] J. J. Grainger and S. H. Lee, “Optimum size and location of shunt capacitors for reduction of losses on distribution feeders,” ***IEEE Transactions on Power Apparatus and Systems***, Volume 100, Number 3, pp. 1105–1118, 1981.

[65] S. H. Lee and J. J. Grainger, “Optimum placement of fixed and switched capacitors on primary distribution feeders,” ***IEEE Transactions on Power Apparatus and Systems***, Volume 100, Number 1, pp. 345–52, 1981.

[66] J. J. Grainger, S. H. Lee, “Capacity release by shunt capacitor placement on distribution feeders: a new voltage dependent model,” ***IEEE Transactions on Power Apparatus and Systems***, Volume 101, Number 5, pp. 1236–44, 1982.

[67] J. J. Grainger, S. H. Lee and A. A. El-kib, “Design of a real-time switching control scheme for capacitive compensation of distribution feeders,” ***IEEE Transactions on Power Apparatus and Systems***, Volume 101, Number 8, pp. 2420–2428, 1982.

[68] M. Ponnavaikko and K. S. P. Rao, “Optimal choice of fixed and switched shunt capacitors on radial distribution feeders by the method of local variations,’ ***IEEE***

Transactions on Power Apparatus and Systems, Volume 102, Number 6, pp.1607–1614, 1983.

[69] T. S. A. Salama, A. Y. Chikhani and R. Hackam, "A new technique for loss reduction using compensating capacitors applied to distribution systems with varying load condition," ***IEEE Transactions on Power Delivery***, Volume 9, Number 2, pp. 819–27, 1994.

[70] M. Chis, M. M. A. Salama, and S. Jayaram, "Capacitor placement in distribution systems using heuristic search strategies," ***IEE Proceedings on Generation, Transmission and Distribution***, Volume 144, Number 2, pp. 225–230, 1997.

[71] M. H. Haque, "Capacitor placement in radial distribution systems for los reduction," ***IEE Proceedings on Generation, Transmission and Distribution***, Volume 146, Number 5, pp. 501–505, 1999.

[72] H. D. Chiang, J. C. Wang, O. Cockings and H. D. Shin, "Optimal capacitor placements in distribution systems, parts I and II," ***IEEE Transactions on Power Delivery***, Volume 5, Number 1, pp. 634–49, 1990.

[73] Y. C. Huang, H. T. Yang and C. L. Huang, "Solving the capacitor placement problem in a radial distribution system using tabu search approach," ***IEEE Transactions on Power Systems***, Volume 11, Number 11, pp. 1868–1873, 1996.

[74] K. N. Miu, H. S. Chiang and G. Darling, "Capacitor placement, replacement and control in large distribution systems by a GA based two-stage algorithms," ***IEEE Transactions on Power Systems***, Volume 12, Number 8, pp. 1160–1166, 1997.

[75] G. Levitin, A. Kalyuzhny, A. Shenkman and M. Chertkov, "Optimal capacitor allocation in distribution systems using a genetic algorithm and a fast energy loss

computation technique," ***IEEE Transactions on Power Delivery***, Volume 15, Number 4, pp. 621–628, 2000.

[76] M. A. S. Masoum, A. Jafarian, M. Ladjevardi, E. F. Fuchs, and W. M. Grady, "Fuzzy approach for optimal placement and sizing of capacitor banks in the presence of harmonics," ***IEEE Transactions on Power Delivery***, Volume 19, Number 2, pp. 822–829, 2004.

[77] D. Das, "Optimal placement of capacitors in radial distribution system using a Fuzzy-GA method," ***Electric Power and Energy Systems***, Volume 30, pp. 361–367, 2008.

[78] S. Sarkar and S. Chakravorty, "Node voltage improvement by capacitor placement in distribution network: A soft computing approach," ***International Journal of Engineering Science and Technology***, Volume 2, Number, 10, pp. 5575-5582, 2010.

[79] A. Goswami and G. K. Singh, "Minimization of voltage sag induced losses in distribution systems using FACTS devices," ***Electric Power Systems Research***, Volume 81, Number 1, 2011, pp. 767-774.

[80] D. I. Sun, D. R. Farris, "Optimal distribution substation and primary feeder planning via the fix charge network formulation," ***IEEE Transactions on Power Apparatus and Systems***, Volume 102, Number 6, pp. 1178- 1187, 1983.

[81] A. Merlin and H. Back, "Search for a minimal-loss operating spanning tree configuration in an urban power distribution system," ***Proceedings of 5th Power System Computation Conference***, Cambridge, U.K., 1975, pp. 1–18.

[82] D. Shirmohammadi and H. W. Hong, “Reconfiguration of electric distribution networks for resistive line loss reduction,” ***IEEE Transactions on Power Delivery***, Volume 4, Number 1, pp. 1492–1498, 1989.

[83] V. Borozan, D. Rajicic, and R. Ackovski, “Improved method for loss minimization in distribution networks,” ***IEEE Transactions on Power Systems***, Volume 10, Number 3, pp. 1420–1425, 1995.

[84] S. Civanlar, J. J. Grainger, H. Yin, and S. S. H. Lee, “Distribution feeder reconfiguration for loss reduction,” ***IEEE Transactions on Power Delivery***, Volume 3, Number 3, pp. 1217–1223, 1988.

[85] M. E. Baran and F. F. Wu, “Network reconfiguration in distribution systems for loss reduction and load balancing,” ***IEEE Transactions on Power Systems***, Volume 4, Number 3, pp. 1401–1407, Aug. 1989.

[86] C. C. Liu, S. J. Lee, and K. Vu, “Loss minimization of distribution feeders: Optimality and algorithms,” ***IEEE Transactions on Power Delivery***, Volume 4, Number 1, pp. 1281–1289, 1989.

[87] T. Taylor and D. Lubkeman, “Implementation of heuristic search strategies for distribution feeder reconfiguration,” ***IEEE Transactions on Power Delivery***, Volume 5, Number 1, pp. 239–246, 1990.

[88] H. D. Chiang and R. M. Jean-Jameau, “Optimal network reconfiguration in distribution systems, part 1: A new formulation and a solution methodology,” ***IEEE Transactions on Power Delivery***, Volume 5, Number 4, pp. 1902–1909, 1990.

[89] H. D. Chiang, R. J. Jumeau, “Optimal network reconfigurations in distribution systems, part 2: Solution algorithms and numerical results,” ***IEEE Transactions on Power Delivery***, Volume 5, Number 3, pp. 1568–1574, 1990.

[90] Y. J. Jeon, J. C. Kim, J. O. Kim, J. R. Shin, and K. Y. Lee, “An efficient simulated annealing algorithm for network reconfiguration in large-scale distribution systems,” ***IEEE Transactions on Power Delivery***, Volume 17, Number 4, pp. 1070–1078, 2002.

[91] T. P. Wagner, A. Y. Chikhani, and R. Hackam, “Feeder reconfiguration for loss reduction,” ***IEEE Transactions on Power Delivery***, Volume 6, Number 4, pp. 1922–1933, 1991.

[92] C. S. Chen and M. Y. Cho, “Energy loss reduction by critical switches,” ***IEEE Transactions on Power Delivery***, Volume 8, Number 3, pp. 1246–1253, 1993.

[93] Q. Zhou, D. Shirmohammadi, and W. H. E. Liu, “Distribution feeder reconfiguration for service restoration and load balancing,” ***IEEE Transactions on Power Systems***, Volume 12, Number 2, pp. 724–729, 1997.

[94] R. Taleski and D. Rajicic, “Distribution network reconfiguration for energy loss reduction,” ***IEEE Transactions on Power Systems***, Volume 12, Number 1, pp. 398–406, 1997.

[95] V. Borozan and N. Rajakovic, “Application assessments of distribution network minimum loss reconfiguration,” ***IEEE Transactions on Power Delivery***, Volume 12, Number 4, pp. 1786–1792, 1997.

[96] W. M. Lin and H. C. Chin, “A new approach for distribution feeder reconfiguration for loss reduction and service restoration,” ***IEEE Transactions on Power Delivery***, Volume 13, Number 3, pp. 870–875, 1998.

[97] C. C. Liu, S. J. Lee, and S. S. Venkata, “An expert system operational aid for restoration and loss reduction of distribution systems,” ***IEEE Transactions on Power Systems***, Volume 3, Number 2, pp. 619–626, 1988.

[98] K. Nara, A. Shiose, M. Kitagawa, and T. Ishihara, “Implementation of genetic algorithm for distribution system loss minimum reconfiguration,” ***IEEE Transactions on Power Systems***, Volume 7, Number 3, pp. 1044–1051, 1992.

[99] K. Nara, T. Satoh, and M. Kitagawa, “Distribution system loss minimum reconfiguration by genetic algorithm,” ***Proceedings of 3rd Symposium Expert System Application to Power Systems***, Tokyo and Kobe, Japan, 1991, pp. 724–730.

[100] D. Das, “A Fuzzy Multi-objective Approach for Network Reconfiguration of Distribution Systems,” ***IEEE Transactions on Power Delivery***, Volume 21, Number 1, pp. 202-209, 2006.

[101] Y. C. Huang, “Enhanced genetic algorithm-based fuzzy multi-objective approach to distribution network Reconfiguration,” ***IET Proceedings on Generation Transmission and Distribution***, Volume 149, Number 5, pp-615-620, 2002.

[102] J. S. Savier and D. Das, “Impact of network reconfiguration on loss allocation of radial distribution systems,” ***IEEE Transactions on Power Delivery***, Volume 22, Number 4, pp. 2473-2480, 2007.

[103] A. S. Bouhouras and D. P. Labridis, "Influence of load alterations to optimal network configuration for loss reduction," ***Electric Power Systems Research***, article in press (2011).

[104] K. N. Miu, H. D. Chiang and R. J. Mc-Nulty, "Multi-Tier service restoration through network reconfiguration and capacitor control for large-scale radial distribution networks," ***IEEE Transactions on Power Systems***, Volume 15, Number 3, pp. 1001-1007, 2000.

[105] M. A. Kashem, V. Ganapathy and G. B. Jasmon, "Network reconfiguration for enhancement of voltage stability in distribution networks," ***IEE Proceedings on Generation Transmission and Distribution***, Volume 147, Number 3, pp. 171-175, 2000.

[106] B. Venkatesh, R. Ranjan, and H. B. Gooi, "Optimal reconfiguration of radial distribution systems to maximize loadability," ***IEEE Transactions on Power Systems,*** Volume 19, Number 1, pp. 260-264, 2004.

[107] A. González, F.M. Echavarren, L. Rouco, T. Gómez and J. Cabetas, "Reconfiguration of large-scale distribution networks for planning studies," ***Electrical Power and Energy Systems***, Accepted 5 December 2011 Article in press (2012).

[108] B. Amanulla, S. Chakrabarti and S. N. Singh, "Reconfiguration of power distribution systems considering reliability and power loss," ***IEEE Transactions on Power Delivery***, accepted November 30, 2011.

[109] A. A. M Zin, A. K. Ferdavani, A. B. Khairuddin, and M. M. Naeini, "Reconfiguration of radial electrical distribution network through minimum-

current circular-updating-mechanism method," ***IEEE Transactions on Power Systems,*** accepted October 25, 2011.

[110] F. V. Gomes, S. C. Jr, J. L. R. Pereira, M. P. Vinagre, P. A. N. Garcia and L. R. Araujo, "A new distribution system reconfiguration approach using optimum power flow and sensitivity analysis for loss reduction," ***IEEE Transactions on Power Systems***, Volume 21, Number 4, pp. 1616-1623, 2006.

[111] N. D. R. Sarma, V.C. Prasad, K. S. P. Rao and V. Sankar, "A new network reconfiguration technique for service restoration in distribution networks," ***IEEE Transactions on Power Delivery***, Volume 9, Number 4, pp. 1936-1942, 1994.

[112] Y. Y. Hong, S. Y. Ho, "Determination of network configuration considering multi-objective in distribution systems using genetic algorithms," ***IEEE Transactions on Power Systems***, Volume 20, Number 2, pp. 1062-1069, 2005.

[113] J. Y. Fan, L. Zhang and John D. McDonald, "Distribution network reconfiguration: single loop optimization," ***IEEE Transactions on Power Systems***, Volume 11, Number 3, pp. 1643 -1647, 1996.

[114] C. T. Sua, C. F. Changb, and J. P. Chiou, "Distribution network reconfiguration for loss reduction by ant colony search algorithm," ***Electric Power Systems Research***, Volume 75 pp. 190–199, 2005.

[115] S. Chakravorty and S. Ghosh, " Distribution planning based on reliability and contingency criteria," ***International Journal of Computer and Electrical Engineering,*** Volume 1, Number 2, pp. 148-153, 2009.

[116] L. Remesh, S. P. Chowdhury, A. A. Natarajan, C. T. Gaunt, " Minimization of power loss in distribution networks by different techniques," ***International***

Journal of Electrical Engineering and Electronics Engineering, Volume 3, Number 9, 2009.

[117] R. S. Rao, S. V. L. Narasimham, "A new heuristic approach for optimal network reconfiguration in distribution systems," ***International Journal of Engineering and Applied Sciences,*** Volume 5, Number 1, pp. 15-21, 2009

[118] H. M. Khodr, J. Martínez-Crespo, M. A. Matos and J. Pereira, "Distribution systems reconfiguration based on opf using benders decomposition," ***IEEE Transactions on Power Delivery***, Volume 24, Number 4, pp. 2166-2176, 2009.

[119] L. W. Oliveira, S. C. Jr, E. J. de Oliveira, J.L.R. Pereira, I. C. Silva Jr., J. S. Costa, "Optimal reconfiguration and capacitor allocation in radial distribution systems for energy losses minimization," ***Electrical Power and Energy Systems***, Volume 32, 840–848, 2010

[120] K. S. Kumar and T. Jayabarathi, "Power system reconfiguration and loss minimization for a distribution systems using bacterial foraging optimization algorithm," ***Electrical Power and Energy Systems***, Article in press, Accepted 29 October 2011.

Appendix-A

3.6 Proof of convergence:

It is mathematically established in this section of the thesis that the formulation proposed in **Section 3.3** (**Chapter 3**) has a surety of convergence. This is because the voltage that is being calculated in the ongoing iteration depends upon the voltage and the voltage drop calculated in the previous iteration. The voltage drop in any branch is also a function of the previous iteration voltage. Figure A1 graphically shows the convergence of the load-flow solution.

From Eq. (3.14) and Eq. (3.15) of **Chapter 3**

$$V_{k+1}\cos\delta_{k+1} + C_{jj}{}^{2} + V_{k+1}\sin\delta_{k+1} + D_{jj}{}^{2} = V_k\cos\delta_k{}^{2} + V_k\sin\delta_k{}^{2} \quad \text{(A1)}$$

By rearranging Eq. (A1)

$$V_{k+1}^2 + 2V_{k+1}(C_{jj}\cos\delta_{k+1} + D_{jj}\sin\delta_{k+1}) + (C_{jj}{}^{2} + D_{jj}^2) = V_k^2 \quad \text{(A2)}$$

Let $V_{k+1}^2 + \Delta V_{jj} = V_k^2$ (A3)

$$V_{k+1}^2\left(1 + \frac{\Delta V_{jj}}{V_{k+1}^2}\right) = V_k^2 \quad \text{(A4)}$$

$$V_{k+1}\left(1 + \frac{\Delta V_{jj}}{V_{k+1}^2}\right)^{\frac{1}{2}} = V_k \quad \text{(A5)}$$

$$V_{k+1}\left(1 + \frac{\Delta V_{jj}}{2V_{k+1}^2}\right) = V_k \quad \text{(A6)}$$

$$V_{k+1} = V_k - \frac{\Delta V_{jj}}{2V_{k+1}} \quad \text{(A7)}$$

$$V_{k+1} = V_k - \frac{\Delta v_{jj}}{V_{k+1}} \tag{A8}$$

Here

$$\Delta v_{jj} = \frac{V_{jj}}{2} = V_{k+1}(C_{jj}\cos\delta_{k+1} + D_{jj}\sin\delta_{k+1}) + \frac{1}{2}(C_{jj}{}^2 + D_{jj}^2) \tag{A9}$$

$$\frac{\Delta v_{jj}}{V_{k+1}} = C_{jj}\cos\delta_{k+1} + D_{jj}\sin\delta_{k+1} + \frac{C_{jj}{}^2 + D_{jj}^2}{2V_{k+1}} \tag{A10}$$

From Eq. (A8) and Eq. (A10)

$$V_{k+1} = V_k - (C_{jj}\cos\delta_{k+1} + D_{jj}\sin\delta_{k+1}) - \left(\frac{C_{jj}{}^2 + D_{jj}^2}{2V_{k+1}}\right) \tag{A11}$$

C_{jj} and D_{jj} has link with V_{k+1} and the nodes beyond the node under consideration. Hence convergence of V_{k+1} gives assurance the convergence of the V's of the other nodes beyond this node. In this case the solving of V_{k+1}, the present value of V_k and the past value of V's of m=k+1th node and nodes beyond this are used.

Let $g(V_{k+1}) = V_k - (C_{jj}\cos\delta_{k+1} + D_{jj}\sin\delta_{k+1}) - \left(\frac{C_{jj}{}^2 + D_{jj}^2}{2V_{k+1}}\right)$ (A12)

Hence C_{jj} and D_{jj} are functions of $f\left(\frac{1}{V_m}\right)$ where m=k+1, k+2, ……

In the above graph shown in Fig. A1 $V_{k+1}(0)$ is the initial value of V_{k+1}. $V_{k+1}(n)$ and $V_{k+1}(n+1)$ are the value of V_{k+1} at the nth and n+1th iteration respectively ξ_{k+1} is the final value of V_{k+1}.

Here $\varepsilon_{k+1}(n) = V_{k+1}(n) - \xi_{k+1}$ (A13)

and $\varepsilon_{k+1}(n+1) = V_{k+1}(n+1) - \xi_{k+1}$ (A14)

$$V_{k+1}(n) = \varepsilon_{k+1}(n) + \xi_{k+1} \tag{A15}$$

And $$V_{k+1}(n+1) = \varepsilon_{k+1}(n+1) + \xi_{k+1} \tag{A16}$$

$$V_{k+1}\ 1 \ = \ g\ V_{k+1}\ 0 \tag{A17}$$

$$V_{k+1}\ 2 \ = g\ V_{k+1}\ 1 \tag{A18}$$

$$V_{k+1}\ 3 \ = g\ V_{k+1}\ 2 \tag{A19}$$

:

:

$$V_{k+1}\ n+1 \ = g\ V_{k+1}\ n \tag{A20}$$

$$\xi_{k+1} + \varepsilon_{k+1}\ n+1 \ = g \quad \xi_{k+1} + \varepsilon_{k+1}\ n \ =$$

$$\xi_{k+1} + \varepsilon_{k+1}\ n\ g'\ \xi_{k+1} + \frac{1}{2!}\varepsilon^2_{k+1}\ n\ g''\ \xi_{k+1} + \text{--------} \tag{A21}$$

$$g'\ \xi_{k+1} = \frac{\Delta v_{jj}}{V_{k+1}^2} \tag{A22}$$

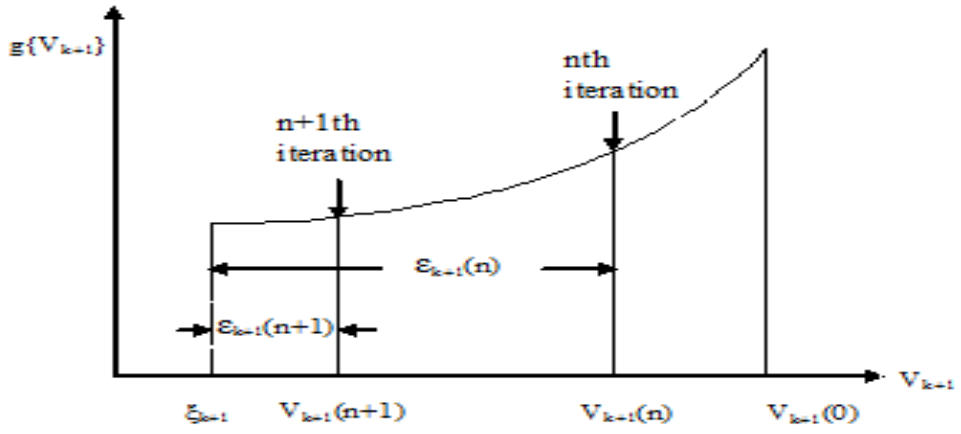

Fig. A1 Plot of g{V_{k+1}} v/s V_{k+1}

$$g'' \quad \xi_{k+1} = \frac{-2\Delta v_{jj}}{V_{k+1}^3} \tag{A23}$$

For $V_{k+1} = \xi_{k+1}$,

(A24)

$$g' \quad \xi_{k+1} = \frac{\Delta v_{jj}}{\xi_{k+1}^2} \tag{A25}$$

$$g'' \quad \xi_{k+1} = \frac{-2\Delta v_{jj}}{\xi_{k+1}^3} \tag{A26}$$

$$\text{So } \varepsilon_{k+1}(n+1) = \varepsilon_{k+1}(n)\left(1 - \frac{\varepsilon_{k+1}(n)}{\xi_{k+1}}\right)\frac{\Delta v_{jj}}{\xi_{k+1}^2} = \varepsilon_{k+1}(n)\left(1 - \frac{\varepsilon_{k+1}(n)}{\xi_{k+1}}\right)g'\{\xi_{k+1}\} \tag{A27}$$

Since $\frac{\varepsilon_{k+1}(n)}{\xi_{k+1}}$ can be neglected,

$$\varepsilon_{k+1}(n+1) = \varepsilon_{k+1}(n)g'\{\xi_{k+1}\} \tag{A28}$$

Since the $\sin\delta_{k+1}$ and $\cos\delta_{k+1}$ are approximately equal to 0 and 1. Δv_{jj} becomes $\Delta v_{jj} = V_{k+1}C_{jj} + \frac{1}{2}\left(C_{jj}^2 + D_{jj}^2\right)$. Which is function of R, X, P and Q. Hence the convergence of the proposed method becomes linear in this case and Δv_{jj} becomes very small and hence $g' \quad \xi_{k+1}$ less than 1. This gives the guarantee of the convergence of the proposed method.

Appendix-B

Table B1 Line data and load data for 33-node distribution system

Branch no.	SEN	REN	Active power load (kW)	Reactive power load (kVA)	Resistance (ohm)	Reactance (ohm)
1	1	2	100	60	0.0922	0.0477
2	2	3	90	40	0.4930	0.2511
3	3	4	120	80	0.3660	0.1864
4	4	5	60	30	0.3811	0.1941
5	5	6	60	20	0.8190	0.7070
6	6	7	200	100	0.1872	0.6188
7	7	8	200	100	1.7114	1.2351
8	8	9	60	20	1.0300	0.7400
9	9	10	60	20	1.0400	0.7400
10	10	11	45	30	0.1966	0.0650
11	11	12	60	35	0.3744	0.1238
12	12	13	60	35	1.4680	1.1550
13	13	14	120	80	0.5416	0.7129
14	14	15	60	10	0.5910	0.5260
15	15	16	60	20	0.7463	0.5450
16	16	17	60	20	1.2890	1.7210
17	17	18	90	40	0.7320	0.5740
18	2	19	90	40	0.1640	0.1565
19	19	20	90	40	1.5042	1.3554
20	20	21	90	40	0.4095	0.4784
21	21	22	90	40	0.7089	0.9373
22	3	23	90	50	0.4512	0.3083
23	23	24	420	200	0.8980	0.7091
24	24	25	420	200	0.8960	0.7011

25	6	26	60	25	0.2030	0.1034
26	26	27	60	25	0.2842	0.1447
27	27	28	60	20	1.0590	0.9337
28	28	29	120	70	0.8042	0.7006
29	29	30	200	600	0.5075	0.2585
30	30	31	150	70	0.9744	0.9630
31	31	32	210	100	0.3105	0.3619
32	32	33	60	40	0.3410	0.5302

Appendix-C

Table C1 Line data and load data for 69-node distribution system

Branch No.	SEN	REN	Active power load (kW)	Reactive power load (kVA)	Resistance (ohm)	Reactance (ohm)
1	1	2	0.0	0.0	0.0005	0.0012
2	2	3	0.0	0.0	0.0005	0.0012
3	3	4	0.0	0.0	0.0015	0.0036
4	4	5	0.0	0.0	0.0251	0.0294
5	5	6	2.6	2.2	0.3660	0.1864
6	6	7	40	30	0.3811	0.1941
7	7	8	75	54	0.0922	0.0470
8	8	9	30	22	0.0493	0.0251
9	9	10	28	19	0.8190	0.2707
10	10	11	14	104	0.1872	0.0619
11	11	12	145	104	0.7114	0.2351
12	12	13	8	5	1.0300	0.3400
13	13	14	8	5.5	1.0440	0.3450
14	14	15	0.0	0.0	1.0580	0.3496
15	15	16	45	30	0.1966	0.0650
16	16	17	60	35	0.3744	0.1238
17	17	18	60	35	0.0047	0.0016
18	18	19	0.0	0.0	0.3276	0.1083
19	19	20	1	0.6	0.2106	0.0690
20	20	21	114	81	0.3416	0.1129
21	21	22	5	3.5	0.0140	0.0046
22	22	23	0.0	0.0	0.1591	0.0526
23	23	24	28	20	0.3463	0.1145
24	24	25	0.0	0.0	0.7488	0.2475
25	25	26	14	10	0.3089	0.1021

26	26	27	14	10	0.1732	0.0572
27	3	28	26	18.6	0.0044	0.0108
28	28	29	26	18.6	0.0640	0.1565
29	29	30	0.0	0.0	0.3978	0.1315
30	30	31	0.0	0.0	0.0702	0.0232
31	31	32	0.0	0.0	0.3510	0.1160
32	32	33	14	10	0.8390	0.2816
33	33	34	9.5	14	1.7080	0.5646
34	34	35	6	4	1.4740	0.4873
35	3	36	26	18.54	0.0044	0.0108
36	36	37	26	18.54	0.0640	0.1565
37	37	38	0.0	0.0	0.1053	0.1230
38	38	39	24	17	0.0304	0.0355
39	39	40	24	17	0.0018	0.0021
40	40	41	1.2	1	0.7283	0.8509
41	41	42	0.0	0.0	0.3100	0.3623
42	42	43	6	4.3	0.0410	0.0478
43	43	44	0.0	0.0	0.0092	0.0116
44	44	45	39	26.30	0.1089	0.1373
45	45	46	39	26.30	0.0009	0.0012
46	4	47	0.0	0.0	0.0034	0.0084
47	47	48	79	56.4	0.0851	0.2083
48	48	49	384.7	274	0.2898	0.7091
49	49	50	384.7	274.	0.0822	0.2011
50	8	51	40.50	28.29	0.0928	0.0473
51	51	52	3.6	2.7	0.3319	0.1114
52	52	53	4.35	3.5	0.1740	0.0886
53	53	54	26.4	19	0.2030	0.1034
54	54	55	24	17.2	0.2842	0.1447
55	55	56	0.0	0.0	0.2813	0.1433
56	56	57	0.0	0.0	1.5900	0.5337

57	57	58	0.0	0.0	0.7837	0.2630
58	58	59	100	72	0.3042	0.1006
59	59	60	0.0	0.0	0.3861	0.1172
60	60	61	1244	888	0.5075	0.2585
61	61	62	32	23	0.0974	0.0496
62	62	63	0.0	0.0	0.1450	0.0738
63	63	64	227	162	0.7105	0.3619
64	64	65	59	42	1.0410	0.5302
65	65	66	18	13	0.2012	0.0611
66	66	67	18	13	0.0047	0.0014
67	67	68	28	20	0.7394	0.2444
68	68	69	28	20	0.0047	0.0016

Appendix-D

Table D1 Line data and load data for 41-node distribution system

S N	R N	Conductor Type	Len. in km	kVA load on RN	Cap. at RN in μF
1	27	6	1	175	0.005153
27	35	5	1.87	185	0.008786
35	8	4	1.76	60	0.008046
8	33	4	1.34	165	0.006126
33	20	4	1.41	85	0.006446
20	39	4	1.63	95	0.007452
39	4	4	1.58	90	0.007223
4	34	4	1.08	85	0.004937
34	32	4	1.96	85	0.008960
32	16	3	1.87	90	0.008237
16	21	2	1.08	73	0.004544
21	17	1	1.75	82	0.007109
27	18	4	1.9	155	0.008686
18	22	4	1.56	175	0.007132
22	11	4	1.84	158	0.008412
11	13	4	1.06	155	0.004846
13	14	4	1.43	196	0.006537
14	40	3	1.22	170	0.005133
40	6	3	1.25	195	0.005259
6	12	1	1.31	220	0.005321
27	15	4	1.5	150	0.006857
15	30	4	0.73	165	0.003337
30	29	3	2.10	150	0.009250
29	41	2	1.39	80	0.005848
41	28	2	1.11	113	0.004670

28	2	1	1.66	140	0.006743
35	26	3	1.5	155	0.006607
26	24	2	1.88	163	0.007910
24	23	1	1.88	166	0.007637
08	37	1	1.46	100	0.005931
33	10	1	1.5	75	0.006093
10	5	1	1.5	75	0.006093
5	9	1	1.91	65	0.007758
39	3	1	1.43	80	0.005809
32	36	1	1.7	90	0.006905
16	31	1	1.4	176	0.005687
21	38	1	1.3	90	0.005281
14	7	1	1.9	163	0.007718
30	19	1	2.02	90	0.008205
26	25	1	1.96	55	0.007962

Table D 2 Technical data of the conductors used in 41-node distribution system

Cond. type.	Code name.	Dia. Of cond. (mm)	Area of X-section.(mm^2) Nominal Copper area Sq. mm.	Resistance (ohm/km)	Reactance (ohm/km)	Max. Current carrying capacity (amp.) at 45° C ambient temp.
1	Squirrel	6.33	12.90	1.3760	0.3896	107
2	Weasel	7.77	19.35	0.9810	0.3797	139
3	Rabbit	10.05	32.26	0.5441	0.3673	193
4	Raccoon	12.27	48.46	0.3657	0.3579	250
5	Dog	14.15	65	0.2745	0.3112	300
6	Lion	22.26	140	0.1223	0.2446	515
The spacing between the two conductors is 1.2 meter. System voltage is 11kV. Power factor is 0.8. Base voltage = 11kV, base power = 100MVA.						

Appendix-E

Table E1 The line data and load data for 30-node network

SN	RN	Length In km	Cond. Type*	Load kVA
1	2	0.2	1	100
2	3	0.2	1	100
3	4	0.43	2	100
4	5	0.6	2	300
5	6	0.22	3	100
6	7	0.16	5	100
7	8	0.3	5	250
8	9	0.1	5	50
9	10	0.4	5	50
1	11	0.6	1	150
11	12	0.24	2	250
12	13	0.24	3	100
13	14	0.6	4	350
14	15	0.5	5	250
15	16	0.25	5	100
16	17	0.11	5	350
17	18	0.11	5	160
18	19	0.32	5	150
19	20	0.25	5	100
20	21	0.1	1	100
1	22	0.2	1	100
22	23	0.3	1	100
23	24	0.1	2	150
24	25	0.5	3	150
25	26	0.1	3	50

26	27	0.43	3	150
27	28	0.25	5	50
28	29	0.15	5	100
29	30	0.2	5	110
TL_1		0.11	5	--
TL_2		0.11	5	--
TL_3		0.32	5	--
TL_4		0.16	5	--

Table E2 Conductor sizes available in inventory for 30-node network.

Cond. no	Code name	Resistance Ohm/km	Reactance Ohm/km	Diameter mm	Weight kg/km	Area mm^2	Current carrying capacity (A)
1	Mink	0.4565	0.366	10.98	255.3	72.64	218
2	Rabbit	0.5449	0.372	10.05	214	61.70	197
3	Ferret	0.6795	0.376	9.00	172	49.48	168
4	Weasel	0.9116	0.382	7.77	128	36.88	139
5	Squirrel	1.374	0.3915	6.33	85	24.48	114

Appendix-F

Table F1 Line data and load data for 32-node radial distribution network.

SN	RN	Conductor number*	Branch length in km	Load in kVA
1	2	1	0.2	100
2	3	1	0.2	100
3	4	1	0.43	100
4	5	1	0.6	300
5	6	1	0.22	0
6	7	1	0.16	63
7	8	1	0.3	100
8	9	1	0.1	250
9	10	1	0.4	500
10	11	1	0.6	500
11	12	1	0.24	250
12	13	1	0.24	250
13	14	1	0.6	0
14	15	1	0.5	350
6	16	1	0.25	250
16	17	1	0.11	100
17	18	1	0.11	350
18	19	1	1	63
19	20	1	0.32	0
20	21	1	0.25	250
21	22	1	0.1	0
22	23	1	0.2	100
23	24	1	0.3	100
24	25	1	0.1	200
25	26	1	0.5	350
19	27	1	0.1	250

27	28	1	0.43	550
20	29	1	0.25	200
22	30	1	0.1	250
30	31	1	0.15	100
14	32	1	0.2	313
* The conductor sizes are same as shown in Table E2 in **Appendix-E**				

Appendix-G

Table G1 Line data and load data for 123-node radial power distribution network.

SN	RN	Conductor number	Length of branch in feet	Connected kVA load
1	2	4	100	10.5
2	3	4	400	9.4
3	4	9	175	8.5
3	5	9	250	16
5	6	9	200	5.5
5	7	9	325	10.9
7	8	9	250	12.6
3	9	4	300	40.25
9	10	4	200	10.9
10	11	9	225	12.5
10	12	9	225	19.5
12	13	9	425	28.4
13	14	9	250	14.7
13	15	9	250	18.5
10	16	4	300	17.5
16	17	9	150	19.2
17	18	9	100	16
18	19	9	350	18.5
18	20	9	100	120
16	21	8	825	60.5
21	22	9	250	18.5
22	23	9	325	117.3
21	24	9	300	56.45
24	25	9	525	55.9
24	26	9	250	40.7

26	27	9	550	51.25
26	28	9	275	16.4
28	29	9	350	12
29	30	9	275	16.9
30	31	9	500	40.4
29	32	9	225	17.5
32	33	9	300	13.5
28	34	9	200	12
34	35	9	300	18.75
35	36	9	350	5
36	37	9	200	40
21	38	8	100	29.3
38	39	8	375	26.5
39	40	9	650	89.7
40	41	9	300	56.3
40	42	9	250	23.4
42	43	9	325	52.6
39	44	9	250	19.8
44	45	9	325	20
44	46	9	250	6
46	47	9	500	180
46	48	9	200	17.6
48	49	9	200	56
49	50	9	300	76.4
48	51	9	250	21.54
51	52	9	150	32.5
51	53	9	250	64.7
53	54	9	250	19.8
54	55	9	250	56
55	56	9	250	24.5
16	57	7	100	64

57	58	7	400	75
58	59	7	200	18.2
59	60	7	125	24
60	61	9	275	32.5
61	62	9	275	32.4
60	63	7	350	71
63	64	9	250	41
64	65	9	250	17.4
63	66	7	750	24
66	67	7	100	56
66	68	9	250	34
68	69	9	175	56
69	70	9	350	17.4
70	71	9	425	19.5
71	72	9	325	12.5
67	73	7	350	56.7
73	74	9	200	54
74	75	9	275	60
75	76	9	325	20
76	77	9	275	40
73	78	8	275	60
78	79	9	275	18.7
79	80	9	350	63.9
80	81	9	400	92.4
78	82	8	200	194
82	83	9	400	80.2
83	84	9	100	46.4
84	85	9	225	16
84	86	9	475	29
86	87	9	475	28
87	88	9	250	25

88	89	9	250	15
87	90	9	675	40
90	91	9	475	6
82	92	9	700	65
92	93	9	450	36
93	94	9	275	54
94	95	9	225	12
95	96	9	225	16.8
96	97	9	300	45.6
97	98	9	200	47.9
96	99	9	275	23.5
95	100	9	300	69.4
94	101	9	225	56.7
93	102	9	175	49.7
73	103	8	250	69.4
103	104	9	275	18.7
104	105	9	550	54.2
105	106	9	300	56.4
106	107	9	800	85
103	108	8	100	120
108	109	9	250	110
109	110	9	225	12.8
110	111	9	325	39.6
111	112	9	700	15.76
109	113	9	275	39.4
113	114	9	225	23.5
114	115	9	575	89.5
113	116	9	325	45.8
116	117	9	450	79.4
117	118	9	300	63.4
118	119	9	575	12.7

118	120	9	125	56.4
120	121	9	525	85.4
121	122	9	325	14.5
116	123	9	1000	12.4

Table G 2 The available conductor sizes in inventory for 123-node distribution network.

Cond. No.	Code name	Resistance Ohm/km	Reactance Ohm/km	Diameter mm	Weight kg/km	Area mm^2	Current carrying capacity Amp.
1	Lynx	0.1589	0.381	19.53	844	226.2	445
2	Wolf	0.1844	0.381	18.13	727	194.9	406
3	Tiger	0.2211	0.381	16.5	591	161.8	361
4	Dog	0.2745	0.381	14.15	394	118.5	312
5	Horse	0.365	0.381	13.95	537.3	116.2	241
6	Mink	0.456	0.381	10.98	255.3	73.71	218
7	Rabbit	0.5449	0.381	10.5	214	61.7	197
8	Squirrel	1.376	0.381	6.33	85	24.5	114
9	Mole	2.702	0.381	4.5	43	12.4	92

List of publication

1. Kultar Deep Singh and Smarajit Ghosh, **"**A New Efficient Method for Load-Flow Solution for Radial Distribution Networks", ***Przeglad Elektrotechniczny (Electrical Review),*** vol.12a'11, pp. 66-73, December 2011. (Impact Factor 0.24)
2. Kultar Deep Singh and Smarajit Ghosh, "Voltage stability index and Line loadability index for radial power distribution networks", ***International Review of Electrical Engineering,*** Vol. 6, no. 7, pp-3111-3121, December 2011. (Impact Factor 1.364)

Biography

Kultar Deep Singh: Born in Ludhiana, Punjab, India on 22nd February, 1978. He did B. Tech. (Elect. Engg.), M. Tech.(Power Engg.) from Punjab Technical University, Jalandhar Punjab, India, in 2001 and 2004 respectively. He is pursuing Ph. D. as regular research scholar in Department of Electrical and Instrumentation Engineering of Thapar University, Patiala, Punjab, India Under the supervision of Prof. Smarajit Ghosh.

His areas of interest are load-flow, line loadability, optimal conductor size selection, optimal capacitor placement etc. for electrical power distribution networks.

Contact email: kultar22@yahoo.com

Smarajit Ghosh: Born in Ghatal, West Bengal, India on 16 August, 1967. He did his B. Tech., M. Tech. in Electrical Machines and Power Systems from Calcutta University in 1994 and 1996 respectively. Finally, he did his Ph.D. from Indian Institute of Technology, Kharagpur, India in 2000.

His research areas include load–flow study, network reconfigurations, optimum capacitor allocation, application of soft computing in Electrical Power Distribution Systems, data-sequrity. He has already served REC (Durgapur), BITS Pilani and Sikkaim Manipal University, as a lecturer, Assistant Professor and Professor respectively.

He has authored a number of books published by Printice Hall of India Private Limted and Pearson Education as a single auther.

Smarajit Ghosh is serving as a Professor in Thapar University Patiala, Department of Electrical and Instrumentation Engineering.

Contact email: smarajitg@hotmail.com